

**Partitioning of the response to cAMP via two specific Ras  
proteins during *Dictyostelium discoideum* development**

by

PARVIN BOLOURANI

B.Sc., Kerman University, 1987  
M.Sc., Utah State University, 1993

A THESIS SUBMITTED IN PARTIAL FULFILLMENT OF  
THE REQUIREMENTS FOR THE DEGREE OF

DOCTOR OF PHILOSOPHY

in

THE FACULTY OF GRADUATE STUDIES

(Microbiology and Immunology)

THE UNIVERSITY OF BRITISH COLUMBIA

(Vancouver)

May 2008

© Parvin Bolourani, 2008

## ABSTRACT

Following starvation, *Dictyostelium discoideum* cells aggregate, a response that requires chemotaxis to cyclic AMP (cAMP) and the relay of the cAMP signal by the activation of adenylyl cyclase (ACA).

Insertional inactivation of the *rasG* gene resulted in delayed aggregation and a partial inhibition of early gene expression, suggesting that RasG does have a role in early development. When the responses of *rasG*<sup>-</sup> cells to cAMP were compared with the responses of *rasC* strain, these studies revealed that signal transduction through RasG is more important in chemotaxis and early gene expression, but that signal transduction through RasC is more important in ACA activation. Characterization of a *rasC/rasG*<sup>-</sup> mutant revealed that both cAMP chemotaxis and adenylyl cyclase (ACA) activation were negligible in this strain.

The ectopic expression of *carA* from the *actin 15* promoter restored early developmental gene expression to the *rasC/rasG*<sup>-</sup> strain, rendering it suitable for an analysis of cAMP signal transduction. Since there was negligible signaling through either the cAMP chemotactic pathway or the adenylyl cyclase activation pathway in this strain, it is clear that RasG and RasC are the only two Ras subfamily proteins that directly control these pathways. The mutational analysis of Switch I and Switch II regions also defined the key residues that generate functional differences between RasC and RasG.

Rap1 is also activated in response to cAMP but its position in the signal transduction cascade was clarified by the finding that its activation was totally abolished in *rasC/rasG*<sup>-</sup>/*act15*:*carA* and in *rasG*<sup>-</sup> cells, but only slightly reduced in *rasC* cells. The finding that *in vitro* guanylyl cyclase activation is also abolished in the *rasC/rasG*<sup>-</sup>

$\Delta[act15]:carA$  strain identifies RasG/RasC as the presumptive monomeric GTPases required for this activation.

The phenotypes of the vegetative *ras* null mutants were also examined. The results indicate that RasG plays an important role in cytokinesis. The partial absence of chemotaxis to folate in *rasG*<sup>-</sup> cells compared to the total absence of chemotaxis to folate in *rasC/rasG*<sup>-</sup>, and *rasC/rasG*<sup>-</sup> $\Delta[act15]:carA$  cells suggests a compensatory role of RasC for RasG during this process, a similar phenomenon to that observed for cAMP chemotaxis by aggregating cells.

# TABLE OF CONTENTS

ABSTRACT .....	ii
TABLE OF CONTENTS .....	iv
LIST OF TABLES .....	viii
LIST OF FIGURES .....	ix
LIST OF ABBREVIATIONS .....	xii
ACKNOWLEDGEMENTS .....	xv
<b>1 INTRODUCTION.....</b>	<b>1</b>
<b>1.1 The heterotrimeric GTPases .....</b>	<b>1</b>
<b>1.2 The monomeric GTPase superfamily.....</b>	<b>2</b>
<b>1.3 The structure and localization of Ras subfamily proteins .....</b>	<b>3</b>
<b>1.4 Ras proteins as molecular switches .....</b>	<b>4</b>
<b>1.5 RasGEFs and RasGAPs .....</b>	<b>6</b>
<b>1.6 Ras activation by receptor stimulation in mammalian cells .....</b>	<b>7</b>
<b>1.7 Ras effectors .....</b>	<b>9</b>
<b>1.8 <i>Dictyostelium</i> as a model organism.....</b>	<b>12</b>
<b>1.9 <i>Dictyostelium discoideum</i> life cycle .....</b>	<b>13</b>
<b>1.10 cAMP signalling during <i>Dictyostelium</i> aggregation.....</b>	<b>15</b>
<b>1.11 <i>Dictyostelium</i> Ras proteins .....</b>	<b>21</b>
<b>1.12 Thesis Objective .....</b>	<b>26</b>
<b>2 Materials and Methods.....</b>	<b>28</b>
<b>2.1 Materials .....</b>	<b>28</b>
<b>2.1.1 Reagents .....</b>	<b>28</b>
<b>2.1.2 Services.....</b>	<b>28</b>
<b>2.1.3 <i>Dictyostelium</i> Strains.....</b>	<b>29</b>
<b>2.1.4 Plasmids and DNA .....</b>	<b>29</b>
<b>2.2 Methods.....</b>	<b>33</b>
<b>2.2.1 Plasmid construction .....</b>	<b>33</b>
<b>2.2.2 DNA amplification .....</b>	<b>33</b>
<b>2.2.3 Generation of mutated constructs .....</b>	<b>38</b>

2.2.4	Generation of null mutant strains .....	40
2.2.5	Growth of <i>Dictyostelium discoideum</i> .....	41
2.2.6	cAMP pulsing .....	42
2.2.7	Multicellular development .....	43
2.2.8	Nuclear staining .....	43
2.2.9	F-actin staining.....	44
2.2.10	Chemotaxis assays.....	44
2.2.11	Western blot analysis.....	45
2.2.12	PKB phosphorylation assays.....	46
2.2.13	Northern blot analyses.....	47
2.2.14	Southern blot analyses.....	48
2.2.15	cAMP accumulation.....	49
2.2.16	Adenylyl cyclase assay .....	50
2.2.17	cAMP binding assay .....	50
2.2.18	cGMP production.....	51
2.2.19	Guanylyl cyclase assay.....	51
2.2.20	RasG, RasC and Rap1 activation assay .....	52
3	RESULTS .....	53
3.1	Comparison of the roles of RasG and RasC in cAMP signaling during aggregation .....	53
3.1.1	Generation of <i>rasG</i> null strain .....	53
3.1.2	Developmental phenotype of the <i>rasG</i> null strains .....	58
3.1.3	Early developmental gene expression .....	62
3.1.4	Comparison of chemotaxis by <i>rasG</i> and <i>rasC</i> cells .....	64
3.1.5	cGMP production in response to cAMP .....	70
3.1.6	Guanylate cyclase activation.....	70
3.1.7	PKB phosphorylation .....	73
3.1.8	cAMP production.....	76
3.1.9	Adenylyl cyclase activation .....	76
3.1.10	Activation of RasC and RasG in <i>rasG</i> and <i>rasC</i> cells in response to cAMP .....	81

3.1.11	Summary.....	83
3.2	cAMP relay and chemotaxis in a <i>rasC/rasG</i> strain in response to cAMP	84
3.2.1	Generation of <i>rasC/rasG</i> strain .....	84
3.2.2	Developmental phenotype of the <i>rasC/rasG</i> cells.....	84
3.2.3	Early developmental gene expression .....	90
3.2.4	Restoration of early developmental gene expression in a <i>rasC/rasG</i> strain by the ectopic expression of <i>carA</i> .....	92
3.2.5	cAMP binding assay .....	96
3.2.6	Developmental phenotype of the <i>rasC/rasG</i> [ <i>act15</i> ]: <i>carA</i> cells.....	100
3.2.7	The RasG and RasC pathways are essential for adenylyl cyclase (ACA) activation .....	102
3.2.8	The RasG and RasC pathways are essential for chemotaxis, PKB phosphorylation, and guanylyl cyclase activation .....	104
3.2.9	Rap activation in <i>ras<sup>-</sup></i> cells.....	111
3.2.10	Summary.....	113
3.3	Identification of the amino acid residues in RasC and RasG required for specificity during aggregation.....	114
3.3.1	RasC and RasG expression from introduced <i>rasC</i> and <i>rasG</i> transgenes in <i>rasG</i> and <i>rasC</i> strains.....	114
3.3.2	Determination of the residues important for RasC activity .....	120
3.3.3	Chimeric constructs .....	122
3.4	Role of RasG and RasC proteins in vegetative cells .....	126
3.4.1	RasG is important for cell growth.....	126
3.4.2	RasG is important for cytokinesis .....	128
3.4.3	Chemotaxis to folate .....	128
3.4.4	F-actin distribution .....	132
4	DISCUSSION.....	136
4.1	RasG is involved in <i>Dictyostelium</i> aggregation.....	136
4.2	Chemotaxis and ACA activation during <i>Dictyostelium</i> aggregation.....	137
4.3	Rap1 activation occurs downstream of RasG activation.....	142

<b>4.4</b>	<b>The production of cGMP plays a more important role in the chemotactic process than does the production of PIP3.....</b>	<b>143</b>
<b>4.5</b>	<b>Specificity of Ras protein interactions .....</b>	<b>144</b>
<b>4.6</b>	<b>The role of RasG and RasC in the regulation of the cytoskeleton during aggregation .....</b>	<b>147</b>
<b>4.7</b>	<b>Proposed model of Ras signaling during aggregation .....</b>	<b>149</b>
<b>4.8</b>	<b>The role of RasG and RasC in vegetative cells.....</b>	<b>151</b>
<b>4.9</b>	<b>Concluding remarks .....</b>	<b>154</b>
	<b>REFERENCES.....</b>	<b>155</b>

## LIST OF TABLES

Table 1. <i>Dictyostelium</i> strain description .....	30
Table 2. Plasmid description.....	31
Table 3. Sequence and description of oligonucleotides primers used .....	35
Table 4. Sequence and description of oligonucleotides used for the site directed mutagenesis on <i>rasG</i> cDNA.....	37
Table 5. Description of probes used for blot hybridization analysis.....	48
Table 6. Chemotaxis analysis of <i>Dictyostelium</i> cells in a spatial gradient of cAMP.	69
Table 7. Cell surface associated-cAMP binding activity.....	97
Table 8. Chemotaxis analysis of <i>Dictyostelium</i> cells in a spatial gradient of cAMP. .....	106
Table 9. Aggregation and cAMP accumulation in cells expressing RasG with a variety of point mutations. ....	124
Table 10. Aggregation and cAMP accumulation in cells expressing chimeric constructs of RasG and RasC. ....	125
Table 11. Nuclei number of <i>Dictyostelium</i> cells grown in suspension. ....	130
Table 12. Chemotaxis analysis of <i>Dictyostelium</i> cells in a spatial folate chemoattractant gradient.....	134

## LIST OF FIGURES

Figure 1. The RasGTPase molecular switch.....	5
Figure 2. Multicellular development of <i>Dictyostelium discoideum</i> . ....	14
Figure 3. Genetic disruption of <i>rasG</i> gene. ....	56
Figure 4. Western blot analysis of Ras protein levels of JH10, JH10/ <i>rasC</i> , JH10/ <i>rasG</i> , AX2, AX2/ <i>rasC</i> , and AX2/ <i>rasG</i> .....	57
Figure 5. Multicellular development of JH10, <i>rasG</i> , and <i>rasC</i> on bacterial growth plates.....	59
Figure 6. Multicellular development of Ax2 and <i>rasG</i> on bacterial growth plates. ....	60
Figure 7. Aggregation of JH10, <i>rasG</i> , and <i>rasC</i> on a plastic surface.....	61
Figure 8. Development of JH10, <i>rasG</i> , and <i>rasC</i> on nitrocellulose filters. ....	63
Figure 9. Northern-blot analysis of early developmental gene expression of JH10, <i>rasG</i> , and <i>rasC</i> .....	65
Figure 10. Chemotaxis of starved JH10, <i>rasG</i> , and <i>rasC</i> cells towards a source of cAMP.....	67
Figure 11. Chemotaxis of pulsed JH10, <i>rasG</i> , and <i>rasC</i> cells towards a source of cAMP.....	68
Figure 12. cGMP production of JH10, <i>rasG</i> , and <i>rasC</i> in response to cAMP.....	71
Figure 13. <i>In vitro</i> GTP $\gamma$ S stimulation of guanylyl cyclase activity of JH10, <i>rasG</i> , and <i>rasC</i> . ....	72
Figure 14. PKB phosphorylation of JH10, <i>rasG</i> , and <i>rasC</i> in response to cAMP. .	75
Figure 15. cAMP accumulation and ACA activation of 5h pulsed JH10, <i>rasG</i> , and <i>rasC</i> .....	78
Figure 16. cAMP accumulation and ACA activation of 8h pulsed JH10, <i>rasG</i> , and <i>rasC</i> .....	80
Figure 17. Ras subfamily protein activation of JH10, <i>rasG</i> , and <i>rasC</i> in response to cAMP.....	82
Figure 18. Western blot analysis of Ras protein levels of JH10, <i>rasC</i> , <i>rasG</i> , and <i>rasC/rasG</i> .....	85
Figure 19. Multicellular development of JH10, and <i>rasC/rasG</i> on bacterial growth plates.....	86

Figure 20. Aggregation of JH10, and <i>rasC/rasG</i> on a plastic surface.....	88
Figure 21. Development JH10, and <i>rasC/rasG</i> on nitrocellulose filters. ....	89
Figure 22. Northern-blot analysis of early developmental gene expression of JH10, <i>rasC/rasG</i> , and <i>rasC/rasG</i> Δ <i>act15</i> : <i>carA</i> .....	91
Figure 23. Expression profiles of early developmental genes. ....	94
Figure 24. Multicellular development of JH10, <i>rasC/rasG</i> , and <i>rasC/rasG</i> Δ <i>act15</i> : <i>carA</i> on bacterial growth plates.....	98
Figure 25. Development of JH10, <i>rasC/rasG</i> , and <i>rasC/rasG</i> Δ <i>act15</i> : <i>carA</i> on nitrocellulose filters.....	99
Figure 26. Aggregation of JH10, <i>rasC/rasG</i> , and <i>rasC/rasG</i> Δ <i>act15</i> : <i>carA</i> on a plastic surface.....	101
Figure 27. <i>In vitro</i> GTPγS stimulation of adenylyl cyclase activity of JH10, <i>rasC/rasG</i> , and <i>rasC/rasG</i> Δ <i>act15</i> : <i>carA</i> . ....	103
Figure 28. Chemotaxis of JH10, <i>rasC/rasG</i> , and <i>rasC/rasG</i> Δ <i>act15</i> : <i>carA</i> cells towards a source of cAMP. ....	105
Figure 29. PKB phosphorylation of JH10, <i>rasC/rasG</i> , and <i>rasC/rasG</i> Δ <i>act15</i> : <i>carA</i> cells in response to cAMP.....	107
Figure 30. cGMP production in response to cAMP and <i>In vitro</i> GTPγS stimulation of guanylyl cyclase activity of JH10, <i>rasC/rasG</i> , and <i>rasC/rasG</i> Δ <i>act15</i> : <i>carA</i> cells. ....	110
Figure 31. Rap activation in response to cAMP.....	112
Figure 32. Western blot analysis of Ras protein levels of JH10, <i>rasG</i> , <i>rasG</i> Δ <i>rasC</i> : <i>rasC</i> , <i>rasC</i> , and <i>rasC</i> Δ <i>rasG</i> : <i>rasG</i> .....	115
Figure 33. Western blot analysis of Ras protein levels of JH10, <i>rasG</i> , <i>rasG</i> Δ <i>rasG</i> : <i>rasC</i> , <i>rasC</i> , and <i>rasC</i> Δ <i>rasC</i> : <i>rasG</i> .....	118
Figure 34. cAMP accumulation in JH10, <i>rasG</i> , <i>rasC</i> , <i>rasC</i> Δ <i>rasC</i> : <i>rasG</i> , and <i>rasG</i> Δ <i>rasG</i> : <i>rasC</i> strains. ....	119
Figure 35. Amino acid comparison of switch I and switch II regions of RasC and RasG.....	121
Figure 36. cAMP accumulation in the various <i>ras</i> mutant strains.....	123
Figure 37. Cell growth in suspension culture. ....	127

<b>Figure 38. Nuclear staining.....</b>	<b>129</b>
<b>Figure 39. Chemotaxis in a spatial folate chemoattractant gradient. ....</b>	<b>131</b>
<b>Figure 40. F-actin distribution.....</b>	<b>135</b>
<b>Figure 41. Model of cAMP signaling via RasC and RasG. ....</b>	<b>138</b>

## LIST OF ABBREVIATIONS

A	ampere or amp, unit measure for electric current
ACA	adenylyl cyclase
ATP	adenosine triphosphate
APS	ammonium persulphate
b, bp	base, base pair
BSA	bovine serum albumin
<i>bsr</i>	blasticidin resistance gene
cAMP	adenosine 3',5'-cyclic monophosphate
cAR	cAMP receptor
cDNA	complementary DNA
cGMP	guanosine 3',5'-cyclic monophosphate
CRAC	cytosolic regulator of adenylyl cyclase
DAG	diacylglycerol
<sup>32</sup> P- $\alpha$ -dCTP	<sup>32</sup> P labeled deoxycytidine triphosphate
ddH <sub>2</sub> O	distilled, deionized water
DEPC	diethylpyrocarbonate
DMSO	dimethyl sulfoxide
DNA	deoxyribonucleic acid
dNTP	deoxynucleoside triphosphate
DTT	dithiothreitol
EDTA	ethylene diamine tetraacetic acid
EGF	epidermal growth factor
ERK	extracellular regulated protein kinase
g	gravity, unit measure for centrifugal force
GAP	GTPase activating protein
GC	guanylyl cyclase
GDP	guanosine 5'-diphosphate
GEF	guanine nucleotide exchange factor

GFP	green fluorescent protein
GPCR	G protein coupled receptor
GST	glutathione-S-transferase
GTP	guanosine 5'-triphosphate
GTP $\gamma$ S	guanosine 5'-O-(3-thiotriphosphate)
h	hour(s)
HL5	nutrient rich axenic growth media
HRP	horseradish peroxidase
HVR	hypervariable region
IP3	inositol (1,4,5) trisphosphate
ITAM	immunoreceptor tyrosine-based activation motifs
kbp	kilo base pair
kDa	kilo Dalton
KK <sub>2</sub>	potassium phosphate non-nutrient buffer
MAP	mitogen activated protein
MEK	MAP kinase kinase
MHC	myosin heavy chain
MHCK	myosin heavy-chain kinase
min	minute(s)
MLC	myosin light chain
MLCK	myosin light chain kinase
mRNA	messenger ribonucleic acid
nt	nucleotide
PAGE	polyacrylamide gel electrophoresis
PBS	phosphate-buffered saline
PDK	phosphoinositide dependent kinase
PH	pleckstrin homology
PtdIns(4,5)P <sub>2</sub>	phosphatidylinositol 4,5-bisphosphate
PtdIns(3,4,5)P <sub>3</sub>	phosphatidylinositol 3,4,5-trisphosphate
PI3K	phosphoinositide 3-kinase
PKA	protein kinase A

PKB	protein kinase B
PLA2	phospholipase A2
PLC	phospholipase C
PTEN	phosphatase and tensin homologue deleted on chromosome ten
PTK	protein tyrosine kinase
RA	Ras associating domain
RalGDS	Ral GTPase dissociation stimulator
RBD	Ras binding domain
RGS	regulator of G protein signaling
RIP	Ras interacting protein
RLC	regulatory light chain
RNA	ribonucleic acid
rpm	revolutions per minute
RTK	receptor tyrosine kinase
s	second(s)
SDS	sodium dodecyl sulphate
SH2	Src homology 2
SH3	Src homology 3
SOS	Son of sevenless, a RasGEF
V	volt(s), unit measure for electric potential
YFP	yellow fluorescent protein

## ACKNOWLEDGEMENTS

It is a pleasure to thank the many people who made this thesis possible.

I would like to express my sincere gratitude to my supervisors, Gerry and George. Working beside them has been an honor and a true pleasure. You both guided me during my studies with valuable lessons. Gerry, your wide knowledge, understanding and encouragement have been of great value to me. George, your logical way of thinking and personal guidance have provided a good basis for the present thesis. To the members of my supervisory committee, Dr. P. Hieter, Dr. P. Johnson, and Dr. J. Kronstad, thanks for your guidance and constructive criticism. My special thanks to Dr. M. Gold for all his encouraging words and his help in many ways.

In the laboratory, my sincere thanks to Meenal, for her friendship and keeping me company. My special thanks to Helmut for being a wonderful friend, for all the support and help in many different ways. Thanks to past and present members of the Weeks laboratory, whose time in the lab coincided with mine: James, Dave, Michelle, Brent, and Megan, for your friendship and helpful discussions. Thanks to the members of the Spiegelman laboratory, Steven and Brett for always being willing to help as they learnt from their mentor.

Thanks to my first biology mentor, Dr. Kalantari, for his special friendship and encouragement throughout my studies.

To my parents, Mansour and Nosrat, for always believing in me. You have been so supportive in too many ways to list; I really appreciate all the help. To my brother and sisters, thanks for the encouragement throughout my academic experience.

My deepest appreciation to my husband, Nosratollah, for an enormous amount of faith in me and lots of wise words. Thanks for creating an environment in which following this path seemed so natural. You have loved, helped, encouraged and supported me to pursue my dreams, thanks. Thanks to my children, Ameen and Mahta, for their understanding and patience. I never forget the everyday question from Mahta: "Are you going to finish your thesis today?" You make everything worthwhile.

# 1 INTRODUCTION

G proteins are regulatory proteins involved in signal transduction pathways. They bind GDP in their inactive state and GTP in the activated state and the change of GDP for GTP and vice-versa constitutes the important regulatory function. There are two distinct families: The monomeric GTPases or “small G proteins” and the heterotrimeric G proteins, sometimes referred to as the “large G proteins”. There is a certain amount of sequence homology between the  $\alpha$  subunits of the heterotrimeric G proteins and the monomeric GTPases.

## 1.1 The heterotrimeric GTPases

Heterotrimeric G proteins are composed of  $G\alpha$ ,  $G\beta$ , and  $G\gamma$  subunits, and function to transduce signals from G protein-coupled receptors (GPCR) to intracellular effector proteins. G protein regulated signaling pathways mediate a vast number of physiological responses, and deregulation of these pathways contributes to many diseases, such as cancer, heart disease, hypertension, endocrine disorders, and blindness (Melien, 2007). Agonist binding to a GPCR at the extracellular cell surface induces a conformational change in the GPCR that allows it to directly promote GDP release from the inactive  $G\alpha$  subunit and its exchange for GTP. This promotes the dissociation of the heterotrimeric complex, giving rise to signaling-competent GTP-bound  $G\alpha$  and free  $G\beta\gamma$  subunits. To complete the G protein cycle, the bound GTP is hydrolyzed to GDP, a reaction catalyzed by a group of proteins referred to as Regulators of G-protein Signaling (RGS), and then GDP-bound  $G\alpha$  reassociates with  $G\beta\gamma$  (Cabrera-Vera *et al.*, 2003).

## 1.2 The monomeric GTPase superfamily

The monomeric GTPases comprise a large superfamily of small GTP-binding proteins with molecular masses of 20-40 kDa (Takai *et al.*, 2001). The family members are highly conserved and are found in eukaryotic organisms ranging from yeast to human. The proteins function as molecular switches in intracellular signaling and control a wide range of cellular functions. The family members share ~30% overall amino acid sequence identity mostly in four conserved GTP-binding domains, required for the recognition of GDP, GTP and the GTPase activity (Bourne *et al.*, 1991).

There are over one hundred members of the monomeric GTPase superfamily that are divided on the basis of sequence and functional similarities into five subfamilies: Rho, Rab, Ran, Arf and Ras. Members within each of the subfamilies share ~50% amino acid sequence identity and exhibit conserved motifs in effector domains, and carboxy terminal sequences that undergo various post-translational modifications (Bourne *et al.*, 1991; Corbett and Alber, 2001; Takai *et al.*, 2001). Each subfamily appears to regulate distinct functions within the cell; the Rho proteins regulate cytoskeletal rearrangement and gene expression; Rab and Arf proteins regulate vesicular trafficking; Ran proteins regulate nuclear trafficking and microtubule organization; Ras proteins are linked to numerous biological functions such as differentiation, proliferation, apoptosis and the regulation of gene expression (Takai *et al.*, 2001). Ha-Ras was the first member of the monomeric G protein superfamily to be described and hence the superfamily is also referred to as the Ras superfamily (Takai *et al.*, 2001). A great deal has been learned about each of the five subfamilies but the remainder of this introduction will focus on the Ras subfamily proteins, the subject of this thesis.

### **1.3 The structure and localization of Ras subfamily proteins**

In mammalian cells three *ras* genes encode four highly related well studied proteins H-Ras, K-RasA, K-RasB, and N-Ras of 188-189 amino acids in length (Barbacid, 1987). All the important domains for GTPase function (sequences important for nucleotide binding and GTP hydrolysis) are located within the N-terminal (165 amino acids) sequence (Lowy and Willumsen, 1993). Based on primary sequence comparisons, these proteins consist of three regions: 1) the N-terminal 86 amino acids, which are 100% identical for the four mammalian Ras proteins and constitutes the Ras effector binding domain (amino acids 32 to 40) that is critical for downstream interactions; 2) the subsequent 80 amino acids, that exhibit 85% identity; 3) the remaining C-terminal sequence, known as the hypervariable region which starts at amino acid 165 and exhibits no sequence similarity, except for a conserved CAAX motif (C, cysteine; A, aliphatic amino acid; X, methionine or serine) at the C-terminal end of the proteins (Clarke, 1992). The other members of the mammalian Ras subfamily proteins exhibit some divergence in these three regions but exhibit overall more than 50% sequence identity. The CAAX motif is the target for posttranslational prenylation, either a farnesyl or a geranylgeranyl moiety, which is involved in anchoring the proteins to the membranes. Fatty acids, especially palmitate, can also be added to Ras proteins at cysteine residues other than the terminal cysteine, which contributes to subcellular localization (Pechlivanis and Kuhlmann, 2006).

The presence of the prenylated hypervariable region (HVR) suggested the possibility that the various Ras subfamily proteins exhibit different subcellular localizations. In fact H-Ras is associated both with lipid raft and non-raft plasma

membrane structures (Chen and Resh, 2001), while, K-Ras is localized exclusively to non-raft plasma membrane structures (Prior *et al.*, 2001). Mammalian Ras proteins have also been visualized on the Golgi and ER membranes (Choy *et al.*, 1999), suggesting that Ras protein activation is not limited to the plasma membrane. Thus a difference in localization of Ras proteins is possibly important in the linking to different types of receptors, which may be important for the downstream regulation of signals.

#### **1.4 Ras proteins as molecular switches**

As noted previously, the Ras subfamily proteins have two interconvertible forms: a GDP-bound inactive form and a GTP-bound active form (Figure 1). Thus, they function as nucleotide-dependent regulatable molecular switch (Vetter and Wittinghofer, 2001). An upstream signal stimulates the exchange of GDP for GTP. GTP-binding results in the conformational change of the two key regions of the protein termed Switch I (residues 21-40 relative to H-Ras) and Switch II (residues 57-75) (Quilliam *et al.*, 2002). Switch I is part of the effector loop and enables the binding of a variety of different effector proteins when Ras is in its GTP-bound form.

The GTP-bound form is converted back to the GDP bound form by the action of the intrinsic GTPase activity, resulting in the release of effectors and thus the completion of one cycle of activation and inactivation. By this means small G proteins serve as molecular switches that transiently transduce an upstream signal to downstream effectors. Interconversion between Ras-GDP and Ras-GTP is extremely slow and enhanced and regulated by two types of regulatory proteins: guanine nucleotide exchange factors (GEFs) that promote the release of GDP, and GTPase activating proteins (GAPs) that enhance the GTPase activity.

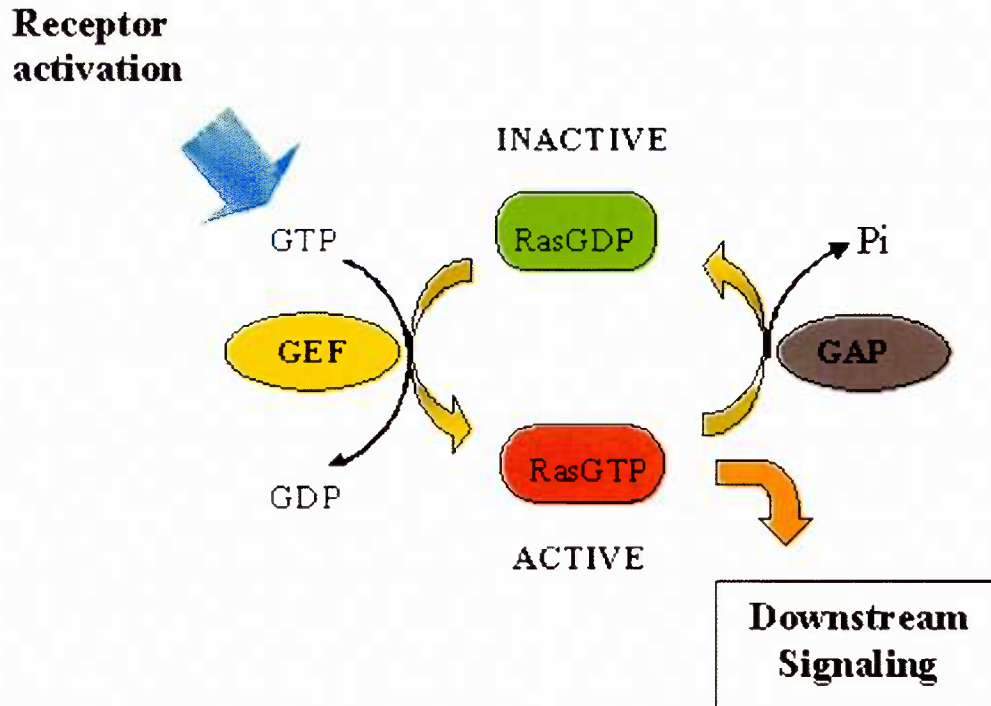


**Figure1. The RasGTPase molecular switch.** Model depicting the GTPase cycle of monomeric Ras superfamily proteins. Stimulation by an activating signal leads to displacement of GDP by GTP, catalyzed by guanine nucleotide exchange factors (GEFs). GTP binding to Ras promotes a structural change facilitating the binding of Ras to various downstream effectors, propagating the signal. Ras is subsequently turned off through the action of GTPase activating proteins (GAPs), which enhance the intrinsic GTPase activity of Ras proteins.

A regulated balance between the activity of GEFs and GAPs is believed to be important in the proper regulation of GTPase activity (Takai *et al.*, 2001). The Ras cycle can be interrupted by various mutations which lock the protein in GTP or GDP-bound forms. Single amino acid substitution at position 12 or 61 keeps Ras in the GTP-bound form and this mutation is often associated with human tumors, while substitution at position 17 prevents Ras activation (Barbacid, 1987). Mutated forms of three human *ras* genes have been detected in 20-30% of human cancers (Bos, 1989; Shields *et al.*, 2000). Since Ras proteins regulate diverse extracellular signaling pathways, the deregulated function of other cellular components can also cause aberrant Ras function even in the absence of mutation in the *ras* genes themselves.

### **1.5 RasGEFs and RasGAPs**

The *Saccharomyces cerevisiae* CDC25 was the first RasGEF to be identified and loss of the encoding gene arrested growth by blocking Ras activation of adenylyl cyclase (Broek *et al.*, 1987; Jones *et al.*, 1991). This discovery was soon followed by the identification of the *Drosophila* Son of sevenless (Sos) (Bonfini *et al.*, 1992) and the mammalian hSos1 (Fath *et al.*, 1993), which both contain a catalytic domain related to that of CDC25. At least 100 RasGEFs have now been identified but the family is diverse and can be grouped into more than ten different classes based on substrate specificities and structural similarities (Bos *et al.*, 2007). While RasGEFs are typically multi-domain containing proteins, they all share at least two discrete domains: an amino-terminal domain of unclear function and a carboxy-terminal domain that mediates GTP-GDP exchange, that has significant homology to CDC25. This latter domain is often referred to as the CDC25 domain. Three regions of Ras have been implicated in the RasGEF-Ras

interaction: Switch I, Switch II, and  $\alpha$ -helix 3 (residues 102-107) (Wittinghofer, 1998). RasGEFs can also serve as dual specificity GEFs, catalyzing the activation of more than one GTPase. SOS, for example, contains a catalytically active RacGEF domain in addition to the RasGEF domain (Nimnual *et al.*, 1998). The dual specificity of SOS provides a mechanism for the regulation of Rac mediated cytoskeletal rearrangement by Ras, which creates a network of GTPase signaling cascades.

The RasGAPs promote the conversion of RasGTP to RasGDP by stimulating the Ras protein's weak intrinsic GTP hydrolyzing activity by the insertion of an arginine side-chain into its active site (Ahmadian *et al.*, 1997). The RasGAPs are highly related to each other (Boguski and McCormick, 1993). p120 RasGAP was the first protein shown to bind to Ras and was initially classified as an effector of Ras (Adari *et al.*, 1988). In addition to a catalytic domain, p120 RasGAP has multiple other domains including: SH2 (Src homology 2), SH3 (Src homology 3), and PH (pleckstrin homology) domains (Gibbs *et al.*, 1988). The RasGEFs have been more extensively studied, but evidence suggests that GAPs may play equally important roles in GTPase regulation (Takai *et al.*, 2001).

## **1.6 Ras activation by receptor stimulation in mammalian cells**

In mammalian cells Ras is activated in response to the stimulation of receptor tyrosine kinases (RTKs), receptor-associated protein tyrosine kinases (PTKs) or G-protein coupled receptors (GPCRs) (Genot and Cantrell, 2000; Schlessinger, 2000; Marinissen and Gutkind, 2001). The role of the RTKs in Ras activation has been extensively studied (Schlessinger, 2000). RTKs consist of an extracellular domain required for ligand binding, a transmembrane domain that anchors the receptor to the membrane, and a cytoplasmic catalytic domain. The general mechanism for RTK

activation begins with ligand binding, which induces dimerization of the RTK and this promotes the phosphorylation of various tyrosine residues in the cytoplasmic domain resulting in activation of the kinase (Olson and Marais, 2000). The phosphorylated tyrosines then function as recruitment sites for SH2 (Src homology 2) domain containing proteins such as Shc and Grb2, which mediate the translocation of a RasGEF, such as SOS, from the cytosol to the activated receptor (receptor-adaptor complex) through an interaction between the C-terminus of the SOS and the SH3 domain of Grb2 (Pawson and Schlessinger, 1993). The process effectively localizes SOS into close proximity with Ras at the plasma membrane, allowing Ras activation through GDP/GTP exchange. Epidermal growth factor (EGF) mediated Ras activation is an example of this process (Schlessinger, 2000).

Ras activation can also occur through the stimulation of receptor-associated PTKs, such as those in B-cell and T-cell lymphocytes (Genot and Cantrell, 2000). These receptors are hetero-dimers consisting of a large extracellular fragment, a transmembrane domain, and a short cytoplasmic tail. These receptors possess no intrinsic tyrosine kinase activity and instead recruit PTKs to the membrane. Once recruited, the PTKs phosphorylate the tyrosine residues referred to as ITAMs (immunoreceptor tyrosine-based activation motifs) on the receptor cytoplasmic tails. These phosphorylated tyrosine residues further recruit various SH2 domain containing proteins such as Syk/Zap70 and adaptor proteins such as LAT and Shc. This ultimately leads to the recruitment of the Grb2-SOS complex from the cytosol to the membrane and the activation of Ras.

A third type of Ras activation pathway involves G-protein coupled receptors (GPCRs). GPCRs are characterized structurally by an extracellular domain, a seven

transmembrane domain (7TMD) and a carboxyterminal intracellular domain. Ligand binding at the extracellular domain leads to a conformational change in the 7TMD, which allows association of the receptor with an heterotrimeric G protein and the initiation of the signaling cascade within the cell (Prinster *et al.*, 2005). The mechanism of Ras activation upon GPCR stimulation has remained more elusive, but is believed to involve the G $\beta\gamma$  subunits of heterotrimeric G-protein and Src kinase as possible intermediates (Marinissen and Gutkind, 2001).

### **1.7 Ras effectors**

Ras activation leads to an interaction with a variety of downstream effector proteins, and this in turn transmits the signal through a cascade of cytoplasmic proteins (Marshall, 1996). The Ras effectors can be organized into 3 groups: kinases, GEFs for other Ras superfamily proteins, and a still expanding group of other effectors with, for the most part, uncertain catalytic functions.

The first Ras effector to be identified was the serine/threonine kinase Raf (Vojtek *et al.*, 1993), the initial component of the best-characterized Ras regulated signal transduction pathway, the mitogen-activated protein (MAP) kinase cascade. This cascade, leading to Erk (Extracellular regulated protein kinase) activation, begins with the binding of Ras to members of the Raf family of serine/threonine kinases, Raf-1, A-Raf, and B-Raf (Stokoe *et al.*, 1994). The precise mechanism through which binding of activated Ras to Raf results in activation of Raf is not completely understood, but probably involves the phosphoserine binding protein, 14-3-3, and members of Src tyrosine kinase family (Morrison and Cutler, 1997). Activated Raf then phosphorylates and activates MEK (MAP kinase kinase), which in turn, phosphorylates and activates the

Erks (Arbabi and Maier, 2002). Activated Erk translocates into the nucleus where it phosphorylates and stimulates a variety of transcription factors, including Elk1 and Jun, coupling Ras activation to gene expression.

The second group of well-characterized mammalian Ras effectors are the phosphoinositide 3-kinases (PI3Ks) (Rodriguez-Viciana *et al.*, 1997), which upon activation in cells regulate apoptosis and actin cytoskeleton rearrangement (Shields *et al.*, 2000). Class I PI3Ks are heterodimers comprising a 110 kDa catalytic subunit (p110) and a smaller regulatory subunit and the p110 subunit interacts directly with GTP-bound Ras (Vanhaesebroeck and Waterfield, 1999; Katso *et al.*, 2001). PI3K catalyzes the conversion of the lipid substrate phosphatidylinositol 4,5-bisphosphate (PtdIns(4,5)P<sub>2</sub> or PIP<sub>2</sub>) to phosphatidylinositol 3,4,5-trisphosphate (PtdIns(3,4,5)P<sub>3</sub> or PIP<sub>3</sub>) which is anchored in the plasma membrane and acts as a docking site for the recruitment of pleckstrin homology (PH) domain containing proteins such as PKB (Akt) and PDK1 (phosphoinositide dependent kinase-1) (Vanhaesebroeck and Waterfield, 1999; Fresno Vara *et al.*, 2004).

While PH domain dependent translocation is required for PKB to function (Bellacosa *et al.*, 1998), activation is dependent upon phosphorylation on two sites, T308 and S473. PDK1 directly phosphorylates the T308 site (Fresno Vara *et al.*, 2004), while the TORC2 complex is responsible for phosphorylation at the S473 site (Sarbasov *et al.*, 2005). Activated PKB then phosphorylates various downstream target proteins including the apoptotic protein BAD, and nuclear transcription factors of the Forkhead family. Upon phosphorylation the transcription factors relocate to the cytosol, resulting in a downregulation of gene transcription (Datta *et al.*, 1997; Biggs *et al.*, 1999; Dijkers *et al.*,

2002). In addition, Ras activation of PI3K can lead to the activation of Sos1/2 and Vav which then activate Rac, resulting in the actin cytoskeletal rearrangement required for cell motility (Nimnual *et al.*, 1998).

The third group of well characterized effectors are the RalGEFs, including RalGDS, Rgl, Rlf, and Rgr, which interact through their Ras association (RA) domains with various activated members of the Ras subfamily including Ras, Rap, and Rit (Wolthuis and Bos, 1999). The RalGEFs activate the Ras subfamily protein, Ral, but the downstream pathways beyond Ral activation are less well defined (Feig, 2003).

Other Ras effector proteins, such as phospholipase C $\epsilon$  (PLC $\epsilon$ ), Rin1, AF6, calmodulin, and Nore-1 have been shown to exhibit preferential binding to Ras-GTP, but have not been well characterized. The PLC family of proteins, of which only PLC $\epsilon$  contains a RBD, cleave PIP<sub>2</sub> at the plasma membrane to generate two important intracellular second messengers, diacylglycerol (DAG) and inositol (1,4,5) trisphosphate (IP3) (Kelley *et al.*, 2001). DAG subsequently leads to the activation of the protein kinase PKC, while IP3 stimulates an increase of intracellular Ca<sup>2+</sup>. Interaction of Ras with other effectors such as Rin1, AF6, calmodulin, and Nore-1, results in regulation of endocytosis, cell-cell junction formation, Ca<sup>2+</sup> signaling and apoptosis respectively (Campbell *et al.*, 1998; Boettner *et al.*, 2000; Cullen, 2001; Tall *et al.*, 2001; Villalonga *et al.*, 2001; Radziwill *et al.*, 2003; Vos *et al.*, 2003). Recently comprehensive searches have been conducted for RA domains and have uncovered several additional possible effectors (Goldfinger *et al.*, 2007). The growing number of Ras effectors indicates involvement of Ras in a variety of signaling pathways.

Given the complexity of Ras signaling pathways in mammalian cells, Ras has been studied in several model organisms, most notably *Drosophila*, *C.elegans*, yeast and *Dictyostelium discoideum*. In fact early studies of *Drosophila* and *C.elegans* helped elucidate the activation by Ras of the MAPK cascade (Wassarman *et al.*, 1995; Sternberg and Han, 1998).

Since all the studies described in this thesis concern the role of Ras in *Dictyostelium discoideum*, the remainder of the introduction will be devoted to a description of the state of knowledge of this topic prior to starting the thesis work.

### **1.8 *Dictyostelium* as a model organism**

Early studies based on rRNA sequence homology suggested that the social amoeba *Dictyostelium discoideum* diverged before the evolution of plants, animals, and fungi (Olsen *et al.*, 1983), but more recent analysis based on protein sequence have indicated that *Dictyostelium* diverged from the animal lineage after the divergence from plants (Loomis and Smith, 1990). The predicted proteome analysis derived from the complete *Dictyostelium* genome sequence (Eichinger *et al.*, 2005) has confirmed this latter view.

*Dictyostelium* is a free-living soil organism that feeds on bacteria in the wild as its natural nutrient source. Starvation induces an interesting developmental program, during which individual cells chemotax to form a multicellular organism and then differentiate into either stalk or spore cells. The separation between growth and differentiation allows for the characterization of growth specific or development specific genes, although some genes are required for both functions (Souza *et al.*, 1998). The haploid nature of the organism, along with the recent completion of the genome sequence, allows for efficient

genetic manipulation either by targeted or random gene disruption and the generation of mutants by homologous recombination. The *Dictyostelium* genome encodes many components that are also involved in mammalian cell functions, and it has proven to be a useful model organism for studying a variety of biological processes such as cell signaling (Van Haastert and Devreotes, 2004; Weeks *et al.*, 2005), cell migration (Parent, 2004), cytoskeletal organization (Affolter and Weijer, 2005) and phagocytosis (Rupper and Cardelli, 2001). *Dictyostelium* also has been used to study action of medically relevant compounds such as lithium and valproic acid, drugs used to treat various depressive disorders (Eickholt *et al.*, 2005; Boeckeler *et al.*, 2006) and cisplatin, a drug used to treat cancer (Li *et al.*, 2000). The simple developmental program, ease of cultivation in the laboratory and the combination of cellular, genetic and molecular biology techniques that are available has made *Dictyostelium* an attractive organism for research in cell and developmental biology.

### **1.9 *Dictyostelium discoideum* life cycle**

The following section provides an overview of the *Dictyostelium discoideum* life cycle (Kessin, 2001). The entire differentiation process from the starvation of vegetative amoeba to the formation of the final fruiting body, consisting of stalk and spore cells, takes about 24 hours (Figure 2). Starving cells begin to emit pulses of cAMP every 6 minutes and this serves as a chemoattractant signal for up to 100,000 neighboring cells to aggregate. In addition to the chemotactic response, cAMP activates adenylyl cyclase (ACA), generating additional cAMP, which relays the signal throughout the population, and also induces early developmental gene expression. As the cellular components required for production and detection of cAMP are made, chemotaxing cells converge

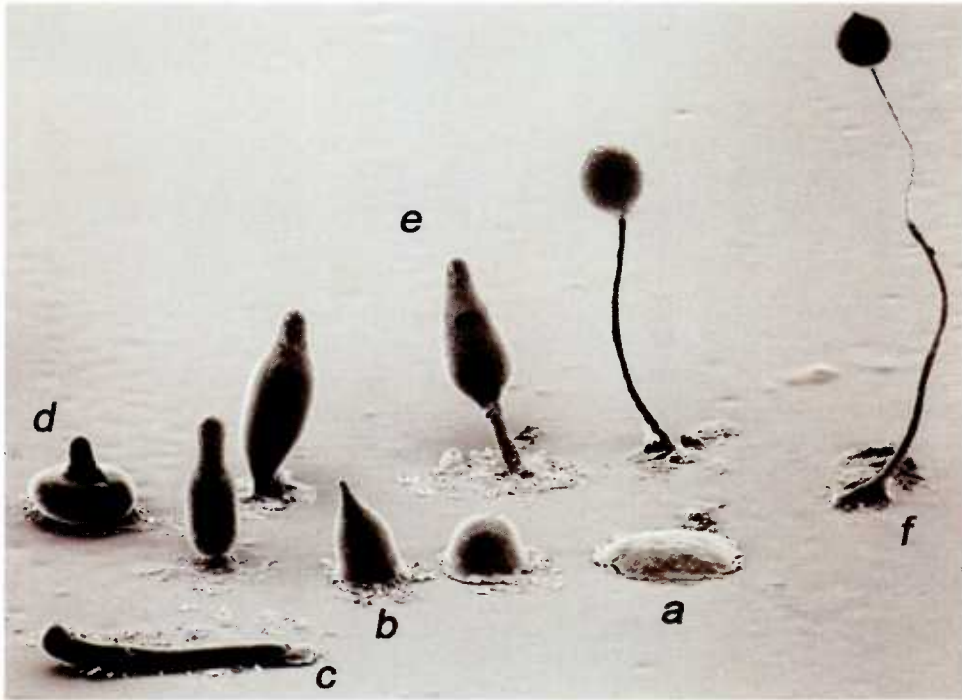


**Figure 2. Multicellular development of *Dictyostelium discoideum*.** *Dictyostelium discoideum* developmental progression are shown in a clockwise pattern beginning with (a) a mound of aggregated cells, (b) standing slug or finger, (c) migrating slug, (d) 'mexican hat', (e) culminating structures, and (f) a terminal fruiting body. The entire process is completed in approximately 24 hours following the onset of starvation. Electron micrograph image is by Mark J. Grimson and R. Lawrence Blanton, Texas Tech University, Lubbock, Texas. © M. J. Grimson and R. L. Blanton.

toward an aggregation center to form a 'mound', which eventually forms a tip. As development proceeds, the tip elongates and forms a finger like structure, which then falls over onto the surface to form a phototactic and thermotactic migrating slug. During migration of the slug prestalk cells differentiate at the front and prespore cells differentiate at the rear. After a period of migration, the slug rounds up and the anterior tip rises resulting in the formation of a fruiting body, a process called 'culmination'. Culmination involves the movement of the prestalk cells downwards through the middle of the cell mass, which lifts the prespore cells off the substratum. The prestalk cells differentiate into vacuolated dead stalk cells (20% of the cells) that support the spore head containing spore cells (80% of the cells). In the laboratory a compact mound of aggregated cells forms between 10-12 hours following starvation and takes another 12 hours to finish the developmental cycle and form fruiting bodies. The spores can tolerate a wide range of environmental conditions and upon dispersal, in response to favorable growth conditions, temperature and humidity, germinate into vegetative amoebae.

#### **1.10 cAMP signalling during *Dictyostelium* aggregation**

Since the function of Ras proteins during the response to cAMP is the focus of this thesis, this section will provide an overview of the cAMP stimulated signaling events and the role that Ras proteins play in this process, which had determined prior to the outset of my work.

In *Dictyostelium* cAMP serves as chemoattractant. There are two general types of signaling pathways that transmit signals induced by cAMP: those that involve the heterotrimeric G protein associated with the cAMP receptor, and those that do not (Manahan *et al.*, 2004). The key receptor for cAMP at the aggregation stage is cAR1, a

seven transmembrane glycoprotein belonging to the GPCR superfamily (Kessin, 2001), which is thought to mediate all cAMP stimulated events during aggregation (Pupillo *et al.*, 1992). cAR1 is associated with a heterotrimeric G protein, comprising G $\alpha$ 2, G $\beta$  and G $\gamma$  subunits (Parent and Devreotes, 1996). The binding of cAMP to cAR1 stimulates the dissociation of G $\alpha$ 2 from G $\beta\gamma$  and the available evidence suggests that G $\alpha$ 2 stimulates the pathway leading to the activation of the guanylyl cyclases, sGC and GCA (Roelofs and Van Haastert, 2002), whereas G $\beta\gamma$  activates PI3K and the adenylyl cyclase, ACA (Wu *et al.*, 1995; Parent and Devreotes, 1996). cARs are required for the induction of post-aggregation gene expression but this process is independent of G $\alpha$ 2 $\beta\gamma$  (Aubry and Firtel, 1999).

ACA consists of six membrane spanning domains and two large cytoplasmic domains similar to that of the mammalian adenylyl cyclase, but unlike the mammalian enzyme, the *Dictyostelium* ACA does not contain a consensus G $\beta\gamma$  binding site. The activation of *Dictyostelium* ACA is eliminated by mutation of genes for two cytosolic proteins: the cytosolic regulator of adenylyl cyclase (CRAC) and Pianissimo (Pia) (Insall *et al.*, 1994; Chen *et al.*, 1997). CRAC, a PH domain containing protein, translocates to the front of migrating cells in response to cAMP, and its translocation is dependent on PI3K activity (Huang *et al.*, 2003). Experiments using ACA-YFP fusion proteins demonstrated that ACA localizes to the rear of polarized cells (Kriebel *et al.*, 2003). Evidence has been presented recently for the involvement of a TORC2 complex in ACA activation (Lee *et al.*, 2005). This complex contains TOR, LST, RIP3 (Ras interacting protein 3) and Pia. RIP3 and Pia are orthologues of the yeast TORC2 components, AVO1 and AVO3 (Chen *et al.*, 1997; Lee *et al.*, 1999; Lee *et al.*, 2005). Disruption of

either of *pia* or *rip3* in *Dictyostelium* results in mutants that are unable to activate adenylyl cyclase (ACA) in response to chemoattractant stimulation and exhibit serious defects in chemotaxis to cAMP. It has therefore been proposed that TORC2 complex is important for coordinating the two essential arms of the developmental pathway, chemotaxis and signal relay, that leads to multicellularity in *Dictyostelium* (Lee *et al.*, 2005).

Chemotaxis requires the precise regulation of both chemoattractant sensing and directional movement up a chemoattractant gradient. Binding of cAMP to cAR1 leads to the activation of several chemotactic signaling events including the production of second messenger molecules, such as PIP3, and cGMP, recruitment of PH-domain containing proteins to the leading edge of the cells, rearrangement of cytoskeleton components and the activation of small G-proteins (Manahan *et al.*, 2004). A ‘compass model’ has been proposed to explain chemotaxis in eukaryotic cells (Weiner, 2002; Franca-Koh and Devreotes, 2004; Sasaki *et al.*, 2004). According to this model, cells respond to directional signals by integrating three processes; directional sensing, pseudopod extensions, and polarization. First, cells establish the directional sensing by determining the direction of the gradient concentration. Second, cells move by extending the lamellipod or pseudopod in the direction of the chemoattractant gradient as a result of localized F-actin polymerization, in coordination with retraction of the cell posterior via a myosin II mediated pathway. Third, cells establish a distinct polarity as a result of the localization of specific proteins to the front and back of the cell. The class I PI3Ks and PTEN (phosphatase and tensin homologue deleted on chromosome ten) have been implicated as important components in the control of *Dictyostelium* directional sensing,

by generating gradients of PIP3 in the cell. PI3K catalyzes the production of PIP3 by the phosphorylation of PIP2 and PTEN catalyzes the reverse reaction (Funamoto *et al.*, 2002; Iijima *et al.*, 2002; Huang *et al.*, 2003). It has been shown that PI3K is recruited from the cytoplasm to the plasma membrane at the leading edge (Sasaki *et al.*, 2004), which results in dissociation of PTEN from the plasma membrane at the leading edge but not at the back of the cell. It is believed that PIP3 accumulation at the front of the cell induces remodeling of the actin cytoskeleton which largely accounts for the extension of F-actin-filled pseudopodia. How PIP3 promotes actin polarization at the leading edge remains unclear, but it probably exerts its effect by recruiting pleckstrin homology (PH) domain-containing proteins to the plasma membrane. However, the extension of the pseudopod at the front of the cell may be viewed as a more random process. Recently, based on a quantitative analysis of pseudopod generation it has been proposed that cells randomly protrude pseudopods that often split and the one that orients itself spatially closer to the chemoattractant source becomes the dominant pseudopod, and the one that is furthest from the cAMP gradient is retracted (Andrew and Insall, 2007). Clearly chemotaxis is a complex process involving a complex network of signaling pathways that is only just beginning to be understood.

The central role for PI3K in directional sensing has recently been questioned (Sasaki and Firtel, 2006; Hoeller and Kay, 2007). *Dictyostelium* cells have a total of six genes that encode PI3Ks and five of them encode type1 PI3Ks. Initially it was found that when the genes encoding PI3K1 and PI3K2 were both knocked out, PIP3 was undetectable at the leading edge, cells were poorly polarized and chemotaxis to the source of chemoattractant was very slow, suggesting that the compass is upstream of

PI3K signaling (Funamoto *et al.*, 2002). However, more recently it has been reported that inactivation of all five genes encoding type I PI3Ks results in cells that exhibit reduced polarity but nearly normal chemotaxis (Hoeller and Kay, 2007) and inactivation of the genes encoding PI3K1-3 produces a similar result. These results suggest that although PIP3 amplification in front of chemotaxing cells is important for polarity and pseudopod formation, it is not essential for chemotaxis and that other pathways are present. One other pathway involves phospholipase A2 (PLA2) encoded by the *plaA* gene. Inhibition of both PI3K and PLA2 resulted in cells that were defective in chemotaxis (Chen *et al.*, 2007; van Haastert *et al.*, 2007). In addition although *plaA*<sup>-</sup> cells are able to polarize and chemotax similar to wild type cells, *plaA*<sup>-</sup>/*pikA*<sup>-</sup>/*pikB*<sup>-</sup> cells exhibit major defects in polarity and directed migration (Chen *et al.*, 2007).

There is also evidence for a third signaling pathway, involving guanylyl cyclases (GCs) which generate guanosine 3',5'-cyclic monophosphate (cGMP) in response to cAMP in polarized cells. Cells with disruptions in the genes *gcaA* and *sgcA*, encoding guanylyl cyclases, exhibit markedly reduced chemotaxis (Roelofs and Van Haastert, 2002). A *gcaA*/*sgcA*<sup>-</sup> mutant that is defective in the production of cGMP, and a *gbpC*<sup>-</sup> mutant that is defective in transmitting signaling events downstream of cGMP production, both extend pseudopods all over the cell body indicating a role for cGMP in suppressing lateral pseudopods (Bosgraaf *et al.*, 2002; Bosgraaf *et al.*, 2005). cGMP also mediates suppression of pseudopodia by stimulating the formation of myosin filaments in the rear of the cells (Bosgraaf and van Haastert, 2006). cGMP is implicated in the transient phosphorylation of RLC (regulatory light chain) and MHC (myosin heavy chain) of myosin II, that results in disassembly of myosin II at the front of the cell (van

Haastert and Kuwayama, 1997). Disruption of the *mhc* gene in *Dictyostelium* results in cells that extend numerous lateral pseudopods and frequently change their direction, resulting in a velocity that is almost half that of the wild type cells (Heid *et al.*, 2005). Recent studies show that myosin heavy-chain kinase A (MHCK-A) translocates to the leading edge (Liang *et al.*, 2002; Steimle *et al.*, 2002) and thus the localization of MHCK-A at the front of the cell is important in localizing myosin to the back and side of the cell (Rubin and Ravid, 2002). In contrast, phosphorylation of MLC (myosin light chain) promotes myosin II activity. It has been proposed that cGMP is a positive regulator of MLCK (myosin light chain kinase) (Liu and Newell, 1994) and mutants with decreased cGMP phosphodiesterase activity exhibit increased MLC phosphorylation (Bosgraaf *et al.*, 2002; Rubin and Ravid, 2002). It has also been shown that sGC localizes to the leading edge of chemotaxing cells where it possibly acts as a mediator of F-actin protrusion (Veltman and Van Haastert, 2006). Taken together the studies suggest that cGMP is involved in a third signaling pathway that is required to promote the myosin filament formation at the rear of the cell, and suppress the pseudopod formation at the sides and at the back of the cell.

cAMP signaling also induces the expression of a number of genes during early development, for example, the genes encoding the cAMP receptors, G protein subunits, and ACA. In addition, the cAMP-dependent protein kinase A (PKA) level increases during differentiation and this increase is required for the regulation of some of the early developmental genes, such as *acaA* and *carA*, the regulation of intracellular cAMP degradation and cell-type differentiation (Harwood *et al.*, 1992; Shaulsky and Loomis, 1993; Schulkes and Schaap, 1995). PKA is a heterodimer consisting of a catalytic kinase

subunit, PKA-C, and a regulatory subunit, PKA-R (Saran *et al.*, 2002). Dissociation of PKA-R from PKA-C upon cAMP binding to PKA-R results in activation of PKA. Cells lacking PKA-R are constitutively active for PKA, resulting in constitutive induction of early developmental genes (Zhang *et al.*, 2003b). Erk2, a MAPK encoded by *erkB*, is also required for ACA activation, although its role is not clear (Segall *et al.*, 1995; Schenk *et al.*, 2001). It has been suggested that PKA is involved in the regulation of Erk2 (Zhang *et al.*, 2003a). Erk2 also inhibits RegA, an intracellular cAMP specific phosphodiesterase that breaks down the cAMP generated by ACA (Shaulsky and Loomis, 1993). As the levels of internal cAMP rise, PKA is activated and it has been proposed that this activation inhibits Erk2. Erk2 inhibition results in RegA activation and the resulting reduction in intracellular cAMP decreases PKA activity to its basal state, in preparation for another cAMP stimulus.

### 1.11 *Dictyostelium* Ras proteins

The genome of *Dictyostelium discoideum* contains fifteen Ras subfamily protein encoding genes, of which only six have thus far been studied; *rasB*, *rasC*, *rasD*, *rasG*, *rasS*, and *rapA* (Weeks *et al.*, 2005). *Dictyostelium* has a relatively small genome of about 34 Mb, which is far smaller than the 180 Mb genome of *Drosophila* and only a small fraction of the 2,851 Mb of human genome. Despite this relatively small genome size, *Dictyostelium* has almost half the number of *ras* genes found in humans and considerably more than that found in *Drosophila* (Colicelli, 2004; Eichinger *et al.*, 2005; Weeks *et al.*, 2005). The *Dictyostelium* Ras subfamily proteins exhibit between 54% and 68% amino acid identity with the canonical human H-Ras protein, with RasD and RasG sharing the highest identity, 65% and 68%, respectively (Daniel, 1995). The RasG and

RasD proteins are most related to each other, 82% overall amino acid identity, and exhibit identical sequences in their effector regions (Switch I, residues 32-40 relative to H-Ras). RasB, RasC and RasS exhibit variations in their effector sequences relative to each other and to RasG and RasD (Daniel, 1995). Since the residues from Switch I contribute to effector binding specificity, these differences would suggest that each protein would regulate a distinct signaling pathway and targeted gene disruption has supported this idea (Wilkins and Insall, 2001; Weeks and Spiegelman, 2003). The different developmental expression profile for each of the characterized Ras genes is consistent with the idea that each gene mediates a specific set of functions during different stages of the life cycle (Daniel, 1995).

*rasD* was the first *Dictyostelium ras* gene to be characterized (Reymond *et al.*, 1984). *rasD* mRNA is not expressed during vegetative growth, but starts to be expressed during the early aggregation stage (~8 hours from the onset of development) and is maximally expressed during culmination (~18-24 hours) (Reymond *et al.*, 1984). Transformants expressing activated RasD (RasD<sup>G12T</sup>) formed multi-tipped aggregates that were blocked in further development (Reymond *et al.*, 1986). These transformants expressed enhanced levels of prestalk specific genes and decreased levels of prespore specific genes, suggesting a role for RasD in cell fate determination (Louis *et al.*, 1997a). It was thus surprising that *rasD* cells developed normally with a proportion of stalk cells to spore cells that was the same as the wild type, and the only obvious phenotype was a loss of phototactic and thermotactic properties of the migrating slugs (Wilkins *et al.*, 2000). However, although RasG protein levels drop as developmental progresses, there

are still appreciable levels of RasG in late aggregates which might compensate for the loss of RasD function (Weeks and Spiegelman, 2003).

*rasB* appears to be essential for growth. Presumptive *rasB* null cells that grew very slowly and displayed undetectable levels of RasB protein were isolated. However, these cells were unstable, regained RasB protein, and reverted to a wild type phenotype (Sutherland, 2001). The only presumptive *rasB* disruptions that could be isolated were all disrupted in the promoter region and contained two copies of the gene, allowing homologous recombination to regenerate an undisrupted RasB function. Immunofluorescence studies revealed that RasB localized to the nucleus during most of the cell cycle (Sutherland *et al.*, 2001). However, during the mitotic period from metaphase to telophase RasB is not associated with the nucleus and returns to the nucleus only when mitosis is complete, suggesting a role for RasB in the regulation of mitosis. Cells overexpressing activated RasB<sup>G12T</sup> are multinucleate, consistent with the presumptive role of RasB in cell cycle regulation (Sutherland *et al.*, 2001).

*rapA* is expressed throughout growth and development and exhibits a biphasic pattern of expression, with one maximum during aggregation and one during culmination (Robbins *et al.*, 1990). Overexpression of wild type and activated Rap1 resulted in morphologically aberrant vegetative amoebae, cells were spread and flattened, concomitant with an increase in actin staining around the cell periphery (Rebstein *et al.*, 1993; Rebstein *et al.*, 1997). Rap1 also positively regulates the rates of phagocytosis and negatively regulates the rate of pinocytosis (Seastone *et al.*, 1999), suggesting a role for Rap1 during growth. Attempts to disrupt *rapA* have been unsuccessful and reduction of the protein levels by antisense mRNA expression reduced growth and viability,

suggesting that *rapA* is an essential gene (Kang *et al.*, 2002). The accumulation of cGMP was reduced with induction of *rapA* antisense RNA and was enhanced in cells expressing the constitutively activated Rap1<sup>G12V</sup> protein, suggesting a role for Rap1 in the generation of cGMP (Kang *et al.*, 2002). A possible role for Rap1 in development was suggested by the coexpression of Rap1 with RasD<sup>G12T</sup> that resulted the completion of development of the multi-tipped aggregates, that were characteristic of cells only expressing RasD<sup>G12T</sup> (Louis *et al.*, 1997b).

*rasS* is expressed predominantly during growth and early aggregation (Daniel *et al.*, 1994). Disruption of *rasS* resulted in the cells unable to grow in axenic culture, due to impairment in fluid phase endocytosis (Chubb *et al.*, 2000). *rasS*<sup>-</sup> cells are also highly polarized, move rapidly and exhibit increased F-actin localization to their pseudopods. It has been suggested, based on these phenotypes, that RasS regulates the balance between feeding and movement and that one behavior is compromised by the function of the other, due to a competition for cytoskeletal components (Chubb *et al.*, 2000).

*rasC* is expressed throughout growth and development and its expression level peaks during the aggregation and slug stages (Daniel *et al.*, 1994). Direct evidence for a role for Ras signaling pathways in regulating the *Dictyostelium* aggregation process came with the disruption of the *rasC* gene, which produced cells that failed to aggregate (Lim *et al.*, 2001). The aggregation defect observed for the *rasC*<sup>-</sup> cells could be explained by an inability to produce cAMP upon receptor stimulation and this phenotype can be bypassed by administration of exogenous cAMP pulses (Lim *et al.*, 2001). In addition, *rasC* null cells also exhibited reduced phosphorylation of PKB in response to cAMP,

suggesting a role for RasC in the signal transduction pathway that regulates chemotaxis (Lim *et al.*, 2001).

*rasG* is expressed maximally during growth and early development, and its expression is down regulated to negligible levels by the aggregation stage (Robbins *et al.*, 1989; Khosla *et al.*, 1990). Consistent with the idea that RasG might be important for growth, gene ablation of *rasG* resulted in cells that exhibited a reduced growth rate (Tuxworth *et al.*, 1997). *rasG*<sup>-</sup> cells grown axenically become large and multinucleate, indicating a defect in cytokinesis due to an inability to sever the cleavage furrow (Tuxworth *et al.*, 1997). The cytokinesis defect appeared to be related to actin cytoskeleton regulation, since *rasG*<sup>-</sup> cells also exhibited multiple elongated filopodia, aberrant lamellipodia and an unusual punctate actin distribution at the cell surface. *rasG*<sup>-</sup> cells also had a defect in cell motility (Tuxworth *et al.*, 1997). The loss of RasG maybe partially compensated for the fact that *rasG* null cells contain increased levels of RasD (Khosla *et al.*, 2000). Expression of RasD from the *rasG* promoter in *rasG*<sup>-</sup> cells which further increased the level of RasD, rescued the growth and cytokinesis defects, but not the motility defects (Khosla *et al.*, 2000).

Although the major role for RasG appeared to be in *Dictyostelium* growth and other vegetative cell functions (Tuxworth *et al.*, 1997; Khosla *et al.*, 2000), the *rasG*<sup>-</sup> cells exhibited delayed aggregation (Weeks and Insall personal communication). However, since this property was variable and the cells were unstable, this defect was not studied further. However, consistent with a possible role for RasG in aggregation was the finding that RasG interacts with *Dictyostelium* PI3K1 and PI3K2 in yeast two hybrid assays (Funamoto *et al.*, 2002). As noted previously cells lacking both PI3Ks exhibited

defects in aggregation and chemotaxis and since RasG binds to PI3Ks, it was suggested that RasG could play a role in regulating these processes (Funamoto *et al.*, 2001). Furthermore, Ras interacting protein 3 (RIP3) was also identified as a putative RasG interacting protein in a yeast two-hybrid assay (Lee *et al.*, 1999) and *ripA*<sup>-</sup> cells are unable to aggregate or activate adenylyl cyclase, and chemotax slower than wild type cells (Lee *et al.*, 1999; Lee *et al.*, 2005). The specific binding of this protein to RasG also suggests a possible role for RasG in regulating aggregation. Finally it was shown that RasG was activated in response to cAMP (Kae *et al.*, 2004), again suggesting a possible role for RasG in the aggregation process.

### **1.12 Thesis Objective**

Cell aggregation requires chemotaxis to cyclic AMP (cAMP) and the relay of the cAMP signal by the activation of adenylyl cyclase (ACA) (Kessin, 2001). It had been shown previously that RasC is involved in both processes (Lim *et al.*, 2001). However, since the loss of the RasC protein does not result in a total loss of signal transduction down the two branches of the cAMP signal-response pathway and since the pulsed *rasC* cells are able to efficiently chemotax to cAMP, RasC may not be the sole Ras protein responsible for mediating the downstream effects of cAMP. Although, there was suggestive evidence for a role for RasG in aggregation, definitive proof was lacking (Tuxworth *et al.*, 1997; Khosla *et al.*, 2000). The first objective of this thesis therefore was to generate new *rasG* null strains in two different parental backgrounds, since strain variability may have been a factor in the variable results obtained with the previous strains. The study on the newly generated null strains positively confirmed a role for RasG in aggregation. However, since the loss of either of the two Ras proteins, RasC and

RasG, alone did not result in a total loss of signal output down either of the branches of the cAMP/heterotrimeric G protein signal-response pathway, a second objective was to generate a *rasC<sup>-</sup>/rasG<sup>-</sup>* strain to determine if all signaling would be abolished. Furthermore, the recent finding that Rap1 is activated in response to cAMP (Jeon *et al.*, 2007) suggested that the role of Rap1 in cAMP signaling in regard to RasC and RasG needs further investigation. Finally, the availability of the new stable *rasG<sup>-</sup>* strains and the *rasC<sup>-</sup>/rasG<sup>-</sup>* strains provided an opportunity to further evaluate the role of RasG and RasC in vegetative cells.

## **2 Materials and Methods**

### **2.1 Materials**

#### **2.1.1 Reagents**

Growth media components were from Oxoid (Nepean, ON), BBL (Cockeysville, MD), or BD Sciences (Mississauga, ON). Chemicals and reagents were obtained from Fisher Scientific (Ottawa, ON), Invitrogen (Burlington, ON) or Sigma (Oakville, ON), unless otherwise stated. Restriction endonucleases, DNA polymerases and other DNA modifying enzymes were obtained from Invitrogen (Burlington, ON), New England BioLabs (Pickering, Ontario) or Stratagene (La Jolla, CA). All cloning and sub-cloning steps employed the use of chemical or electro-competent *Escherichia coli* strain XL1-Blue MRF' (Stratagene, La Jolla, CA) or Promega (Madison, WI). Hybond P Polyvinylidene difluoride (PVDF) membranes, enhanced chemiluminescence (ECL), horseradish peroxidase (HRP) conjugated goat anti-rabbit secondary antibody for immunoblot analysis were obtained from GE Healthcare (Baie d'Urfe, PQ). The *Dictyostelium* PKB-specific polyclonal antibody was generously provided by Fan Jiang and Dr. Robert Dottin (Hunter College, New York). Phosphothreonine polyclonal antibody (Cat # 9381) was from Cell Signaling Technology (Danvers, MA).

#### **2.1.2 Services**

The RasG, RasC, and Rap specific antibodies were raised in rabbits against the C-terminal hypervariable portion of corresponding proteins at the UBC Animal Care Facility (Khosla *et al.*, 1994; Rebstein *et al.*, 1997; Lim *et al.*, 2001). All oligonucleotides for PCR were generated by Alpha DNA (Montreal, PQ). All DNA

sequencing was performed by the Nucleic Acid and Protein Services (NAPS) unit (University of British Columbia, Vancouver, BC).

### **2.1.3 *Dictyostelium* Strains**

The strains generated during this study are listed in Table 1. The AX2 parental strain, used for the generation of AX2/*rasG*<sup>-</sup> mutant strains was obtained from Dr. Barry Coukell (York University, Toronto). The JH10 parental strain that was used to generate the JH10/*rasG*<sup>-</sup>, and *rasC*/*rasG*<sup>-</sup> mutant strains was obtained from Dr. Jeffrey Hadwiger (Oklahoma State University, Oklahoma). The JH10/*rasC*<sup>-</sup> strain was generated by Meenal Khosla in the Weeks laboratory (Khosla *et al.*, 2005).

### **2.1.4 Plasmids and DNA**

The following plasmids and DNA were generously provided by the indicated sources: pRHI119, pRHI125 and pRASG-G418 from Dr. Robert Insall (University of Birmingham, England); pJH60 from Dr. Jeffrey Hadwiger (Oklahoma State University, Oklahoma); *pga2*-CFP from Dr. Chris Janetopoulos and Dr. Peter Devereotes (John Hopkins University, Baltimore); pBS-*carA* from Dr. Peter Devereotes (John Hopkins University, Baltimore); pEMBL18-*csaA* from Dr. Chi-Hung Siu (University of Toronto, Toronto); and pcAR1-B18 from the Dicty Stock Center (Columbia University, New York). The following plasmids were donated by former members of the Weeks laboratory: pJLW14, pJLW26, and pJLW30 from Dr. Chinten James Lim; pRASG from Dr. Stephen Mark Robbins; pGEX-Byr2-RBD from Dr. Helmut Kae. All other plasmids were constructed during the course of this study. A full description of the plasmids is given in Table 2.

**Table 1. *Dictyostelium* strain description.**

<b>Strain</b>	<b>Description</b>	<b>Selection</b>
<i>AX2/rasG<sup>-</sup></i>	Chromosomal KO of <i>rasG</i> gene in AX2	10 µg/ml blasticidin S
<i>JH10/rasG<sup>-</sup></i>	Chromosomal KO of <i>rasG</i> gene in JH10	No thymidine
<i>rasC<sup>-</sup>/rasG<sup>-</sup></i>	Chromosomal KO of <i>rasC</i> gene in the <i>JH10/rasG</i> null strain	10 µg/ml blasticidin S
<i>rasC<sup>-</sup>/rasG<sup>-</sup>[/act15]:carA</i>	Ectopic over expression of the <i>carA</i> gene in the <i>rasC<sup>-</sup>/rasG<sup>-</sup></i> strain	10 µg/ml blasticidin S 10 µg/ml G418
<i>rasC<sup>-</sup>/[rasG]:rasG</i>	<i>rasC<sup>-</sup></i> transformed with pRASG-G418	10 µg/ml G418
<i>rasG<sup>-</sup>/[rasC]:rasC</i>	<i>rasG<sup>-</sup></i> transformed with pJLW30	10 µg/ml G418
<i>rasC<sup>-</sup>/[rasC]:rasG</i>	<i>rasC<sup>-</sup></i> transformed with pBM2	10 µg/ml G418
<i>rasG<sup>-</sup>/[rasG]:rasC</i>	<i>rasG<sup>-</sup></i> transformed with pBM1	10 µg/ml G418
<i>rasC<sup>-</sup>/[rasC]:RasG<sup>I24T</sup></i>	<i>rasC<sup>-</sup></i> transformed with pBMG1 encoding RasG <sup>I24T</sup>	10 µg/ml G418
<i>rasC<sup>-</sup>/[rasC]:RasG<sup>H27Q</sup></i>	<i>rasC<sup>-</sup></i> transformed with pBMG2 encoding RasG <sup>H27Q</sup>	10 µg/ml G418
<i>rasC<sup>-</sup>/[rasC]:RasG<sup>D30A</sup></i>	<i>rasC<sup>-</sup></i> transformed with pBMG3 encoding RasG <sup>D30A</sup>	10 µg/ml G418
<i>rasC<sup>-</sup>/[rasC]:RasG<sup>D38N</sup></i>	<i>rasC<sup>-</sup></i> transformed with pBMG4 encoding RasG <sup>D38N</sup>	10 µg/ml G418
<i>rasC<sup>-</sup>/[rasC]:RasG<sup>T50V</sup></i>	<i>rasC<sup>-</sup></i> transformed with pBMG5 encoding RasG <sup>T50V</sup>	10 µg/ml G418
<i>rasC<sup>-</sup>/[rasC]:RasG<sup>C51Y</sup></i>	<i>rasC<sup>-</sup></i> transformed with pBMG6 encoding RasG <sup>C51Y</sup>	10 µg/ml G418
<i>rasC<sup>-</sup>/[rasC]:RasG<sup>L52M</sup></i>	<i>rasC<sup>-</sup></i> transformed with pBMG7 encoding RasG <sup>L52M</sup>	10 µg/ml G418
<i>rasC<sup>-</sup>/[rasC]:RasG<sup>M72I</sup></i>	<i>rasC<sup>-</sup></i> transformed with pBMG8 encoding RasG <sup>M72I</sup>	10 µg/ml G418
<i>rasC<sup>-</sup>/[rasC]:RasG<sup>T74S</sup></i>	<i>rasC<sup>-</sup></i> transformed with pBMG9 encoding RasG <sup>T74S</sup>	10 µg/ml G418
<i>rasC<sup>-</sup>/[rasC]:RasC<sup>1-78</sup>+RasG<sup>79-190</sup></i>	<i>rasC<sup>-</sup></i> transformed with pBCSA encoding 1-78 aa of RasC + 79-190 of RasG	10 µg/ml G418
<i>rasC<sup>-</sup>/[rasC]:RasG<sup>1-78</sup>+RasC<sup>79-190</sup></i>	<i>rasC<sup>-</sup></i> transformed with pBCSB encoding 1-78 aa of RasG + 79-190 of RasC	10 µg/ml G418

**Table 2. Plasmid description.**

Plasmid	Description
pRHI119	pBS containing <i>bsr</i> selectable marker
pRHI125	pBS containing <i>rasG</i> genomic DNA minus ExonI
pRASG	pAT153 containing <i>rasG</i> genomic DNA
pRASG-G418	pAT153 containing <i>rasG</i> genomic DNA in G418 selection background
pJLW14	Plasmid containing <i>lacZ</i> gene under <i>rasC</i> promoter in G418 selection background
pJLW26	pBS containing both genomic and cDNA fragments of <i>rasC</i> flanking <i>bsr</i> selectable marker ( <i>rasC-bsr</i> disruption vector)
pJLW30	Plasmid containing <i>rasC</i> cDNA fragment under <i>rasC</i> promoter in G418 selection background
pcARI-B18	Plasmid containing <i>carA</i> cDNA under the control of constitutively active <i>actin 15</i> promoter and a neomycin-resistance cassette
pBS- <i>carA</i>	Plasmid containing <i>carA</i> cDNA
<i>pga2</i> -CFP	Plasmid containing <i>gpaB</i> cDNA
pEMBL18- <i>csaA</i>	Plasmid containing <i>csaA</i> cDNA
pGEX-Byr2-RBD	Plasmid encoding GST-Byr2-Ras Binding Domain
pJH60	Plasmid containing <i>thyl</i> gene
pGEM- <i>rasG</i>	<i>rasG</i> cDNA cloned into pGEM-T Easy
pGEM- <i>rasC</i>	<i>rasC</i> cDNA cloned into pGEM-T Easy
pBW1	<i>Bam</i> HI fragment of pRHI119 containing <i>bsr</i> selectable marker cloned into <i>Bgl</i> II site of <i>rasG</i> promoter in pRASG ( <i>rasG-bsr</i> disruption vector)
pBW2	<i>Bam</i> HI fragment of pJH60 containing <i>thyl</i> gene cloned into <i>Bgl</i> II site of <i>rasG</i> promoter in pRHI125 ( <i>rasG-thyl</i> disruption vector)
pBM1	<i>Bgl</i> II- <i>Xho</i> I fragment of <i>rasC</i> cDNA cloned into <i>Bgl</i> II- <i>Xho</i> I of pRASG-G418
pBM2	<i>Bam</i> HI- <i>Sal</i> I fragment of <i>rasG</i> cDNA cloned into <i>Bgl</i> II- <i>Xho</i> I of pJLW14
pGEM-MG1	Modified <i>rasG</i> cDNA carrying I24T mutation in pGEM-T Easy plasmid
pGEM-MG2	Modified <i>rasG</i> cDNA carrying H27Q mutation in pGEM-T Easy plasmid
pGEM-MG3	Modified <i>rasG</i> cDNA carrying D30A mutation in pGEM-T Easy plasmid
pGEM-MG4	Modified <i>rasG</i> cDNA carrying D38N mutation in pGEM-T Easy plasmid
pGEM-MG5	Modified <i>rasG</i> cDNA carrying T50V mutation in pGEM-T Easy plasmid
pGEM-MG6	Modified <i>rasG</i> cDNA carrying C51Y mutation in pGEM-T Easy plasmid
pGEM-MG7	Modified <i>rasG</i> cDNA carrying L52M mutation in pGEM-T Easy plasmid
pGEM-MG8	Modified <i>rasG</i> cDNA carrying M72I mutation in pGEM-T Easy plasmid
pGEM-MG9	Modified <i>rasG</i> cDNA carrying T74S mutation in pGEM-T Easy plasmid
pBMG1	<i>Bam</i> HI- <i>Sal</i> I fragment of pGEM-MG1 carrying I24T of <i>rasG</i> cDNA cloned into <i>Bgl</i> II- <i>Xho</i> I of pJLW14
pBMG2	<i>Bam</i> HI- <i>Sal</i> I fragment of pGEM-MG2 carrying H27Q of <i>rasG</i> cDNA cloned into <i>Bgl</i> II- <i>Xho</i> I of pJLW14
pBMG3	<i>Bam</i> HI- <i>Sal</i> I fragment of pGEM-MG3 carrying D30A of <i>rasG</i> cDNA cloned into <i>Bgl</i> II- <i>Xho</i> I of pJLW14
pBMG4	<i>Bam</i> HI- <i>Sal</i> I fragment of pGEM-MG4 carrying D38N of <i>rasG</i> cDNA cloned into <i>Bgl</i> II- <i>Xho</i> I of pJLW14
pBMG5	<i>Bam</i> HI- <i>Sal</i> I fragment of pGEM-MG5 carrying T50V of <i>rasG</i> cDNA cloned into <i>Bgl</i> II- <i>Xho</i> I of pJLW14
pBMG6	<i>Bam</i> HI- <i>Sal</i> I fragment of pGEM-MG6 carrying C51Y of <i>rasG</i> cDNA cloned into <i>Bgl</i> II- <i>Xho</i> I of pJLW14
pBMG7	<i>Bam</i> HI- <i>Sal</i> I fragment of pGEM-MG7 carrying L52M of <i>rasG</i> cDNA cloned into <i>Bgl</i> II- <i>Xho</i> I of pJLW14

<b>Plasmid</b>	<b>Description</b>
pBMG8	<i>Bam</i> HI- <i>Sal</i> I fragment of pGEM-MG8 carrying M72I of <i>rasG</i> cDNA cloned into <i>Bgl</i> II- <i>Xho</i> I of pJLW14
pBMG9	<i>Bam</i> HI- <i>Sal</i> I fragment of pGEM-MG9 carrying T74S of <i>rasG</i> cDNA cloned into <i>Bgl</i> II- <i>Xho</i> I of pJLW14
pGEM-CSA	Chimeric construct of 1-78 aa of RasC + 79-190 of RasG cloned in pGEM-T Easy plasmid
pGEM-CSB	Chimeric construct: 1-78 aa of RasG + 79-190 of RasC cloned in pGEM-T Easy plasmid
pBCSA	<i>Bgl</i> II- <i>Sal</i> I fragment of pGEM-CSA cloned into <i>Bgl</i> II- <i>Xho</i> I of pJLW14
pBCSB	<i>Bam</i> HI- <i>Xho</i> I fragment of pGEM-CSB cloned into <i>Bgl</i> II- <i>Xho</i> I of pJLW14

## 2.2 Methods

### 2.2.1 Plasmid construction

The primers PBRG10-F and PBRG8-R (Table 3) were used in a PCR procedure to add a *Bam*HI site prior to ATG start codon and a *Sal*I site after the termination codon of *rasG* cDNA in pBS-*rasG*. The primers PBRC3-F and PBRC3-R were used in a PCR procedure to add a *Bgl*II site prior to ATG start codon and a *Xho*I site after the termination codon of *rasC* cDNA in pBS-*rasC*. The PCR amplified fragments were then ligated into pGEM-T Easy to generate pGEM-*rasG* and pGEM-*rasC* respectively. pBW1, the *rasG* knockout vector, was constructed by inserting a *Bam*HI fragment of pRHI119 containing the *bsr* selectable marker into *Bgl*II site of *rasG* in pRASG (Robbins et al., 1992). pBW2, the *rasG* disruption vector, was constructed by inserting a *Bam*HI fragment of pJH60 containing *thy1* gene into *Bgl*II site of *rasG* in pRHI125. pBM1 and pBM2 were constructed by ligating the *Bgl*II-*Xho*I excised fragment of *rasC* cDNA from pGEM-*rasC* into *Bgl*II-*Xho*I of pRasG-G418 and *Bam*HI-*Sal*I excised fragment of *rasG* cDNA from pGEM-*rasG* into *Bgl*II-*Xho*I of pJLW14 respectively. The construction of pGEM-MG1-9, pBMG1-9, pGEM-CSA, pGEM-CSB, pBCSA and pBCSB are described in section 2.2.3.

### 2.2.2 DNA amplification

DNA amplification was employed to generate DNA fragments for plasmid construction, to generate probes for Southern and Northern blot analysis, to perform site directed mutagenesis, to generate chimeric constructs, and for gene disruption screening. Reactions were performed using either an Idaho RapidCycler (Idaho Technologies, Idaho

Falls, ID) or Whatman Biometra Tgradient Thermocycler (Goettingen, Germany). The sequence and description of the oligonucleotide primers used are shown in Table 3 and 4.

**(a) Standard amplification**

Standard amplification reactions were performed in 10  $\mu$ l reaction volumes in glass capillary tubes containing 5.38  $\mu$ l ddH<sub>2</sub>O (distilled, deionized water), 1  $\mu$ l 10X Idaho PCR buffer (500 mM Tris-Cl, pH 8.3, 2.5 mg/ml BSA, 20% (w/v) sucrose, 1 mM cresol red, 30 mM MgCl<sub>2</sub>), 0.5  $\mu$ l 2.5 mM dNTPs (Invitrogen, Carlsbad, CA), 1  $\mu$ l of each 2.5  $\mu$ M oligonucleotide primers, 1  $\mu$ l DNA template and 0.12  $\mu$ l of 5 U/ $\mu$ l *Taq* DNA Polymerase (Invitrogen, Carlsbad, CA). The cycling parameters were as follows: 2 cycles of 92 °C for 90 s, 55 °C for 10 s, and 72 °C for 120 s; 35 cycles of 91 °C for 7 s, 50-55 °C for 7 s, and 72 °C for  $x$  s and then held at 72 °C for 180 s. The annealing temperature was optimized for each particular set of primers, and the extension time ( $x$ ) was 60 s for every 1000 bp of amplification target.

**(b) Mutagenesis**

Reactions were performed in 50  $\mu$ l reaction volumes in PCR tubes containing 5  $\mu$ l 10X *Pfu Turbo* buffer (Stratagene, La Jolla, CA), 1  $\mu$ l 25 mM dNTPs (Invitrogen, Carlsbad, CA), 5  $\mu$ l of each 2.5  $\mu$ M forward (MG1-9-F) and reverse oligonucleotide primers (MG1-9-R), 5  $\mu$ l *rasG* cDNA template in pGEM-T Easy vector (50 ng/ $\mu$ l), 1  $\mu$ l *Pfu Turbo* DNA Polymerase 2.5 U/ $\mu$ l (Stratagene, La Jolla, CA) and ddH<sub>2</sub>O to total of 50  $\mu$ l. The cycling parameters were as follows: 1 cycle of 95 °C for 30 s followed by 16 cycles of 95 °C for 30 s, 55 °C for 60 s, and 68 °C for  $x$  min (2 min per kb) and then held at 4 °C.

**Table 3: Sequence and description of oligonucleotides primers used.**

F: Forward primer R: Reverse primer

<b>Oligo</b>	<b>Sequence</b>	<b>Brief description of nucleotide changes:</b>
PBRG9-F:	5'CCGCATTTTTTGGCA TTC GC3'	Forward primer for <i>rasG</i> , promoter PCR, in combination with PBRG5-R used for KO screening.
PBRG5-R:	5'TGGTTAAGGCACTTT TAC CG3'	Reverse primer for <i>rasG</i> , exonI, used for KO screening.
PBRC2-F:	PBRC2-F: 5'ATTGCTGAATATGAT CCA AC3'	Forward primer for <i>rasC</i> , 3 bp in ExonI and the rest overlaps IntronI, in combination with PBRC2-R used for KO screening.
PBRC2-R:	5'AAAAAAAAATAATAA ATG AATGC3'	Reverse primer for <i>rasC</i> , Intron II, used for KO screening.
PBbsr2-F:	5'CAGGAGAAATCATTT CGGC3'	Forward primer for <i>bsr</i> cDNA PCR
PBbsr1-R:	5'TACCACAAGGACTTACCA CTCG3'	Reverse primer for <i>bsr</i> cDNA PCR
PBRG3-R:	5'CTAATTTACTCTCTAAAAT G3'	Reverse primer for <i>rasG</i> genomic, 3' untranslated region. Around 100bp after the stop codon.
PBRG10-F	5'ggatccttATGACAGAA TACAAATTAGTTATTGTT GGT3'	Forward primer for <i>rasG</i> cDNA PCR. <i>Bam</i> HI linker at 5' site added.
PBRG8-R	5'gtcgacTTATAAAAGAGT ACAAGCTTTTAATGGTC3'	Reverse primer for <i>rasG</i> cDNA PCR. <i>Sal</i> I site at 3' end after the stop codon added.
PBRG78-F	5'TTCCTTTGTGTCTACTCTA TCACTTC3'	Forward primer for <i>rasG</i> cDNA PCR.
PBRC3-F	5'agatctATGTCAAAATTA TTAATAATTAGTTATCG3'	Forward primer for <i>rasC</i> cDNA PCR. <i>Bg</i> II linker at 5' site before ATG start added.
PBRC3-R	5'ctcgagTTACAATATAAT ACATCCCCTTTT C3'	Reverse primer for <i>rasC</i> cDNA PCR. <i>xho</i> I site after the stop codon added.
PBRC79-F	5'TTTTTAATTGTTTACAGTA TTATATC3'	Forward primer for <i>rasC</i> cDNA PCR.
PBRC78-R+G overhang	5'gtagacacaaggaaTCCTCTACC TGATCTAATATATTG3'	Reverse primer for <i>rasC</i> cDNA PCR plus 15 nucleotides from <i>rasG</i> cDNA .
PBRG77-R+C overhang	5'gtaacaattaaaaACCTTGACC AGTTTCATATATTGG3'	Reverse primer for <i>rasG</i> cDNA PCR plus 15 nucleotides from <i>rasG</i> cDNA .
PBcar1-F2:	5'AGTTTTGCATGTTGGTTGT GGAC3'	Forward primer for <i>carA</i> cDNA PCR
PBcar1-R2:	5'CATTGCACATCATCACCA GTTGG3'	Reverse primer for <i>carA</i> cDNA PCR
PBga2-F1	5'ATGGGTATTTGTGCATCA TC3'	Forward primer for <i>gpaB</i> cDNA PCR

<b>Oligo</b>	<b>Sequence</b>	<b>Brief description of nucleotide changes:</b>
PB $\alpha$ 2-R1	5'TTAAGAATATAAACCAGC TTTC3'	Reverse primer for <i>gpaB</i> cDNA PCR
PBgp80-F2:	5'CCTCGTGCCAAATACAAT CG3'	Forward primer for <i>csaA</i> cDNA PCR
PBgp80-R2:	5'CTGATGAAGGTGCTTCAG TTTCTTC3'	Reverse primer for <i>csaA</i> cDNA PCR

**Table 4: Sequence and description of oligonucleotides used for the site directed mutagenesis on *rasG* cDNA.**

Primer position: is the nucleotide number from the 5' of *rasG* cDNA

<b>Oligo</b>	<b>Sequence</b>	<b>Brief description of nucleotide changes:</b>
MG1-F:	5'CTTAACCATTCAATTAaccCAA AACCATTTTCATTG3'	ATC to acc. I toT (ile to thr) Primer position: 54-88 (35mer) Changed amino acid # 24
MG1-R:	5'CAATGAAATGGTTTTGggtTAATTGAAT GGTTAAG 3'	
MG2-F:	5'CAATTAATCCAAAACcaaTTCATTGATG AATACG 3'	CAT to caa. H to Q (his to gln) Primer position: 64-97 (34mer) Changed amino acid # 27
MG2-R:	5'CGTATTCATCAATGAAttgGTTTTGGATT AATTG 3'	
MG3-F:	5'CAAAACCATTTCATTgetGAATACGATCC AACTATC 3'	GAT to gct. D to A (asp to ala) Primer position: 73-108 (36mer) Changed amino acid # 30
MG3-R:	5'GATAGTTGGATCGTATTCagcaATGAAA TGGTTTTG 3'	
MG4-F:	5'CGATCCAACACTATCGAAaatTCATACAGA AAACAAG 3'	GAT to aat. D to N (asp to asn) Primer position: 96-130 (36mer) Changed amino acid # 38
MG4-R:	5'CTTGTTTTCTGTATGAattTCGATAGTT GGATCG 3'	
MG5-F:	5'CATTGATGAAGAAggtTGTTTATTAGATA TTTTAG 3'	ACT to gtt. T to V (thr to val) Primer position: 135-169 (35mer) Changed amino acid # 50
MG5-R:	5'CTAAAATATCTAATAAACaaacTTCTTC ATCAATG 3'	
MG6-F:	5'CATTGATGAAGAAACTtatTTATTAGATA TTTTAG 3'	TGT to tat. C to Y (cys to tyr) Primer position: 135-169 (35mer) Changed amino acid # 51
MG6-R:	5'CTAAAATATCTAATAAataAGTTTCTTCA TCAATG 3'	
MG7-F:	5'GATGAAGAACTTGTatgTTAGATATTTT AGATACTG 3'	TTA to atg. L to M (leu to met) Primer position: 139-175 (37mer) Changed amino acid # 52
MG7-R:	5'CAGTATCTAAAATATCTAAacatACAAGT TTCTTCATC 3'	
MG8-F:	5'CAATGAGAGACCAATATattAGAACTGG TCAAGG 3'	ATG to att. M to I (met to ile) Primer position: 197-230 (34mer) Changed amino acid # 72
MG8-R:	5'CCTTGACCAGTTCTaatATATTGGTCTCT CATTG 3'	
MG9-F:	5'GACCAATATATGAGAagtGGTCAAGGTT TCCTTTG 3'	ACT to agt. T to S (thr to ser) Primer position: 205-239 (35mer) Changed amino acid # 74
MG9-R:	5'CAAAGGAAACCTTGACCactTCTCATAT ATTGGTC 3'	

The extension products were ethanol precipitated and dissolved in 20  $\mu$ l TE (10 mM Tris-Cl, pH 8.0, 0.1 mM EDTA). The DNA was digested initially with 1.5  $\mu$ l DpnI of 5 U/ $\mu$ l (Invitrogen, Carlsbad, CA) for 1 h, after which 1  $\mu$ l of additional DpnI was added and the DNA further digested for 1 hour to ensure the complete removal of the original plasmid DNA. 5  $\mu$ l of the amplified products were transformed into *E. coli* strain XL1-MRF'. Positive transformants were confirmed by sequencing.

**(c) Gene disruption screening by amplification**

To prepare templates for amplification, cells were lysed in 10 mM Tris-Cl, pH 8.0, 1 mM EDTA, 0.3% Tween-20, 60  $\mu$ g/ml proteinase K, and the lysates were incubated for 1 h at 56 °C. The lysates were then boiled for 10 min, and 1  $\mu$ l of the crude cell lysate was used as template in a 10  $\mu$ l reaction in a glass capillary tube using a Idaho RapidCycler (Idaho Technologies, Idaho Falls, ID), as described for the standard reaction. Amplification was conducted using appropriate primers (Table 3) with the following cycling parameters: 2 cycles of 92 °C for 90 s, 50 °C for 10 s, and 72 °C for 120 s; followed by 35 cycles of 91 °C for 7 s, 50 °C for 7 s, and 72 °C for 60 s; and then held at 72 °C for 180 s.

**2.2.3 Generation of mutated constructs**

Site directed mutants of *rasG* were created using pGEM-*rasG* as the template and the oligonucleotide pairs MG1-9-F and MG1-9-R (Table 4) in accordance to the Stratagene PfuTurbo DNA polymerase-based protocol, as described in the mutagenesis section. pBMG1-9 expression plasmids were generated by ligating the *Bam*HI-*Sal*I excised fragment of pGEM-MG1-9 into *Bgl*III-*Xho*I of pJLW14.

RasG was also modified by two block switches of sequence with RasC. This was accomplished by ligating DNA coding the first 78 amino acids of RasC to DNA encoding amino acids 79-190 of RasG (CSA). In addition a chimeric construct encoding amino acids 1-78 of RasG and 79-190 of RasC was generated (CSB). In more detail, to generate pBCSA and pBCSB chimeric constructs, the following strategy was employed. The primers PBRC3-F and PBRC78-R+G overhang, PBRC79-F and PBRC3-R were used to generate two amplified products of C1 (nt 1-234) and C2 (nt 235-570) from *rasC* cDNA as template. The primers PBRG10-F and PBRG77-R+C overhang, PBRG78-F and PBRG8-R were used to generate 2 amplified PCR products of G1 (nt 1-231) and G2 (nt 232-570) from *rasG* cDNA as template. The 50  $\mu$ l reactions were performed in PCR tubes using the standard PCR protocol except that *Pfu Turbo* DNA polymerase was used instead of *Taq* DNA polymerase to prevent the A-tailing, which would have prevented the proper subsequent cloning. After completion, the amplified products were gel purified, and subjected to a second round of standard amplification. Reactions were performed in 40  $\mu$ l mixtures in PCR tubes containing, 5  $\mu$ l 10X *Pfu Turbo* buffer, 2.5  $\mu$ l 2.5 mM dNTPs, 1  $\mu$ l *Pfu Turbo* DNA Polymerase 2.5 U/ $\mu$ l, 200 ng of each gel purified and amplified DNA (C1 and G2) or (G1 and C2), and ddH<sub>2</sub>O to 40  $\mu$ l. The procedure was interrupted after 10 cycles to add 5  $\mu$ l each of the PBRC3-F and PBRG8-R primers or the PBRG10-F and PBRC3-R primers respectively. The resulting products, CSA (C1+G2) and CSB (G1+C2), were gel purified and then subjected to standard amplification using *Taq* DNA polymerase and the PBRC3-F and PBRG8-R primers or the PBRG10-F and PBRC3-R primers respectively. The PCR amplified products were gel purified and cloned by T/A ligation into the pGEM-T Easy vector (Promega,

Madison, WI) to generate pGEM-CSA and pGEM-CSB. pBCSA and pBCSB were generated by ligating *Bgl*II-*Sal*I fragment of pGEM-CSA and *Bam*HI-*Xho*I fragment of pGEM-CSB into *Bgl*II-*Xho*I of pJLW14 expression plasmid.

#### 2.2.4 Generation of null mutant strains

The AX2/*rasG*<sup>-</sup> strain was generated as described previously (Tuxworth *et al.*, 1997). 270 blasticidin S-resistant transformants were screened by PCR, which yielded three Ax2/*rasG*<sup>-</sup> isolates. To generate *rasG*<sup>-</sup> mutants in the JH10 strain background, a *rasG-thy1* disruption vector was constructed by inserting the *Bam*HI fragment of plasmid pJH60, containing the *thy1* gene (Hadwiger and Firtel, 1992), into the single *Bgl*II site in the *rasG* promoter in plasmid pRHI125, which contains only the promoter and exon II of *rasG* (R. H. Insall, personal communication). The first *rasG* exon was not present in this construct in an attempt to generate a more stable null strain and make PCR screening of the gene disrupted strains easier. Transformants were selected in the absence of thymidine and screened by using PBRG9-F and PBRG5-R primer sets. From 280 screened clones, three JH10/*rasG*<sup>-</sup> cell lines were isolated. Southern blot analysis confirmed each of the presumptive gene disruptions and indicated that each was the result of a single insertion into the genome. Construction of the AX2/*rasC*<sup>-</sup> and JH10/*rasC*<sup>-</sup> strains has been described previously (Lim *et al.*, 2001; Khosla *et al.*, 2005). To make a *rasC/rasG*<sup>-</sup> double-disruption strain, the *rasC* disruption vector pJLW26, carrying the blasticidin-resistance (*bsr*) selectable marker (Lim *et al.*, 2001), was transformed into JH10/*rasG*<sup>-</sup> cells. The second *rasC* intron is not present in this construct, which also provided the opportunity for easier screening. The blasticidin-resistant clones were screened using PBRC2-F and PBRC2-R primer sets. From 700 clones screened, two

*rasC/rasG* cell lines were isolated. *rasG/rasG* rescued strains were generated by transforming the *rasG*-containing plasmid, pRASG-G418, into the *rasG* strain as previously described (Tuxworth *et al.*, 1997). *rasC/rasG/rasC/rasG* rescued strains were created by cotransforming the plasmids, pRASG-G418 and pJLW30 (Tuxworth *et al.*, 1997; Lim *et al.*, 2001) into the double-disruption strain.

For all transformations, 20 µg of the appropriate vector were cleaved with restriction enzymes and electroporated into *Dictyostelium* cells as previously described (Alibaud *et al.*, 2003). Clones containing the selectable marker were isolated 8-15 days following the application of the selection conditions and growth in plastic dishes. These clonal isolates were plaque purified on a bacterial lawn and screened for single or double gene disruptions using *rasG* or *rasC* specific primers as described.

To generate the *rasC/rasG/[act15]:carA* strain, 20 µg of the pcAR1-B18 expression vector, which contains *carA* cDNA under the control of constitutively active *actin 15* promoter and a neomycin-resistance cassette (Johnson *et al.*, 1991) was electroporated into *rasC/rasG* cells as previously described (Alibaud *et al.*, 2003). Clones containing the selectable marker were isolated 8-15 days following the application of the selection conditions and maintained in HL5 media supplemented with 10 µg/ml G418 (Invitrogen, Carlsbad, CA).

### **2.2.5 Growth of *Dictyostelium discoideum***

Strain Ax2 was grown at 22 °C in HL5 medium (14.3 g peptone, 7.15 g yeast extract, 15.4 g glucose, 0.96 g Na<sub>2</sub>HPO<sub>4</sub>·7H<sub>2</sub>O and 0.486 g KH<sub>2</sub>PO<sub>4</sub> per liter of water), supplemented with 50 µg/ml streptomycin sulfate (Sigma, St. Louis, MO) in Nunclon tissue culture dishes (Nunc, Rochester, NY), or in suspension in flasks shaken at 160 rpm

(Watts and Ashworth, 1970). Strain JH10 was grown in HL5 medium supplemented with 100  $\mu\text{g/ml}$  thymidine (Sigma). The JH10/*rasG*<sup>-</sup> cells were grown in HL5 medium without supplement, while JH10/*rasC*<sup>-</sup>/*rasG*<sup>-</sup> cells were grown in HL5 media supplemented with 10  $\mu\text{g/ml}$  blasticidin S (Calbiochem, San Diego, CA). The JH10/*rasG*<sup>-</sup>/*[rasG]:rasG* rescue and the *rasC*<sup>-</sup>/*rasG*<sup>-</sup>/*[act15]:carA* cells were grown in HL5 medium supplemented with 10  $\mu\text{g/ml}$  G418 (Invitrogen, Carlsbad, CA). All cells were maintained on tissue culture dishes, and passaged by scraping confluent plates ( $\sim 2 \times 10^6$  cells/ml) and diluting between 50-100 fold into fresh HL5 on tissue culture plates. For cryopreservation,  $\sim 1 \times 10^8$  cells were frozen in 1.0 ml aliquots of HL5 supplemented with 10% DMSO (Fisher Scientific, Fair Lawn, NJ). All cells were maintained for no more than 6 passages before recovering fresh samples from cryopreserved stocks. For quantitative growth, cells were seeded at an initial density of  $10^5$  cells/ml in flasks of HL5 and cell numbers at various time points was determined in shaken cell suspension by cell counting using a haemocytometer. For plaque purification, *Dictyostelium* cells were diluted and plated (20-30 cells/plate) in association with *Klebsiella oxytoca* on SM agar plates (Sussman, 1987).

### 2.2.6 cAMP pulsing

To obtain cAMP-pulsed cells, vegetative cells were harvested by centrifugation (500 x g, 5 min), washed twice in KK2 (20 mM potassium phosphate, pH 6.1), and resuspended in KK2 to a final density of  $5 \times 10^6$  cells/ml. 30 ml of this cell suspension was shaken at 150 rpm for 1 h and then pulsed with 100  $\mu\text{l}$  of cAMP to a final concentration of 50 nM every 6 min for 5 h, using a Polystaltic pump (Buchler, Fort Lee, NJ) and a Lab Controller timer (VWR, Mississauga, ON). After pulsing, cells were

harvested by centrifugation (500 x g, 5 min), washed two times with KK<sub>2</sub>, and resuspended in KK<sub>2</sub> at appropriate cell density depending on the experiment. For some experiments, the cAMP pulsing was for 8 h.

### **2.2.7 Multicellular development**

To observe multicellular development, vegetative or cAMP-pulsed cells were washed twice in Bonner's salts (10 mM NaCl, 10 mM KCl, 2 mM CaCl<sub>2</sub>), and plated on nitrocellulose filters (Millipore, Bedford, MA) supported by KK<sub>2</sub>-saturated pads and incubated in a moist container at 22 °C. Multicellular development was also observed on bacterial growth plates. To observe aggregation streaming, vegetative or 5 h cAMP-pulsed cells were washed twice in Bonner's salts, seeded at  $\sim 4 \times 10^5$  cells/cm<sup>2</sup> in Nunc tissue-culture dishes submerged under Bonner's salts, and incubated at 22 °C.

### **2.2.8 Nuclear staining**

To determine nuclear number, cells were grown in shake suspension in HL5 for five days.  $3 \times 10^3$  cells/cm<sup>2</sup> were allowed to adhere to glass coverslips for 30 minutes and then washed 3 times with KK<sub>2</sub>. The cells were fixed with 3.7% formaldehyde for 10 minutes and the fixed cells were washed a further 3 times with KK<sub>2</sub>. Cells were then permeabilised with -20 °C acetone, dried, rehydrated with KK<sub>2</sub> and then nuclei stained with 1 μM 4,6-diamidino-2-phenylindole (DAPI, Sigma). Stained cells were washed three times with PBS, air-dried and mounted on glass slides with 50% glycerol. Epifluorescence images of random fields of view were captured using an Olympus IX-70 inverted microscope, a DAGE-MTI CCD-100 camera (Michigan City, IN), and Scion (Frederick, MD) Image 4.0 software. The average number of nuclei per cell was obtained by counting 300-390 cells.

### 2.2.9 F-actin staining

For visualization of F-actin distribution *in situ*, cells were grown in HL5 media in Nunc tissue culture dishes,  $2 \times 10^3$  cells/cm<sup>2</sup> reseeded onto glass coverslips and allowed to adhere for 3 hours. The cells were then fixed and permeabilized with 1% glutaraldehyde, 0.1% Triton X-100 in PBS for 10 minutes. Fixed cells were rinsed three times in PBS and autofluorescence quenched with 1 mg/ml NaBH<sub>4</sub> for 10 minutes. Following three further rinses in PBS, the cells were stained with 0.1 µg/ml fluorescein isothiocyanate (FITC) phalloidin conjugate (Sigma) for 1 hour. The coverslips were then rinsed in PBS, air-dried and mounted onto slides with or without the addition of Prolong antifade (Molecular Probes). Epifluorescent images were taken on a Zeiss Axiovert microscope.

### 2.2.10 Chemotaxis assays

To determine chemotaxis to cAMP, cells were pulsed with cAMP as described above, washed twice with Bonner's salts, and then seeded in Nunc tissue-culture dishes at a cell density of  $\sim 5 \times 10^5$  cell/cm<sup>2</sup> in Bonner's salts. At  $t=0$ , an Eppendorf Femtotip Micropipet (Hamburg, Germany) filled with 100 µM cAMP was placed in the field of view, and cell movements toward the Micropipet were monitored by time-lapse video microscopy and recorded at the rate of 2 frames per minutes (30 s intervals) using an Olympus IX-70 inverted microscope, a DAGE-MTI CCD-100 camera (Michigan City, IN), and Scion (Frederick, MD) Image 4.0 software. The cell movement was followed for a total of 90 frames. Instantaneous velocities and chemotaxis indices were determined as described previously (Wessels *et al.*, 2004). The images were analyzed by *Openlab* software (Improvision, Coventry, England). Motility parameters were

computed from the centroid position of each cell. To measure the instantaneous velocity ( $\mu\text{m}/\text{min}$ ) of a cell in frame  $n$ , a line was drawn from the centroid in frame  $n-1$  to the centroid in frame  $n+1$  and the length of that line was divided by twice the time interval between frames. Chemotaxis index was calculated as the net distance traveled towards the source of chemoattractant divided by the total distance traveled in that time period.

Chemotaxis to folate, was determined using a previously described protocol (Palmieri *et al.*, 2000). Cells were cultivated in HL5 media on Nunc tissue culture dishes to a density of  $\sim 4 \times 10^5$  cells/cm<sup>2</sup>. The cells were then rinsed once and submerged in 20% HL5. At  $t=0$ , an Eppendorf Femtotip Micropipet (Hamburg, Germany) filled with 25 mM folate was positioned in the field of view and cell movements monitored by time-lapse microscopy as described above.

### **2.2.11 Western blot analysis**

Protein samples were prepared by pelleting cells by centrifugation (500 x g, 5 min). For some experiments cells were resuspended in KK2 and lysed by mixing with 6X SDS-PAGE loading buffer (350 mM Tris-Cl, pH 6.8, 10% SDS, 600 mM DTT, 0.012% w/v bromophenol blue, 30% glycerol) in a volume ratio of 5:1. For other experiments cells were lysed directly by resuspending in SDS-PAGE loading buffer. Samples then were boiled at 100 °C for 5 min and used for discontinuous SDS-PAGE or stored at -85 °C (Sambrook, 1989).

Proteins were separated by discontinuous SDS-PAGE gels, consisting of an upper protein stacking gel (3.9% bis-acrylamide (1:19), 125 mM Tris-Cl, pH 6.8, 0.1% SDS, 0.03% ammonium persulfate, 0.1% TEMED) and a lower protein resolving gel (10% bis-acrylamide (1:19), 375 mM Tris-Cl, pH 8.8, 0.1% SDS, 0.03% ammonium persulfate,

0.07% TEMED). Samples were electrophoresed at 100 V for 100 min. The electrophoresis buffer was 25 mM Tris-Cl, 192 mM glycine, 0.1% SDS, pH 8.3. Separated proteins were blotted onto Hybond P PVDF membranes (Amersham, Buckinghamshire, England), using a Mini Protean II electroblot apparatus (Bio-Rad) at 0.2 A for 68 min submerged in ice-cold transfer buffer (25 mM Tris, 192 mM glycine, 20% methanol). To determine if proteins were equally loaded, the gels were stained with Coomassie blue solution (0.025% w/v Coomassie G-250, 10% v/v acetic acid).

After transfer, the membranes were incubated for 1 h at 22 °C with gentle agitation, in blocking buffer consisting of 5 % w/v milk (non-fat dried powder) in TBS-T (50 mM Tris-Cl, pH 7.4, 154 mM NaCl, 0.1% Tween20), and then incubated with anti-Ras specific primary antibodies in 1 % w/v non-fat milk powder/TBS-T overnight at 22 °C on a rotary shaker. Membranes were washed 3 times for 5 min each with TBS-T and incubated with horse radish peroxidase (HRP) conjugated goat anti-rabbit secondary antibody (GE Healthcare) at 1:5000 dilution in 1% w/v milk/TBS-T for 1 h at 22°C on a rotary shaker. Membranes were washed 3 times for 5 min each with TBS-T, detected by enhanced chemiluminescence (ECL, Amersham) according to manufacturer's instructions and exposed to X-OMAT XB-1 X-ray film (Eastman Kodak Company, Rochester, NY) for an appropriate amount of time to visualize the signal.

#### **2.2.12 PKB phosphorylation assays**

PKB phosphorylation was determined as described previously (Lim *et al.*, 2001). Briefly, cAMP-pulsed cells were washed twice in KK2, resuspended to  $5 \times 10^7$  cells/ml in KK2, and then stimulated with cAMP at a final concentration of 100 nM. Aliquots of 100  $\mu$ l were removed at intervals, before and after stimulation, and mixed with 20  $\mu$ l of

6X SDS-PAGE loading buffer. 10 µg of protein were fractionated by SDS-PAGE and then subjected to Western-blot analysis using a phosphothreonine-specific antibody (Cat#9381, Cell Signaling Technologies, Danvers, MA).

Equal sample loading was verified by staining a duplicate gel with Coomassie Blue. To assess equal PKB expression levels in all strains, Western blots were also analyzed using a *Dictyostelium* PKB-specific antibody (a gift from F. Jiang and R. Dottin).

### **2.2.13 Northern blot analyses**

*Dictyostelium* cells were pulsed with cAMP, as described above, and at various intervals total RNA was extracted from  $2 \times 10^7$  cells using guanidinium isothiocyanate (Invitrogen, Carlsbad, CA) (Chomczynski and Sacchi, 1987). Briefly, pelleted cells were lysed in solution containing 6M guanidinium isothiocyanate, 10% sarcosyl, 0.75 M sodium citrate, pH 7.0, and 0.7% BME (2-Mercaptoethanol, Sigma), mixed with 100 µl sodium acetate, pH 4.0, 1.2 ml phenol/chloroform (50:50) and incubated on ice for 15 min. The phases were then separated by centrifugation at 4000 rpm for 10 min. The upper aqueous phase was mixed with 1 volume isopropanol, incubated for 1 h at -20 °C and centrifuged at 8000 rpm for 20 min. The pelleted RNA was resuspended again in 6 M guanidinium isothiocyanate, 10% sarcosyl, 0.75 M sodium citrate, pH 7.0, 0.7% BME and reprecipitated with 1 volume of isopropanol. The RNA pellet was further washed with 1.0 ml 75% ethanol, air dried briefly, dissolved in DEPC-treated ddH<sub>2</sub>O by vortexing and heating in 42 °C water bath and quantitated by absorbance spectrophotometry at 260 nm. 15 µg aliquots were size-fractionated on 1.25% agarose-formaldehyde gels. The gels were blotted onto Hybond-N+ membrane (Amersham) and

hybridized with radioactive probes labeled with [ $\alpha$ - $^{32}$ P]dCTP by the random primer method as described previously (Sambrook, 1989). Probes were derived from PCR amplified fragments of plasmid templates that had been first gel purified using the QIAquick Gel Extraction Kit (Qiagen). Descriptions of the various probes used in this thesis are summarized in Table 5. Equal loading of samples was verified by intensity of ribosomal RNA stained with ethidium bromide.

**Table 5. Description of probes used for blot hybridization analysis.**

<b>Probe</b>	<b>Description</b>	<b>Size (kbp)</b>	<b>Source</b>	<b>PCR primers</b>
<i>rasG</i>	Full length cDNA	0.6	pGEM- <i>rasG</i>	PBRG10-F, PBRG8-R
<i>bsr</i>	Partial cDNA	0.2	PCR-pRHI119	PBbsr2-F, PBbsr1-R
<i>carA</i>	Partial cDNA	0.7	pBS- <i>carA</i>	PBcar1-F2, PBcar1-R2
<i>gpaB</i>	Full length cDNA	1.1	pga2-CFP	PBga2-F1, PBga2-R1
<i>csaA</i>	Full length cDNA	1.0	pEMBL18- <i>csaA</i>	PBgp80-F2, PBgp80-R2

#### 2.2.14 Southern blot analyses

To isolate genomic DNA,  $2 \times 10^7$  *Dictyostelium* cells grown in HL5 were washed in KK2 and resuspended in 1.0 ml solution containing 40 mM Tris-Cl pH 7.8, 1.5% sucrose, 0.1 mM EDTA, 6 mM MgCl<sub>2</sub>, 40 mM KCl, 5 mM DTT and 0.4% NP-40, centrifuged at 13000 rpm for 10 min, and the supernatant discarded. The pellet was resuspended in 100  $\mu$ l 0.1 M EDTA, mixed with 100  $\mu$ l 10% SDS and incubated at 55 °C for 15 min. Following addition of 225  $\mu$ l 4 M ammonium acetate, the precipitated

nucleic acid was pelleted by centrifugation at 13000 rpm for 15 min and subsequently washed with 1.0 ml 75% ethanol. The pellet was redissolved in TE and treated with RNaseA (final concentration of 1.6  $\mu\text{g/ml}$ ) for 1 h at 37  $^{\circ}\text{C}$ , extracted with phenol/chloroform and reprecipitated with ethanol. Purified genomic DNA was dissolved in TE buffer (10 mM Tris-Cl, pH 8.0, 0.1 mM EDTA) and the concentration determined by absorbance spectrophotometry at 260 nm. 10  $\mu\text{g}$  of DNA was digested with the indicated restriction enzymes and size fractionated by electrophoresis in 0.7% agarose in TBE buffer (89 mM Boric Acid, 89 mM Trisbase, 2 mM EDTA) gels.

Fractionated nucleic acids were blotted onto nylon membranes (Hybond N+, Amersham) and hybridized with radioactive probes labeled with [ $\alpha$ - $^{32}\text{P}$ ]dCTP by the random primer method as described previously (Sambrook, 1989). Probes were derived from PCR amplified fragments of plasmid templates that had been first gel purified using the QIAquick Gel Extraction Kit (Qiagen). Descriptions of the various probes used in this thesis are summarized in Table 5.

#### **2.2.15 cAMP accumulation**

cAMP production was measured by a previously described method (van Haastert, 1984). Briefly, cells were pulsed with cAMP, as described above, washed twice and then resuspended in KK2 at a density of  $6.25 \times 10^7$  cells/ml. The cell suspension was stimulated with 10  $\mu\text{M}$  2'-deoxy cAMP, and 100  $\mu\text{l}$  samples were lysed at intervals by addition of 100  $\mu\text{l}$  of 3.5% perchloric acid and 50  $\mu\text{l}$  of 50% saturated  $\text{KHCO}_3$ . cAMP levels were then measured using a cAMP binding-protein assay kit (Amersham TRK432).

### 2.2.16 Adenylyl cyclase assay

cAMP-pulsed cells were treated with 2 mM caffeine for 30 min, centrifuged and washed twice with ice-cold KK2 buffer. Cell pellets were then resuspended to a density of  $5 \times 10^7$  cells/ml in ice-cold 2 mM MgSO<sub>4</sub>/KK2, mixed with an equal volume of 20 mM Tris-Cl pH 8.0, 2 mM MgSO<sub>4</sub> and immediately frozen on dry ice, thawed, and then vortexed in the presence of glass beads (<106 microns) (Sigma, St. Louis, MO, USA). For stimulation by GTP $\gamma$ S, 80  $\mu$ M GTP $\gamma$ S and 2  $\mu$ M cAMP were included in the lysis buffer. Lysates were kept chilled on ice for 5 min, 200  $\mu$ l samples were then incubated for 2 min at 22 °C in a reaction mix containing 10 mM Tris-Cl, pH 8.0, 0.1 mM ATP, 1.0 mM cAMP, 10 mM DTT, and 10<sup>6</sup> cpm  $\alpha$ <sup>32</sup>P-ATP (Amersham). Mn<sup>2+</sup> stimulated activity was measured by inclusion of 5 mM MnSO<sub>4</sub> in the reaction mix. Reactions were terminated by the addition of 100  $\mu$ l 1% SDS containing 1 mM cAMP and 9 mM ATP. cAMP was purified by sequential chromatography through Dowex-50 and alumina, as previously described (Salomon, 1979). The eluted <sup>32</sup>P-cAMP was mixed with 5.0 ml water miscible scintillation fluid (ReadySafe, Beckman Coulter) and counted in the <sup>3</sup>H-channel for 4.0 min per sample in a Beckman LS6000IC scintillation counter.

### 2.2.17 cAMP binding assay

cAMP-pulsed cells were treated with 2 mM caffeine for 30 min, washed twice in ice-cold KK2 and resuspended to a density of  $1.5 \times 10^8$  cells/ml. The binding of <sup>3</sup>H-cAMP to the cell surface was measured by the ammonium sulfate stabilization assay (Van Haastert and Kien, 1983). Cells ( $1.5 \times 10^7$ ) were incubated with 100  $\mu$ l of KK2 containing 10 nM <sup>3</sup>H-cAMP (0.9 TBq/mmol) (GE Healthcare, Little Chalfont, Buckinghamshire, England) and 5 mM DTT (Sigma, St. Louis, MO, USA) for 1 min at

0 °C. One ml of saturated ammonium sulfate was then added, followed immediately by the addition of 100 µl of bovine serum albumin (10 mg/ml) (Sigma, St. Louis, MO, USA). After 5 min incubation at 0 °C, the samples were centrifuged at  $8000 \times g$  for 2 min. The supernatant was removed and the pellet was resuspended in 110 µl of 1 M acetic acid. One hundred µl of the resuspended pellet was mixed with 4 ml scintillation cocktail (Ready Safe liquid scintillation cocktails, Beckman Coulter, Fullerton, CA, USA) and the amount of bound  $^3\text{H}$ -cAMP was measured using a Beckman LS6000IC scintillation counter.

#### **2.2.18 cGMP production**

To measure cGMP production, cells were pulsed with cAMP as described above, washed twice with KK2, and resuspended to a density of  $1 \times 10^8$  cells/ml in KK2 containing 2 mM caffeine. The cells were stimulated with 100 nM cAMP, and 100 µl samples were lysed at intervals by the addition of 100 µl of 3.5% perchloric acid, followed by the addition of 50 µl of 50% saturated  $\text{KHCO}_3$ . cGMP levels were then measured using a cGMP- $^3\text{H}$ ] assay kit (Amersham TRK500).

#### **2.2.19 Guanylyl cyclase assay**

*In vitro* guanylyl cyclase assay was determined as described previously (Snaar-Jagalska and Van Haastert, 1994). Briefly, cAMP pulsed cells were washed and resuspended to a density of  $2 \times 10^8$  cells/ml in KK2. One volume of cell suspension was mixed with one volume of 10 mM Tris-Cl, pH 8, 1.5 mM EGTA, 500 mM sucrose, in the presence or absence of 200 µM  $\text{GTP}\gamma\text{S}$ , and cells were immediately lysed by pushing the suspension through 5 µm Isopore Membrane Filters (Millipore, Ireland) placed directly between a 1 ml syringe and a 26G1/2 needle. 150 µl of cell lysate was mixed with an

equal volume of assay mix (10 mM Tris-Cl, pH 8, 250 mM sucrose, 40 mM DTT, 1 mM GTP, 5 mM MgCl<sub>2</sub>) and the mixture incubated at 22 °C for 60 s. Aliquots (100 µl) were mixed with 100 µl 3.5% perchloric acid, followed by addition of 50 µl of 50% saturated KHCO<sub>3</sub>. cGMP levels were then measured using a cGMP-[<sup>3</sup>H] assay kit (Amersham TRK500).

#### **2.2.20 RasG, RasC and Rap1 activation assay**

After cAMP pulsing, cells were harvested by centrifugation and resuspended at a density of  $2 \times 10^7$  cells/ml in KK2 containing 1 mM caffeine. After 30 min, aliquots (2 ml) of cell suspension were stimulated by addition of cAMP to 15 µM. Cell suspensions (350 µl) were lysed at the indicated times by mixing with an equal volume of 2X lysis buffer (20 mM sodium phosphate, PH 7.2, 2% Triton X-100, 20% glycerol, 300 mM NaCl, 20 mM MgCl<sub>2</sub>, 2 mM EDTA, 2 mM Na<sub>3</sub>VO<sub>4</sub>, 10 mM NaF, containing two tablets of protease inhibitor (Roche Complete) per 50 ml buffer). The lysates were centrifuged for 10 min and the protein concentrations of the supernatants were determined using the protein assay from Bio-Rad (Hercules, CA). The GST-Byr2-Ras Binding Domain (RBD) was expressed in *Escherichia coli* and purified as described previously (Kae *et al.*, 2004). 400 µg of protein was then incubated with 100 µg of GST-Byr2-RBD on glutathione-sepharose beads (Amersham Biosciences) at 4 °C for 1 hour. The glutathione-sepharose beads were harvested by centrifugation and washed three times in 1X lysis buffer. 50 µl of 1X SDS gel loading buffer was then added to the pelleted beads and the suspension boiled for 5 min. Samples were subjected to SDS-PAGE and Western blots probed with anti-RasG, RasC or Rap1 specific antibodies.

### 3 RESULTS

#### 3.1 Comparison of the roles of RasG and RasC in cAMP signaling during aggregation

##### 3.1.1 Generation of *rasG* null strain

Direct evidence for a role for Ras in early development came with the disruption of the *rasC* gene, which produced cells that failed to aggregate (Lim *et al.*, 2001). Although aggregation was totally defective under certain experimental conditions, it did occur under others, indicating that RasC was important but not essential. Evidence for the involvement of an additional Ras protein came from the finding that like RasC, RasG was also activated in response to cAMP (Kae *et al.*, 2004). This study suggested that the role of RasG in aggregation should be further investigated. The original *rasG*<sup>-</sup> strains, IR15 and IR17, isolated by the Insall laboratory exhibited only slight and variable defects in development, background strain variability and instability (Tuxworth *et al.*, 1997; Khosla *et al.*, 2000). In view of the problems with these strains, I therefore generated new *rasG* null strains in order to reinvestigate the possible role of RasG during early development. To control for possible strain-related variation, the mutants were generated in two different wild type axenic backgrounds that are known to be genetically distinct; AX2 (Watts and Ashworth, 1970) and JH10, a thymidine-requiring derivative of AX3 (Hadwiger and Firtel, 1992). To generate *rasG* null strains, the pBW1 and pBW2 constructs that carried a clone of *rasG* interrupted by a blasticidin and a thymidine gene respectively (Table 2) were digested with EcoRI and KpnI and introduced into AX2 and JH10 by electroporation. Following 8-15 days of selection for blasticidin resistant cells or cells that no longer required thymidine as the supplement, cells were clonally isolated

and screened by PCR. Three positive clones in each background were selected for further analysis by southern and western blotting.

Southern blot analysis of EcoRI and HindIII digested genomic DNA confirmed each of the presumptive gene disruptions (Figure 3), because the expected EcoRI-HindIII fragment was shifted as predicted. When the duplicate blots were hybridized with the *bsr* probe, a single band was detected at 3.2 kb, indicating that each mutant contained of a single insertion into the genome (data not shown). Western blots of total cell protein from the mutants revealed no RasG protein in any of the three AX2/*rasG*<sup>-</sup> or the three JH10/*rasG*<sup>-</sup> isolates (Figure 4). In vegetative *rasG*<sup>-</sup> cells there was a marked increase in the amount of RasC protein (Figure 4) relative to wild type, suggesting the possibility that RasC is capable of partially compensating for the loss of RasG. In contrast in *rasC*<sup>-</sup> cells there was only a slight increase in the amount of RasG protein (Figure 4) suggesting a minor or no compensatory role of RasG for RasC. The AX2/*rasG*<sup>-</sup> and JH10/*rasG*<sup>-</sup> clones all exhibited identical properties, so detailed studies were conducted on a single isolate of each.

Ectopic expression of RasG protein from the *rasG* promoter was accomplished by introducing the 20 µg of undigested pRASG-G418 into *rasG*<sup>-</sup> cells by electroporation. This ectopic expression rescued both the growth and developmental phenotypic defects of *rasG*<sup>-</sup> mutants in both backgrounds, confirming that the observed phenotype was a consequence of *rasG* gene disruption. Unlike the originally isolated strains, IR15 and IR17, both new *rasG* null strains (AX2/*rasG*<sup>-</sup> and JH10/*rasG*<sup>-</sup>) had stable phenotypes during prolonged growth.

*AX2/rasC* and *JH10/rasC* strains were generated previously in the Weeks laboratory (Lim *et al.*, 2001; Khosla *et al.*, 2005) and the availability of these strains allowed direct comparison of the effects of the deletion of *rasG* and *rasC* in isogenic backgrounds. Since the *JH10/rasG* cell line was later used to generate other mutant strains, all subsequent data presented in this thesis is for this strain, unless otherwise indicated.

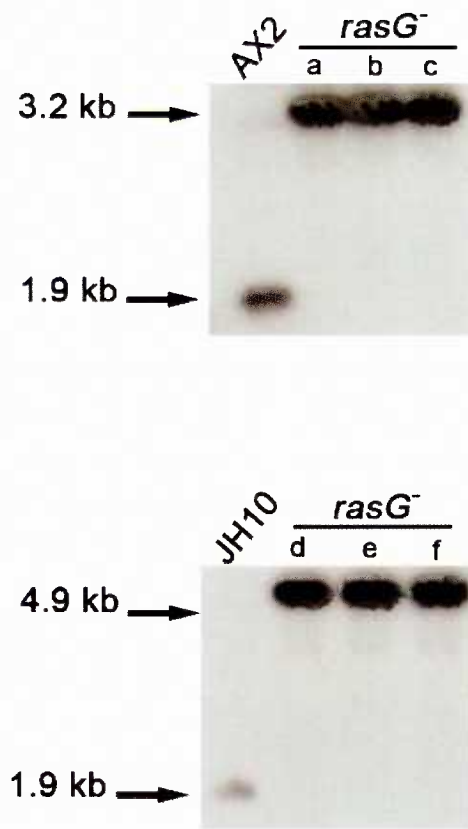


**Figure 3. Genetic disruption of *rasG* gene.** Southern blot of genomic DNA from parental AX2 and JH10 and three disrupted clones derived from cells transformed with pBW1 and pBW2. 10  $\mu$ g genomic DNA was digested with *EcoRI* and *HindIII*, separated in a 0.7% agarose gel, blotted onto nylon membrane and probed with the full length *rasG* cDNA.

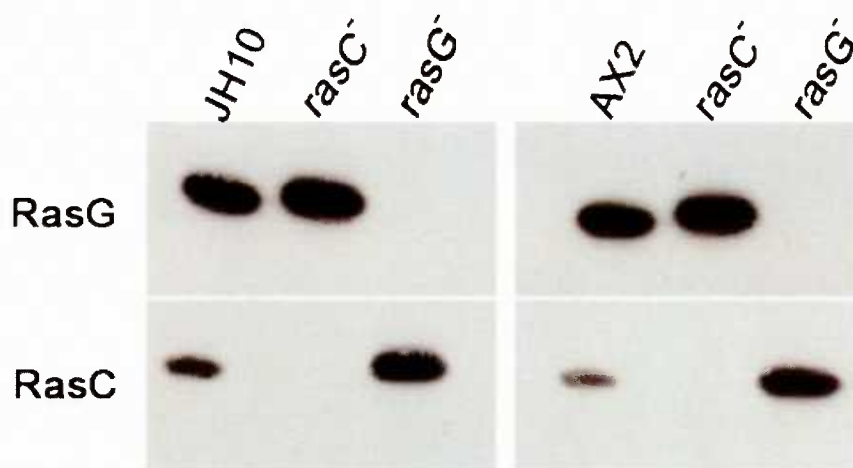


**Figure 4.** Western blot analysis of Ras protein levels of JH10, JH10/*rasC*<sup>-</sup>, JH10/*rasG*<sup>-</sup>, AX2, AX2/*rasC*<sup>-</sup>, and AX2/*rasG*<sup>-</sup>. Cell lysates from the JH10, JH10/*rasC*<sup>-</sup>, JH10/*rasG*<sup>-</sup>, AX2, AX2/*rasC*<sup>-</sup>, and AX2/*rasG*<sup>-</sup> were probed with RasG and RasC specific antibodies, as indicated.

### 3.1.2 Developmental phenotype of the *rasG* null strains

When grown in association with bacteria (*Klebsiella oxytoca*) on SM plates (Sussman, 1987), single *Dictyostelium* cells form distinct plaques; the amoebae clear the plate of the bacteria and subsequently enter development and form fruiting bodies. The plaques of JH10/*rasG*<sup>-</sup> strain showed large clearing zones before differentiation commenced (Figure 5), as observed previously for the original *rasG*<sup>-</sup> strains (R. H. Insall and G. Weeks, unpublished observations) and similar results were obtained for newly generated AX2/*rasG*<sup>-</sup> strain (Figure 6). Ectopic expression of the RasG protein under the control of *rasG* promoter restored multicellular development in the null strain to the wild type phenotype (data not shown), confirming that the observed phenotype was a consequence of *rasG* gene disruption. Developmental phenotype for the JH10/*rasC*<sup>-</sup> strain is also shown in Figure 5 for comparison.

Aggregation of parental and mutant strains was observed in more detail by plating cells in plastic dishes under non-nutrient buffer. Aggregation streams of JH10 cells were observed 8 h after plating, and typical tight aggregates formed by 12 h (Figure 7A). JH10/*rasG*<sup>-</sup> (Figure 7B) and AX2/*rasG*<sup>-</sup> cells (data not shown) formed aggregation streams with a delay of about 4 h relative to wild type, and the final aggregates were smaller. Under these conditions, the JH10/*rasC*<sup>-</sup> cells formed very small clumps (Figure 7C), as observed previously (Khosla *et al.*, 2005). When pulsed with cAMP for 5 h in shaken suspension JH10 cells rapidly formed aggregation streams upon plating in plastic dishes (Figure 7D), whereas JH10/*rasG*<sup>-</sup> cells were again somewhat delayed in aggregate-stream formation (Figure 7E). Under these conditions, JH10/*rasC*<sup>-</sup> cells formed large clumps without detectable aggregate-stream formation (Figure 7F).

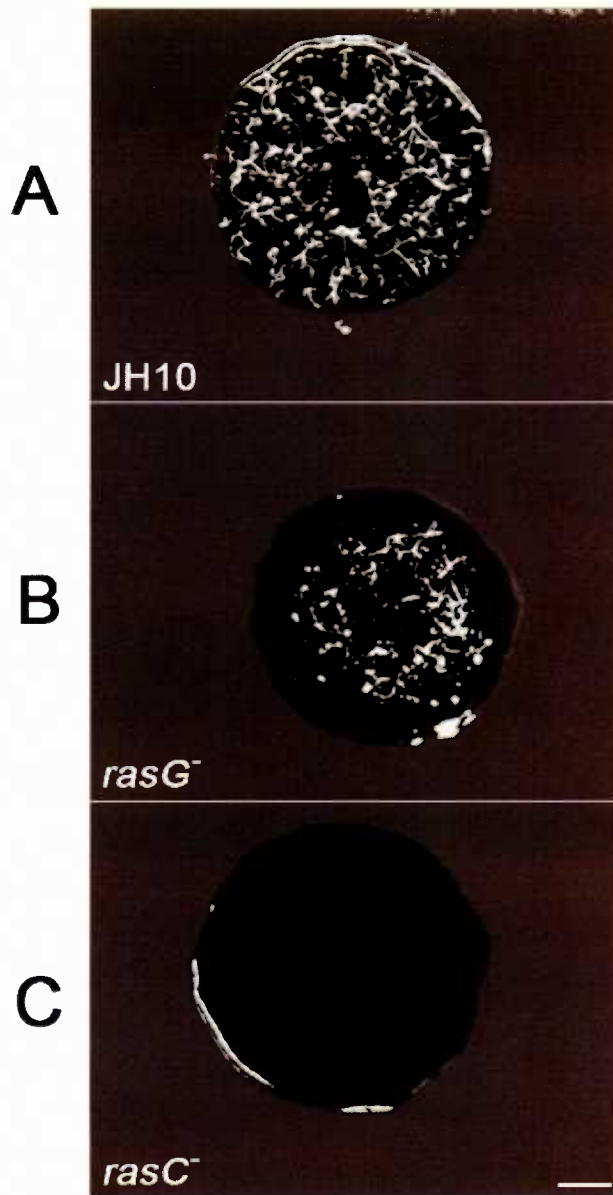


**Figure 5. Multicellular development of JH10, *rasG*, and *rasC* on bacterial growth plates.** Clonal plaque of (A) parental JH10, (B) *rasG*<sup>-</sup> and (C) *rasC*<sup>-</sup> strains after 5 days growth on a bacterial lawn. Images were taken using a Wild Leitz dissecting microscope. Scale bar is 150  $\mu\text{m}$ .

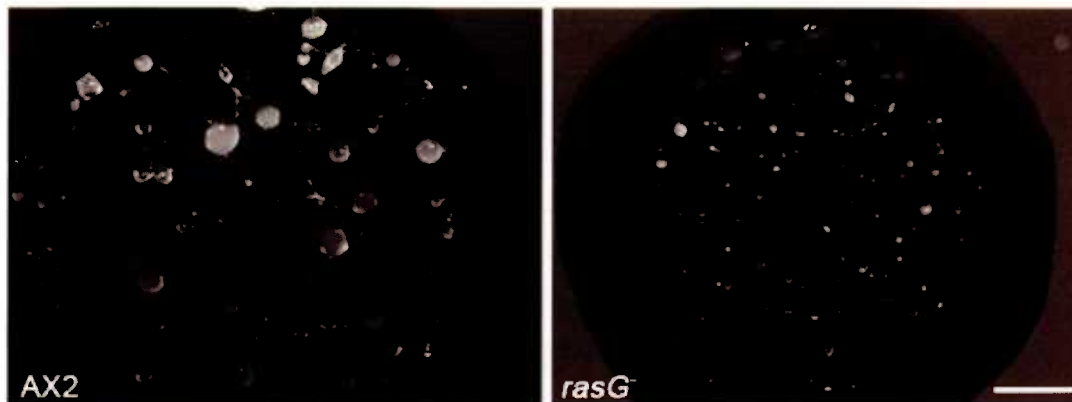


**Figure 6. Multicellular development of Ax2 and *rasG*<sup>-</sup> on bacterial growth plates.** Clonal plaque of parental Ax2 and *rasG*<sup>-</sup> strains after 5 days growth on a bacterial lawn. Images were taken using a Wild Leitz dissecting microscope. Scale bar is 150  $\mu\text{m}$ .

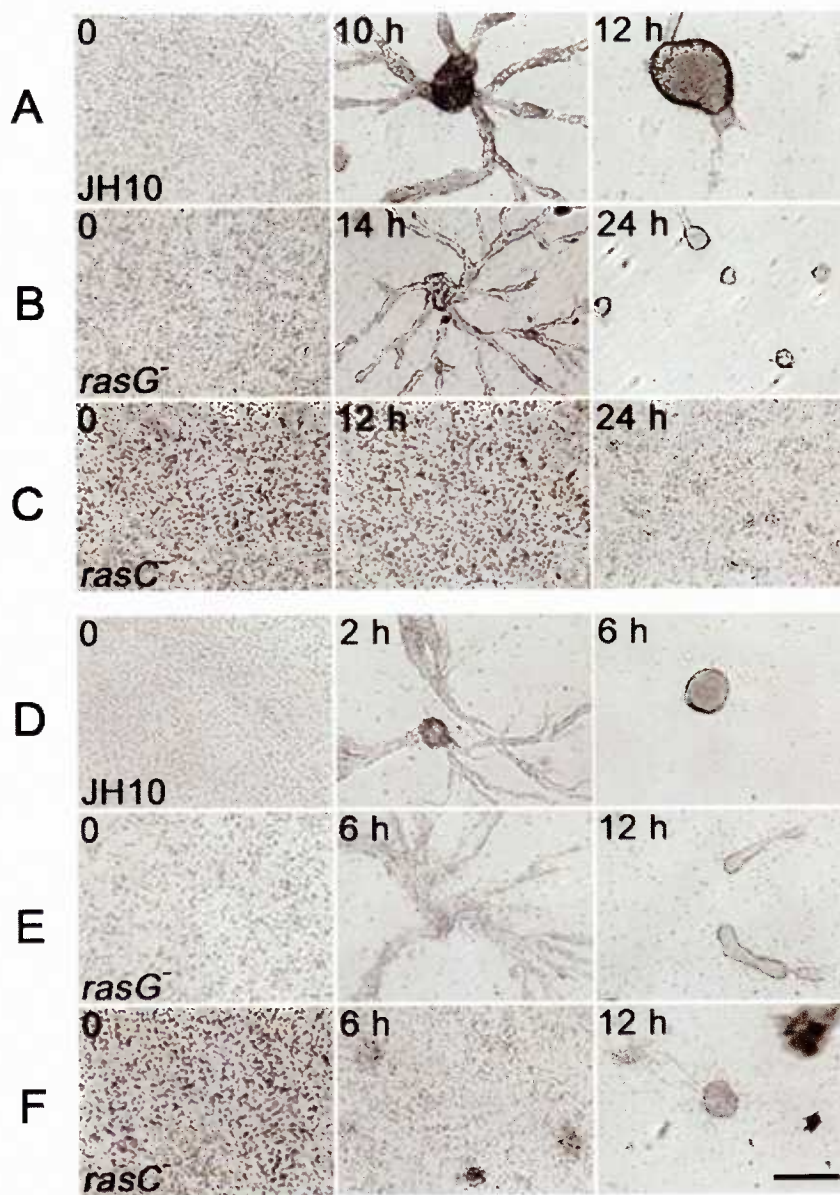


**Figure 7. Aggregation of JH10, *rasG*<sup>-</sup>, and *rasC*<sup>-</sup> on a plastic surface .** Without (A-C) or with (D-F) 5 h of prior pulsing with cAMP (see Materials and Methods). Strains JH10 (A and D), *rasG*<sup>-</sup> (B and E), and *rasC*<sup>-</sup> (C and F) were photographed at the indicated times after plating. Single experiments are shown, but the results for the various strains were highly reproducible. Scale bar is 250  $\mu$ m.

Developmental phenotypes were also observed after cells were plated on nitrocellulose filters under starvation conditions. Under these conditions AX2 and JH10 cells culminate uniformly after 24 h. In contrast, both the JH10/*rasG*<sup>-</sup> and AX2/*rasG*<sup>-</sup> strains did form small fruiting bodies, but culmination was not observed until about 30 h (Figure 8A and data not shown). Although the JH10/*rasC*<sup>-</sup> cells did not routinely undergo development under these conditions (Figure 8A), some filters occasionally contained small fruiting bodies (data not shown), confirming previous results (Khosla *et al.*, 2005). However, as shown JH10/*rasC*<sup>-</sup> cells formed fruiting bodies following the administration of cAMP pulses to cells in suspension (Figure 8B).

### 3.1.3 Early developmental gene expression

The developmental defects in *Dictyostelium* mutants could be due to the misregulation of the genes required for development. A number of genes are known to be expressed soon after the initiation of development (Loomis, 1996). These include the genes for the cAMP receptor (*carA*), for the G $\alpha$  subunit (*gpaB*), for the adenylyl cyclase (*acaA*), and for the cAMP phosphodiesterases (*pdsA* and *regA*) (Loomis, 1996; Parent and Devreotes, 1996). The products of these genes function with the preexisting proteins to generate and relay the cAMP and regulate the cAMP both outside and inside the cells. As the cells aggregate, they stick to each other as a result of expression of aggregation specific genes, *csaA* and *lagC*. It has been known that *Dictyostelium* cells express many developmental genes while suspended in buffer and given pulses of cAMP at 6 min periods for several hours (Kessin, 2001). To investigate the expression of early developmentally regulated genes in the *ras* mutant strains, cells were pulsed with cAMP under starvation conditions. These exogenous pulses mimic the developmental program

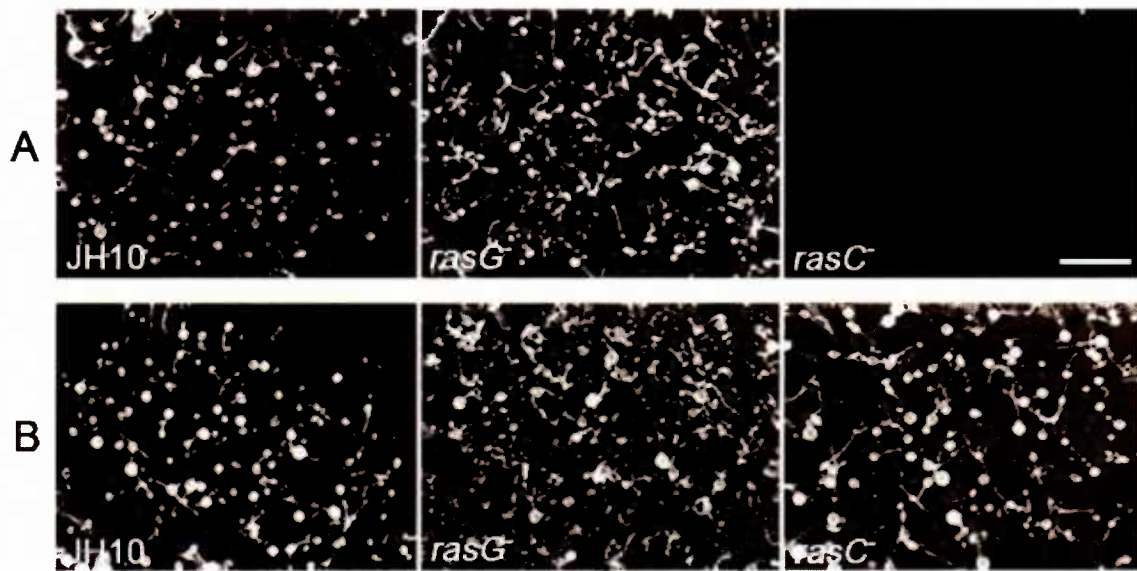


**Figure 8. Development of JH10, *rasG*, and *rasC* on nitrocellulose filters.** (A) Vegetative JH10, *rasG*, and *rasC* cells or (B) cAMP-pulsed JH10, *rasG*, and *rasC* cells plated for development on nitrocellulose filters supported by KK2-saturated pads. Images were taken at 22 h after plating using a Wild Leitz dissecting microscope. Scale bar is 150  $\mu$ m.

of *Dictyostelium*, thus all strains, even those defective in endogenous signaling, undergo synchronized developmental changes and express developmental genes more synchronously. The total RNA was prepared from harvested cells at various time points. The RNA was separated by electrophoresis, and the levels of expression of three representative early developmental genes *carA*, *gpaB*, and *csaA* were determined by northern blot analysis. In the control JH10 cells, the expression of all three genes had increased markedly by 8 h of development (Figure 9A). In these pulsed cells, the expression of two genes (*carA* and *gpaB*) was significantly reduced in JH10/*rasG*<sup>-</sup> cells (Figure 9B), but not appreciably reduced in JH10/*rasC*<sup>-</sup> cells (Figure 9C). In addition, the expression of the *carA* gene was significantly delayed in the JH10/*rasG*<sup>-</sup> cells but not delayed in the JH10/*rasC*<sup>-</sup> cells (Figure 9). Similar results were obtained for the AX2/*rasG*<sup>-</sup> cells (data not shown). These results indicated an involvement of a RasG-dependent signal-transduction pathway for the optimum expression of these genes. For the third gene, the aggregation-specific *csaA*, expression was slightly lower in both the JH10/*rasG*<sup>-</sup> and JH10/*rasC*<sup>-</sup> cells than in JH10 cells. The delayed expression of the *carA* gene in *rasG*<sup>-</sup> cells might partially explain the delayed aggregation phenotype observed in *rasG*<sup>-</sup> cells, since the cAR1 gene product is essential for response to cAMP.

#### **3.1.4 Comparison of chemotaxis by *rasG*<sup>-</sup> and *rasC*<sup>-</sup> cells**

Diffusion of cAMP from the tip of a micropipet establishes a spatial cAMP gradient, and chemotaxis-competent cells placed in this gradient respond by migrating towards the tip (Firtel and Chung, 2000). Chemotaxis assays were first performed with cells that had been starved for 6 h on plastic dishes submerged under non-nutrient buffer without the application of cAMP pulses. At t=0, a micropipet filled with 100 μM cAMP

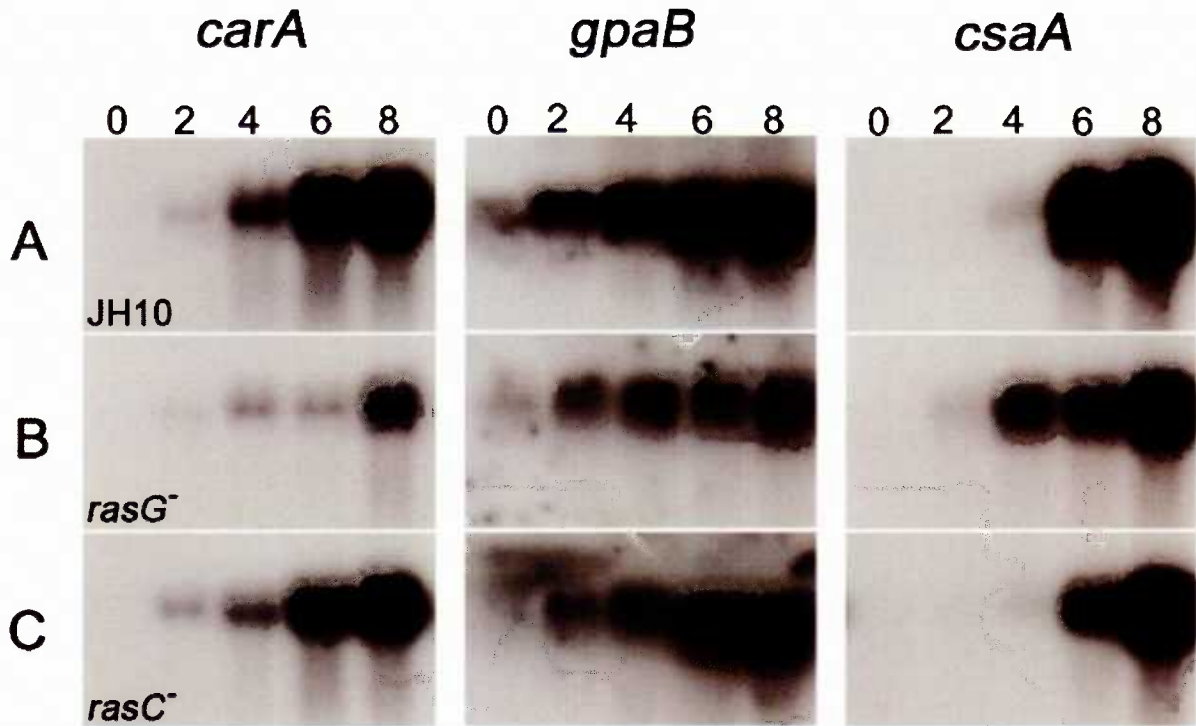


**Figure 9. Northern-blot analysis of early developmental gene expression of JH10, *rasG*<sup>-</sup>, and *rasC*<sup>-</sup>.** Cells of strains JH10 (A), *rasG*<sup>-</sup> (B), and *rasC*<sup>-</sup> (C) were pulsed with cAMP as described in Materials and Methods, and RNA was isolated at the indicated times (in hours) after the onset of pulsing. Blots were hybridized with cDNA probes corresponding to the indicated genes.

was positioned in the microscopic field of view, and the movement of cells was captured by time-lapse microscopy. As shown in Figure 10A, JH10 cells responded to the cAMP gradient by rapidly chemotaxing toward the tip within 20 min. JH10/*rasG*<sup>-</sup> cells were capable of chemotaxis but less number of cells around the micropipet tip was detected at the same time frame (Figure 10B). Similar results were obtained with AX2/*rasG*<sup>-</sup> cells (data not shown). In contrast, under the same conditions, JH10/*rasC*<sup>-</sup> cells responded extremely poorly (Figure 10C), confirming previous results (Khosla *et al.*, 2005).

Chemotaxis assays were then performed with cells that had been pulsed with cAMP in suspension for 5 h prior to the assay. Under these conditions, JH10 and JH10/*rasC*<sup>-</sup> cells were highly polarized at the beginning of the assay. The cells responded quickly and migrated rapidly toward the cAMP source (Figure 11A and 11C). The chemotaxis of JH10/*rasG*<sup>-</sup> cells (Figure 11B) and AX2/*rasG*<sup>-</sup> cells (data not shown) was slower, and the cells exhibited little polarity. Instantaneous velocities and chemotaxis indices were determined using *Openlab* software. To measure the instantaneous velocity of a cell in frame *n*, a line was drawn from the centroid in frame *n*-1 to the centroid in frame *n*+1 and the length of that line was divided by twice the time interval between frames. Chemotaxis index was calculated as the net distance traveled towards the source of chemoattractant divided by the total distance traveled in that time period. The results showed no significant difference between the JH10 and JH10/*rasC*<sup>-</sup> cells, but the motility of the JH10/*rasG*<sup>-</sup> cells was lower (Table 6). The instantaneous velocity values obtained for the JH10 and JH10/*rasC*<sup>-</sup> cells were not significantly different from previously published values for the AX2 and AX2/*rasC*<sup>-</sup> strains (Wessels

*et al.*, 2004). A calculation of chemotactic index revealed no reduction for the JH10/*rasC*<sup>-</sup> cells relative to JH10, but a lower value for the JH10/*rasG*<sup>-</sup> cells (Table 6).

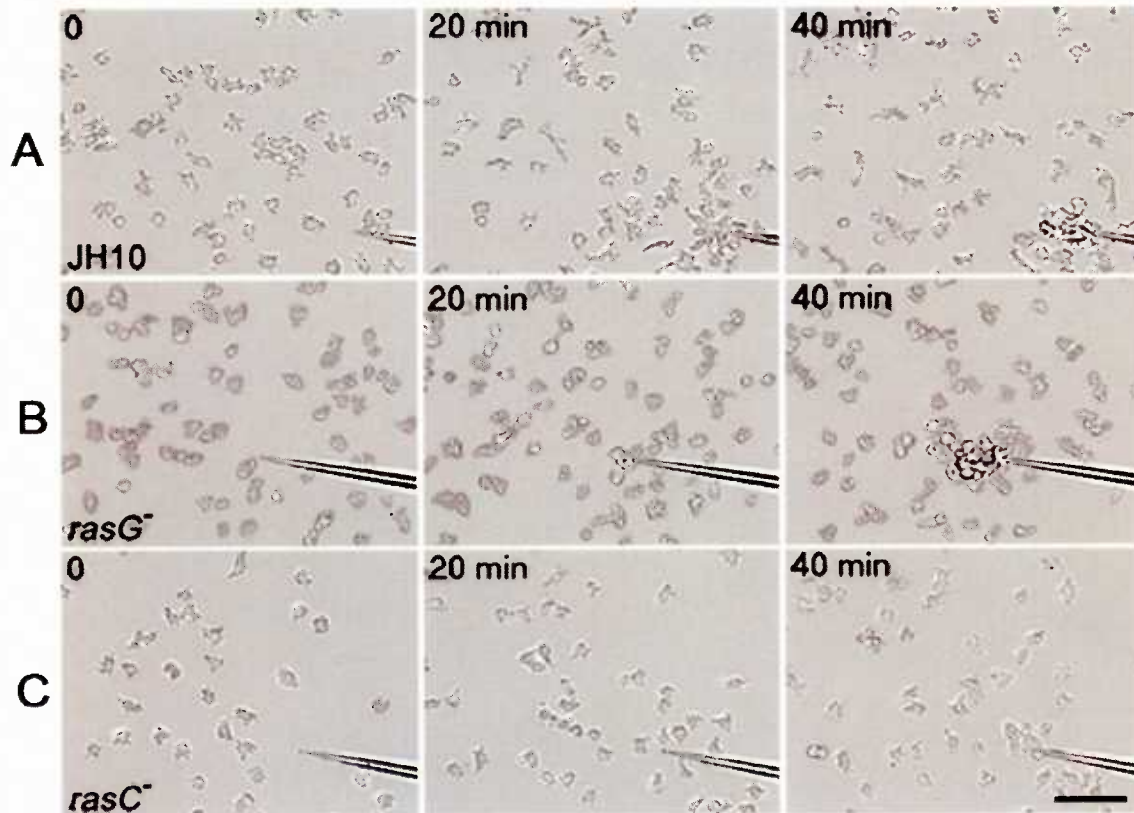


**Figure 10. Chemotaxis of starved JH10, *rasG*<sup>-</sup>, and *rasC*<sup>-</sup> cells towards a source of cAMP .** Cells of strains JH10 (A), JH10/*rasG*<sup>-</sup> (B), and JH10/*rasC*<sup>-</sup> (C) were plated on Nunc dishes, submerged in Bonner's salts and starved for 6 h. A micropipette filled with 100  $\mu$ M cAMP was inserted at t=0. Cells were photographed at the indicated times following the release of cAMP from the micropipette tip. Scale bar is 50  $\mu$ m.

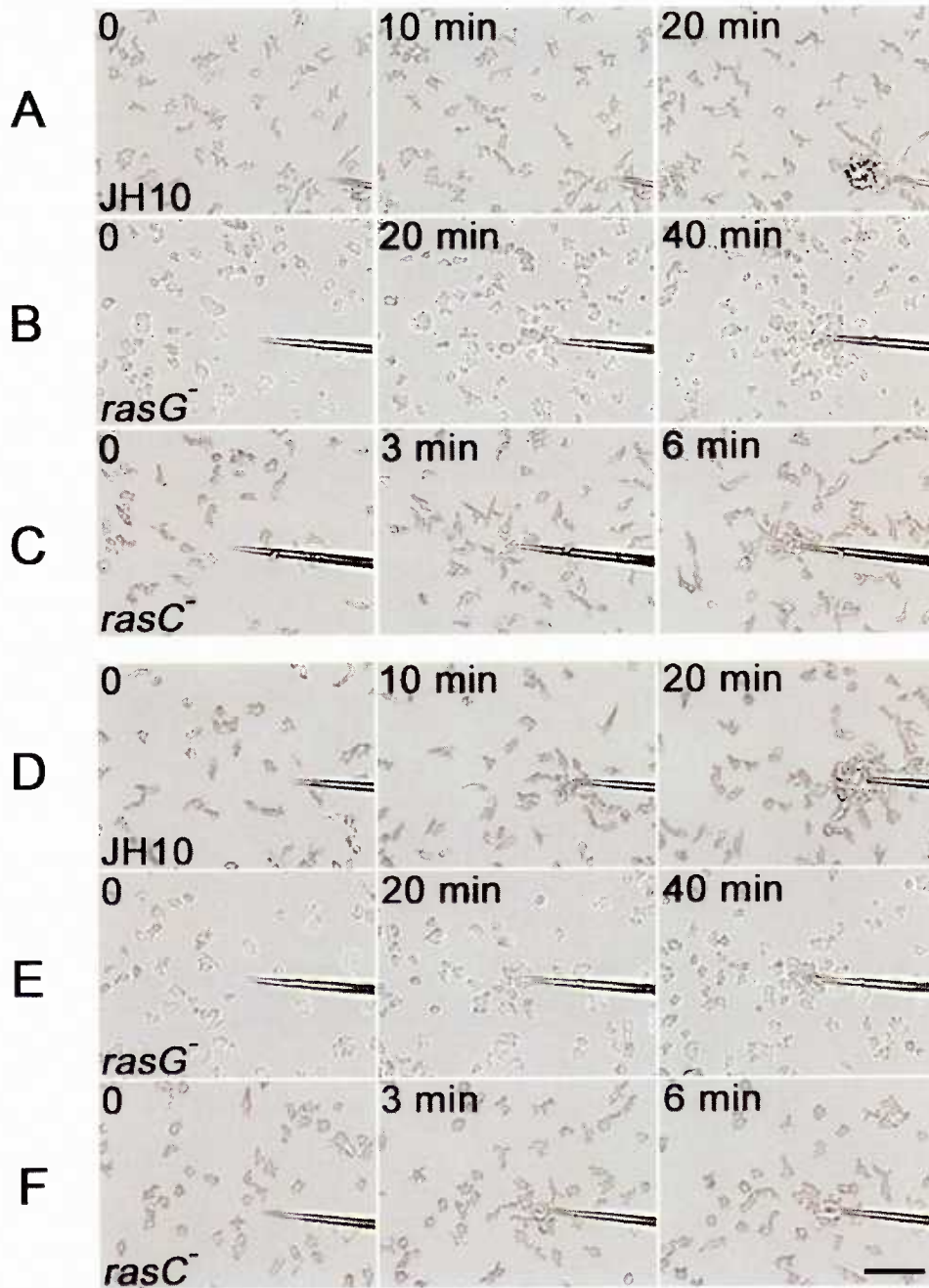


**Figure 11. Chemotaxis of pulsed JH10, *rasG*<sup>-</sup>, and *rasC*<sup>-</sup> cells towards a source of cAMP .** Cells of strains JH10 (A and D), *rasG*<sup>-</sup> (B and E), and *rasC*<sup>-</sup> (C and F) had been pulsed with cAMP for 5 h (A-C) or 8 h (D-F) were photographed at the indicated times following the release of cAMP from the micropipette tip. Scale bar is 50  $\mu$ m.

**Table 6. Chemotaxis analysis of *Dictyostelium* cells in a spatial gradient of cAMP.**

<b>Strain</b>	<b>Instantaneous velocity (<math>\mu\text{m}/\text{min}</math>)</b>	<b>Chemotaxis index <sup>a</sup></b>
<b>JH10 (n = 20)</b>	<b>11.02 <math>\pm</math> 1.6</b>	<b>0.60 <math>\pm</math> 0.1</b>
<b><i>rasG</i> (n = 22)</b>	<b>5.97 <math>\pm</math> 1.7</b>	<b>0.43 <math>\pm</math> 0.2</b>
<b><i>rasC</i> (n = 21)</b>	<b>12.88 <math>\pm</math> 3.3</b>	<b>0.70 <math>\pm</math> 0.1</b>

Values are means  $\pm$  SD; n = number of cells

<sup>a</sup> Chemotaxis index was calculated as the net distance traveled towards the source of chemoattractant divided by the total distance traveled in that time period.

Because the delay of *carA* expression in the JH10/*rasG* cells (Figure 9B) might possibly explain the reduced chemotaxis of the 5 h cAMP pulsed cells, the experiments were repeated with cells that had been pulsed with cAMP for 8 h to ensure maximum expression of *carA*. Results were not significantly different from those for 5 h cAMP-pulsed cells (Figure 11D-F). Thus the reduced chemotaxis exhibited by the JH10/*rasG* cells after five hours of cAMP pulsing is not simply due to reduced levels of cAR1. These results suggest an important role for RasG in the signaling pathway responsible for chemotaxis to cAMP. However, the finding that *rasG* cells are still capable of some chemotaxis suggests either the existence of a RasG independent pathway, or that another Ras family protein can mediate some of the signal transduction normally carried out by RasG.

### 3.1.5 cGMP production in response to cAMP

In *Dictyostelium*, cGMP production has been shown to be associated with the chemotactic response (van Haastert and Kuwayama, 1997). We therefore examined cGMP production in response to cAMP in the *ras* mutant strains. To do these studies, cAMP pulsed cells washed and treated with caffeine, stimulated with cAMP and the cGMP levels were then measured using a cGMP-[<sup>3</sup>H] assay kit as described in material and methods. As previously reported for wild-type cells, there was a burst of cGMP production in JH10 cells, 10 s after the application of cAMP, and a drop back to basal levels after about 30 s. Maximum production of cGMP was significantly reduced in JH10/*rasG*<sup>-</sup> cells (Figure 12) and in AX2/*rasG*<sup>-</sup> cells (data not shown). In the JH10/*rasC*<sup>-</sup> cells, there was also less cGMP produced, but the level was closer to wild type than for the *rasG*<sup>-</sup> cells. Since cGMP production is important for chemotaxis, these results further implicate RasG in chemotaxis signaling. However, since there was also a reduction of cGMP production in the *rasC*<sup>-</sup> cells, RasC appears also to play a subsidiary role in chemotaxis.

### 3.1.6 Guanylate cyclase activation

In *Dictyostelium*, *in vivo* activation of guanylate cyclase is known to be dependent on GPCRs and on heterotrimeric G proteins. cAMP is a well known extracellular ligands that induce a transient rise in cGMP. It has been shown previously that GTPγS stimulates guanylyl cyclase activity (van Haastert and Kuwayama, 1997). However, in lysates of *gβ*<sup>-</sup> cells, this activation still occurs and the involvement of a monomeric G protein in the regulation of GC has therefore been proposed (Wu *et al.*, 1995; Roelofs *et al.*, 2001). I investigated the possibility that either RasC or RasG is the previously invoked

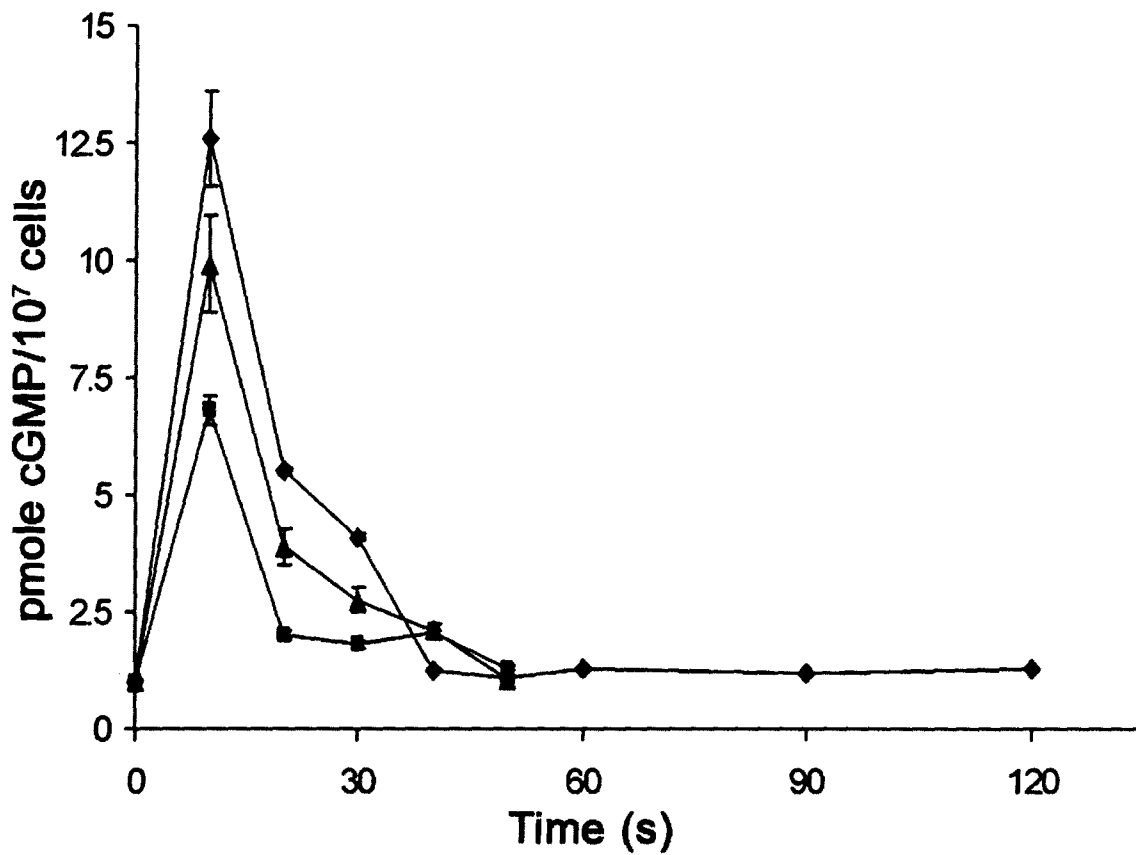


**Figure 12.** cGMP production of JH10, *rasG*, and *rasC* in response to cAMP. JH10 (◆), JH10/*rasG* (■), and JH10/*rasC* (▲) cells were pulsed for 5 h with cAMP, washed, and then stimulated with 100 nM cAMP. Samples were taken at the indicated times and assayed for cGMP accumulation (see Material and Methods). The means and standard deviations for three independent experiments are shown.

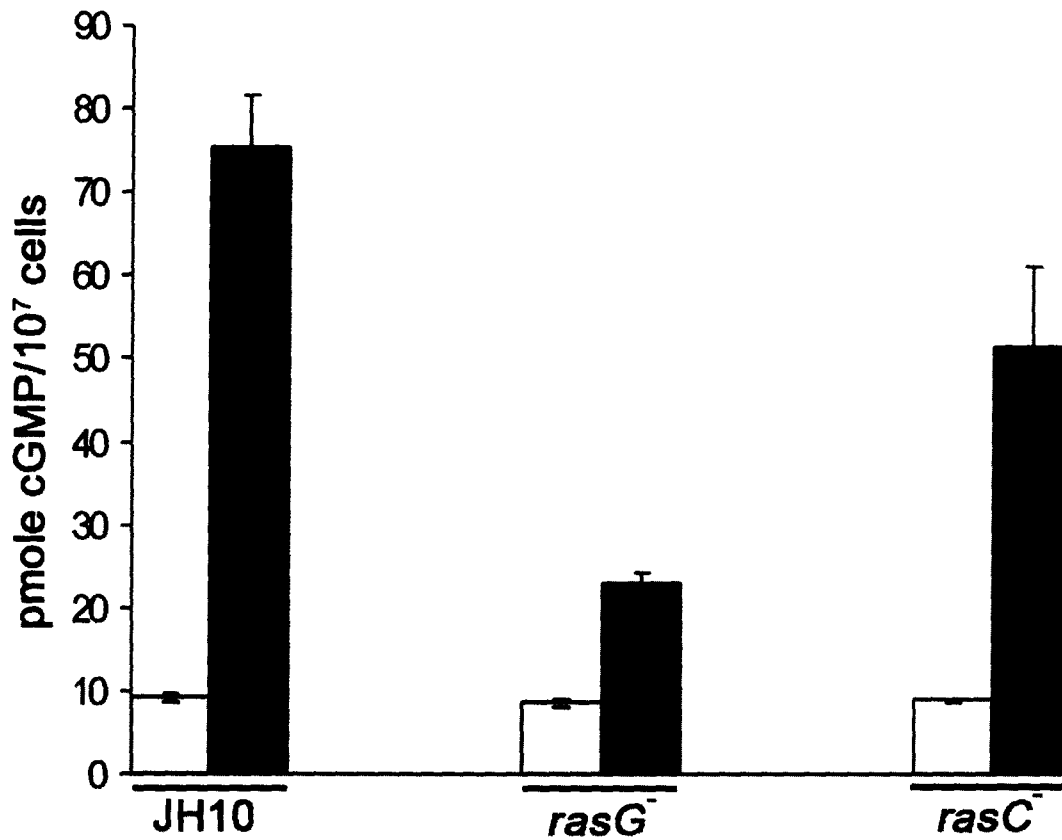


**Figure 13.** *In vitro* GTP $\gamma$ S stimulation of guanylyl cyclase activity of JH10, *rasG*<sup>-</sup>, and *rasC*<sup>-</sup>. JH10, JH10/*rasG*<sup>-</sup>, and JH10/*rasC*<sup>-</sup> cells were pulsed with cAMP for 5 h and lysates were then assayed for guanylyl cyclase activity in the absence (gray bar), or the presence of GTP $\gamma$ S (black bar). The means and standard deviations for three independent experiments are shown.

monomeric G protein, by examining the GTP $\gamma$ S stimulation of guanylyl cyclase activity in the *ras* mutant strains. For this experiment, cAMP pulsed cells were washed and cell suspension was lysed in the presence or absence of GTP $\gamma$ S, and cGMP levels were then measured using a cGMP-[ $^3$ H] assay kit. The guanylyl cyclase activity of JH10 lysates was stimulated ~8 fold, by GTP $\gamma$ S. The activity of *rasG*<sup>-</sup> lysates was stimulated ~2.5 fold and the activity of *rasC*<sup>-</sup> lysates was stimulated ~5.5 fold (Figure 13). This result again suggests an important role for RasG in cAMP signal transduction pathway responsible for guanylyl cyclase activation. However, since lysates from *rasC*<sup>-</sup> cells also exhibit reduced guanylate cyclase activity, there may also be a role for RasC.

### 3.1.7 PKB phosphorylation

The *Dictyostelium* chemotactic response to cAMP involves a PI3K-mediated signaling pathway that leads to the transient phosphorylation of PKB (see introduction). To test the possible involvement of RasG in the PI3K-PKB pathway, cAMP pulsed cells were stimulated with cAMP at a final concentration of 100 nM. Aliquots of cell suspension were removed at intervals, before and after stimulation, and then subjected to western blot analysis using a phosphothreonine-specific antibody that is capable of unambiguously detecting the phosphorylation of PKB (Lim *et al.*, 2001). In JH10 cells, PKB was transiently phosphorylated after 10 s in response to cAMP (Figure 14A). The phosphorylation level then decreased, and there was a second, smaller increase after 120 s. This response was severely reduced in JH10/*rasG*<sup>-</sup> cells (Figure 14A) and in AX2/*rasG*<sup>-</sup> cells (data not shown). It was also reduced in JH10/*rasC*<sup>-</sup> cells, although less markedly (Figure 14A), as observed previously (Khosla *et al.*, 2005). The total amounts of PKB protein, as detected using a specific PKB antibody, were identical in all three

strains (Figure 14A). These results are also consistent with the involvement of RasG in the cAMP stimulated phosphorylation of PKB. However, again since PKB phosphorylation was also reduced in *rasC* cells, a subsidiary role for RasC can not be excluded. When cells were pulsed with cAMP for 8 h rather than for 5 h in an attempt to increase the likelihood that *carA* expression was sufficient, similar results were obtained (Figure 14B).

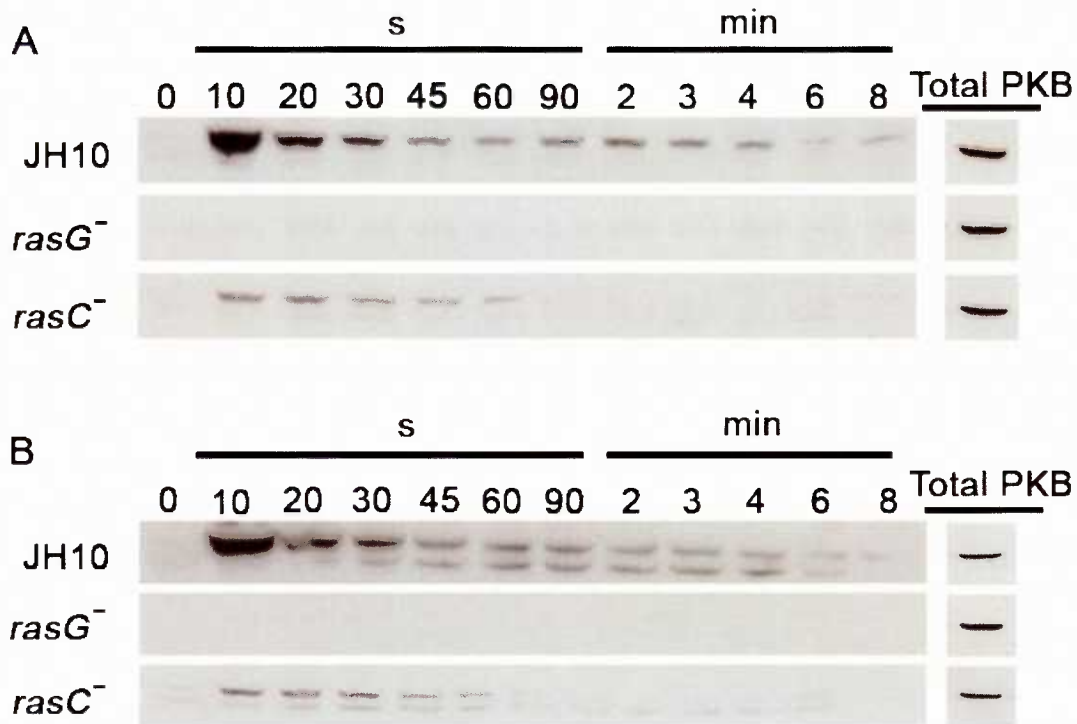


**Figure 14. PKB phosphorylation of JH10, *rasG*<sup>-</sup>, and *rasC*<sup>-</sup> in response to cAMP.** Cells were pulsed with cAMP for 5 h (A) or 8 h (B) and then treated with 100 nM cAMP. Cell extracts from JH10, JH10/*rasG*<sup>-</sup>, and JH10/*rasC*<sup>-</sup> were prepared at the indicated times after the cAMP stimulus and subjected to western-blot analysis. Blots were probed with a phosphothreonine-specific antibody.

### 3.1.8 cAMP production

To compare the roles of RasG and RasC in the cAMP-stimulated activation of adenylyl cyclase, cells that had been pulsed with cAMP for either 5 or 8 h were washed, stimulated with 2'-deoxy-cAMP, and assayed for cAMP accumulation at various time points after stimulation using a cAMP binding-protein assay kit. JH10/*rasG*<sup>-</sup> cells produced lower levels of cAMP than the JH10 wild type cells upon stimulation, but the reduction was far less pronounced than that observed for JH10/*rasC*<sup>-</sup> cells (Figures 15A and 16A). Results for AX2/*rasG*<sup>-</sup> cells were similar to those for JH10/*rasG*<sup>-</sup> cells (data not shown). These results suggest that RasC is more important for cAMP production but that RasG can also make a contribution. Although cAMP production increases in some strains as cells progress through aggregation (Brenner, 1978), our finding that the levels of cAMP production in the JH10 wild-type cells were identical after 5 and 8 h of cAMP pulsing (Figure 15A and 16A) is not surprising, because cells pulsed for 5 h are fully aggregation competent and would not be expected to change appreciably in their physiological responses during the additional 3 h of pulsing.

### 3.1.9 Adenylyl cyclase activation

The potential roles of RasG and RasC in the cAMP relay were also examined by measuring *in vitro* GTP $\gamma$ S-mediated activation of ACA in cell lysates prepared from cAMP pulsed cells. It has been shown that GTP $\gamma$ S stimulates ACA activity by uncoupling the G $\beta\gamma$  subunit from the heterotrimeric G-protein, and this happens without the need for receptor activation (Theibert and Devreotes, 1986; Parent and Devreotes, 1996). GTP $\gamma$ S stimulated the ACA activity of JH10 lysates ~18 fold, JH10/*rasG*<sup>-</sup> lysates ~15 fold, AX2/*rasG*<sup>-</sup> lysates ~15 fold and JH10/*rasC*<sup>-</sup> lysates ~7 fold over the basal levels

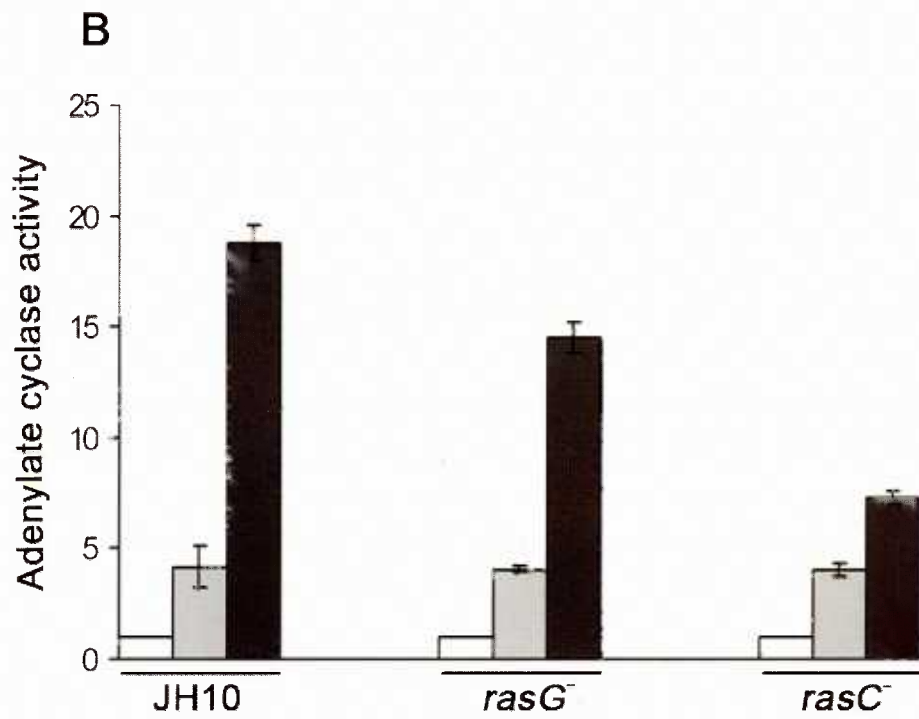
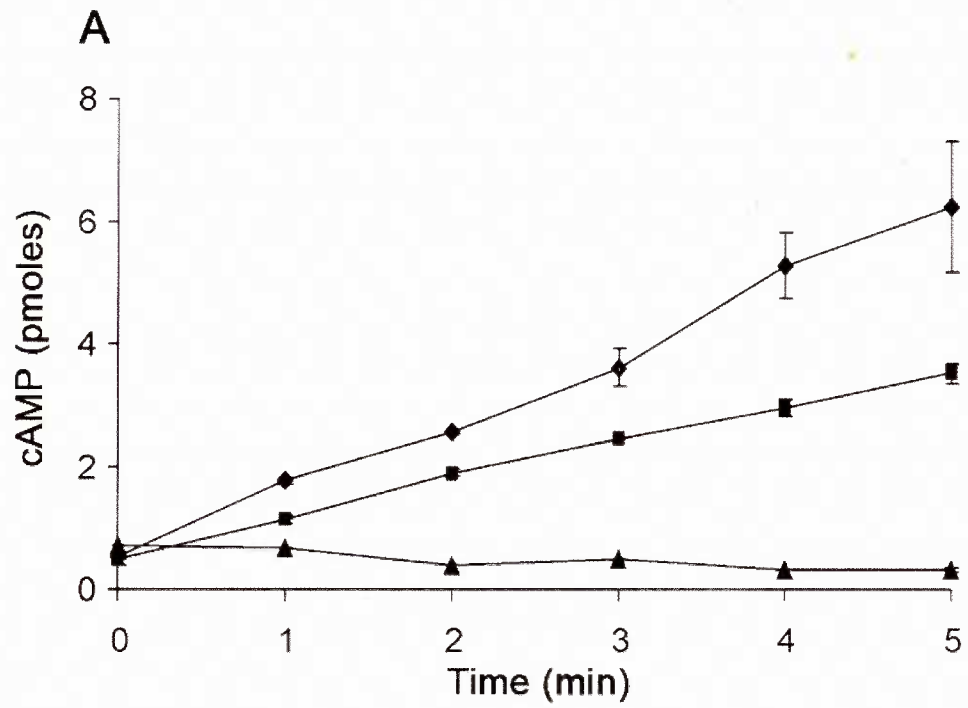


**Figure 15. cAMP accumulation and ACA activation of 5h pulsed JH10, *rasG*, and *rasC*.** (A) Cells of strains JH10 (◆), JH10/*rasG* (■), and JH10/*rasC* (▲) were pulsed with cAMP for 5 h, washed, and then stimulated with 2'-deoxy cAMP (see Materials and Methods). Samples taken at the indicated times were assayed for cAMP accumulation. The means and standard deviations for three independent experiments are shown. (B) The same strains were pulsed with cAMP for 5 h, and then lysates were assayed for ACA activity in the presence of 5 mM MnSO<sub>4</sub> (gray bar), 40 μM GTPγS (black bar), or no additional component (white bar). Plotted values are normalized relative to the unstimulated activity in the absence of MnSO<sub>4</sub> or GTPγS (white bar). Unstimulated activity defined as 1.0. The means and standard deviations for three independent experiments are shown.

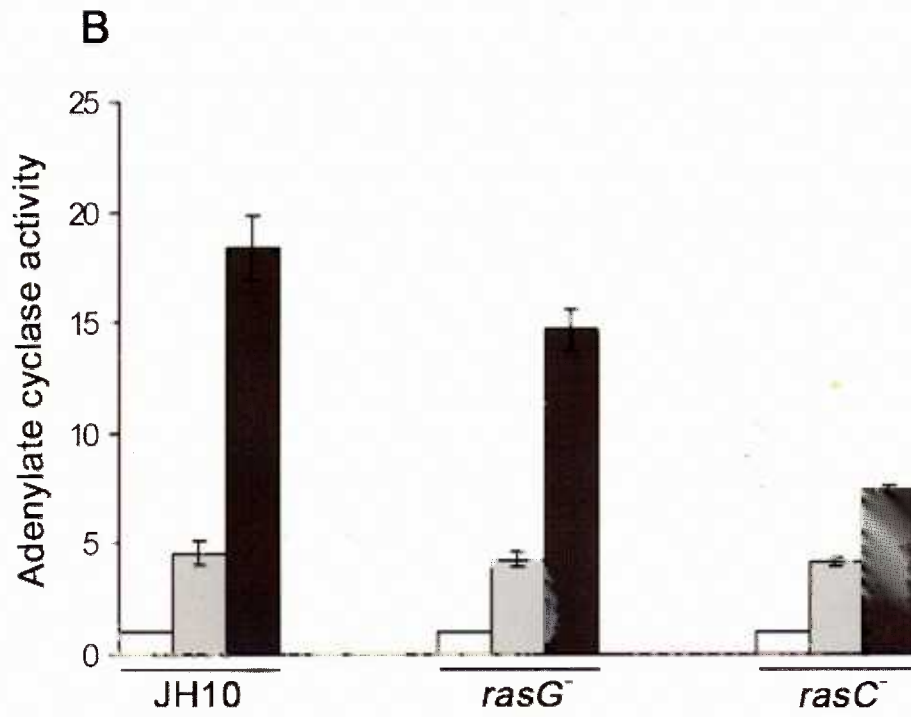
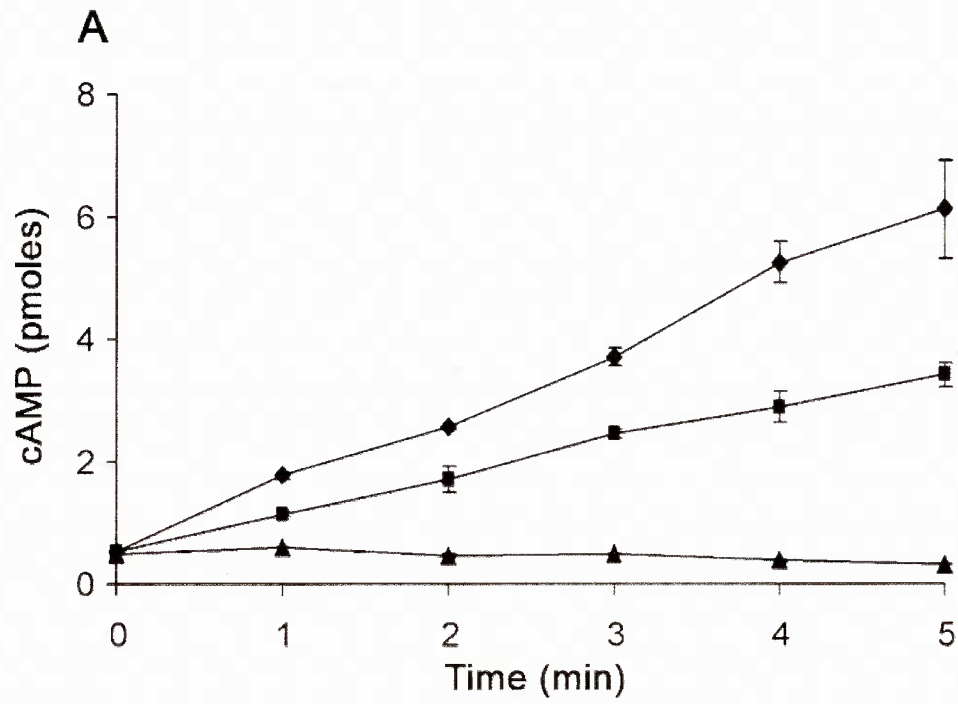


**Figure 16. cAMP accumulation and ACA activation of 8h pulsed JH10, *rasG*, and *rasC*.** (A) Cells of strains JH10 (◆), JH10/*rasG* (■), and JH10/*rasC* (▲) were pulsed with cAMP for 8 h, washed, and then stimulated with 2'-deoxy cAMP (see Materials and Methods). Samples taken at the indicated times were assayed for cAMP accumulation. The means and standard deviations for three independent experiments are shown. (B) The same strains were pulsed with cAMP for 8 h, and then lysates were assayed for ACA activity in the presence of 5 mM MnSO<sub>4</sub> (gray bar), 40 μM GTPγS (black bar), or no additional component (white bar). Plotted values are normalized relative to the unstimulated activity in the absence of MnSO<sub>4</sub> or GTPγS (white bar). Unstimulated activity defined as 1.0. The means and standard deviations for three independent experiments are shown.

(Figures 15B and 16B, and data not shown). These results are consistent with the idea that RasC is more important than RasG for the signal transduction leading to ACA activation. The ACA activity of lysates was also assayed in the presence of  $Mn^{2+}$  (Figures 15B and 16B) to provide an accurate measure of the unstimulated ACA activity. This activity was comparable for JH10, JH10/*rasC*<sup>-</sup>, and JH10/*rasG*<sup>-</sup> lysates, indicating that the lower levels of activation in the latter two cell lysates of these strains was not due to reduced levels of ACA.

### 3.1.10 Activation of RasC and RasG in *rasG*<sup>-</sup> and *rasC*<sup>-</sup> cells in response to cAMP

In vegetative *rasG*<sup>-</sup> cells there was a marked increase in the amount of RasC protein (Figure 4) relative to wild type, suggesting the possibility that RasC is capable of at least partially compensating for the loss of RasG or somehow RasG represses the expression of *rasC*. To determine if the amount of activated RasC produced in response to cAMP was increased in the *rasG*<sup>-</sup> cell, cells were pulsed with cAMP for 5 hours, stimulated with cAMP and the level of GTP bound RasC was determined by an affinity ‘pull-down’ assay (Kae *et al.*, 2004). The activation of RasC in response to cAMP was considerably enhanced in the *rasG*<sup>-</sup> cells (Figure 17A), suggesting that RasC is activated by RasGEFs, that normally target RasG. This higher level of activated RasC might explain why *rasG*<sup>-</sup> cells are reasonably efficient at chemotaxis.

In contrast in *rasC*<sup>-</sup> cells there was only a slight increase in the amount of RasG protein (Figure 4). Similarly, the amount of activated RasG produced 10 seconds following cAMP stimulation was almost identical in the JH10 and *rasC*<sup>-</sup> cells (Figure 17B), indicating no compensatory increase in RasG to account for the loss of RasC. However,

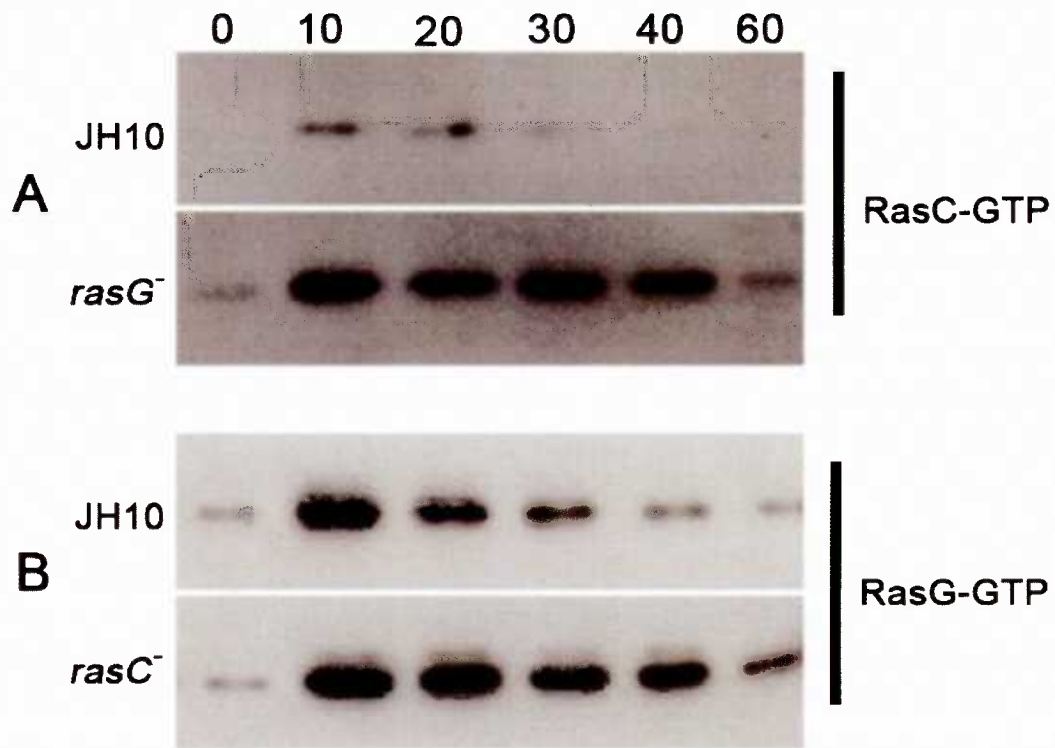


**Figure 17. Ras subfamily protein activation of JH10, *rasG<sup>-</sup>*, and *rasC<sup>-</sup>* in response to cAMP.** Extracts from (A) JH10 and JH10/*rasG<sup>-</sup>*, (B) JH10 and JH10/*rasC<sup>-</sup>* cells, that had been pulsed with cAMP and then subjected to a single cAMP stimulus for the indicated times (in seconds), were bound to GST-Byr2-RBD. The bound material was analyzed by western blots, using antibodies specific for RasC and RasG.

the decrease in RasG after the peak at 10 sec was less pronounced in the *rasC*<sup>-</sup> cells than the JH10 cells suggesting an alteration in the adaptation process in the mutant. These results indicate relatively little compensatory expression of RasG or activation of RasG in response to cAMP in the *rasC*<sup>-</sup> cells. The fact that RasG seems unable to compensate for RasC under these conditions is consistent with the finding that ACA activation is low in these cells.

### 3.1.11 Summary

The study of the newly generated *rasG*<sup>-</sup> strains confirmed a role for RasG in early aggregation and a comparison of the properties of the *rasG*<sup>-</sup> strain with those of the *rasC*<sup>-</sup> strain, in an isogenic background, suggested that RasG was more important for chemotactic functions while RasC was more important for signal relay functions (Bolourani *et al.*, 2006). However, chemotaxis was far from eliminated in *rasG*<sup>-</sup> cells. Furthermore, signal relay functions although very low were not totally eliminated in *rasC*<sup>-</sup> cells. There are three possible explanations for these results: the existence of an additional Ras protein or proteins that fulfill the chemotactic and signal relay function of RasG and RasC in the mutants, an overlap of function between RasG and RasC, and a requirement for both RasG and RasC for optimum activation of ACA and for chemotaxis. To try to distinguish between these possibilities, a *rasC*<sup>-</sup>/*rasG*<sup>-</sup> strain was generated.

## 3.2 cAMP relay and chemotaxis in a *rasC/rasG* strain in response to cAMP

### 3.2.1 Generation of *rasC/rasG* strain

To make a *rasC/rasG* double disruption strain, the *rasC* disruption vector pJLW26, carrying the *rasC* genomic sequences flanking a blasticidin-resistance (*bsr*) selectable marker (Lim et al., 2001), was linearized with EcoRI and transformed into JH10/*rasG* cells by electroporation. Following 8-15 days of selection, the blasticidin-resistant clones were screened by PCR. From 700 clones, two independent *rasC/rasG* cell lines were isolated. Both clones lacked the RasC and RasG proteins and had identical phenotypes. A western blot analysis of one of the strains is shown in Figure 18. Ectopic expression of RasG and RasC protein was accomplished by cotransforming 20 µg of each undigested pRASG-G418 and pJLW30 into *rasC/rasG* cells by electroporation. Ectopic expression of both RasC and RasG restored a wild-type phenotype to the doubly disrupted *rasC/rasG* strain (data not shown). The *rasC/rasG* strains exhibited vegetative growth defects that were similar to those of the *rasG* null strains, defects that are described in detail in a subsequent section (Section 3.4).

### 3.2.2 Developmental phenotype of the *rasC/rasG* cells

When grown in association with bacteria, the *rasC/rasG* cells did not form aggregates on bacterial lawns (Figure 19), a property shared with the JH10/*rasC* cells (Khosla et al., 2005). Aggregation of parental and mutant strains was observed in more detail by plating cells in plastic dishes under non-nutrient buffer and observing cells with an inverted microscope as described. Aggregation streams of JH10 cells were observed 8 h after plating, and typical tight aggregates formed by 12 h (Figure 20A). The *rasC/rasG* strains showed no sign of aggregation or clumping when plated on plastic, even

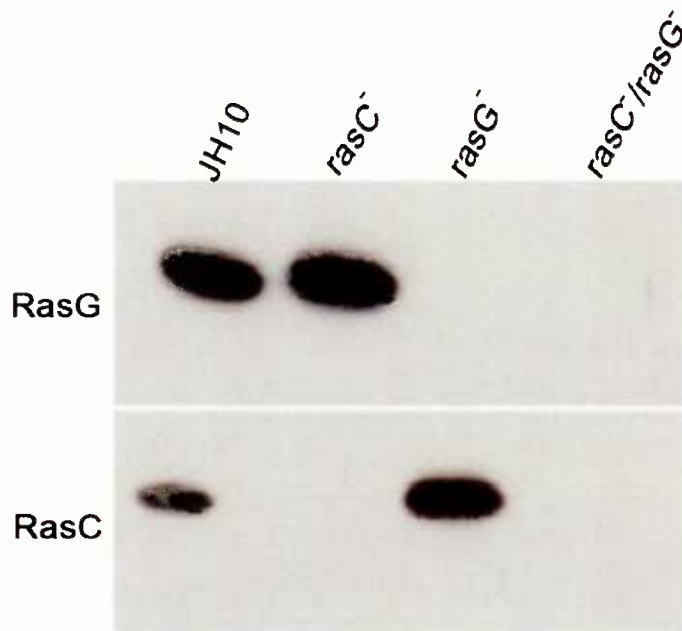


**Figure 18.** Western blot analysis of Ras protein levels of JH10, *rasC*, *rasG*, and *rasC/rasG*. Cell lysates from the JH10, JH10/*rasC*<sup>-</sup>, JH10/*rasG*<sup>-</sup>, and JH10/*rasC*<sup>-</sup>/*rasG*<sup>-</sup> were probed with RasG and RasC specific antibodies, as indicated.

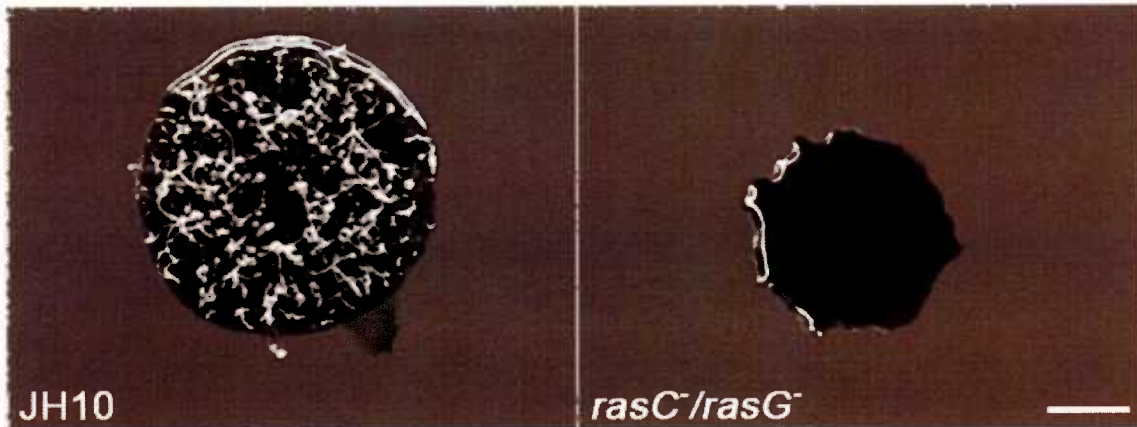


**Figure 19. Multicellular development of JH10, and *rasC*/*rasG* on bacterial growth plates.** Clonal plaque of parental JH10 and *rasC*/*rasG* strains after 5 days growth on a bacterial lawn. Images were taken using a Wild Leitz dissecting microscope. Scale bar is 150  $\mu\text{m}$ .

after prolonged incubation at 22°C (Figure 20B). When pulsed with cAMP for 5 h in shaken suspension prior to plating in plastic dishes, JH10 cells rapidly formed aggregation streams (Figure 20C), whereas *rasC/rasG*<sup>-</sup> cells exhibited no detectable cell-cell association (Figure 20D).

Developmental phenotypes were also assessed by plating cells on nitrocellulose filters under starvation conditions, resting on KK2 saturated support pads, and incubated in a moist container at 22°C. Under these conditions JH10 cells culminated after 24 h. In contrast the *rasC/rasG*<sup>-</sup> cells did not aggregate or form any developmental structures (Figure 21A). To check whether pulsing with cAMP could allow a bypass the aggregation minus phenotype of *rasC/rasG*<sup>-</sup> strain, cells in suspension were pulsed for 5 h and then plated for development on nitrocellulose filters. Although JH10/*rasC*<sup>-</sup> cells formed fruiting bodies under these conditions (Figure 8B), the *rasC/rasG*<sup>-</sup> cells failed to form any developmental structures (Figure 21B).

The finding that the developmental defect of the *rasC/rasG*<sup>-</sup> cells was far more pronounced than that of JH10/*rasC*<sup>-</sup> cells provided additional evidence for an involvement of RasG in early development. A detailed investigation of the ability of doubly disrupted null strain in both chemotactic and signal relay functions was undertaken.

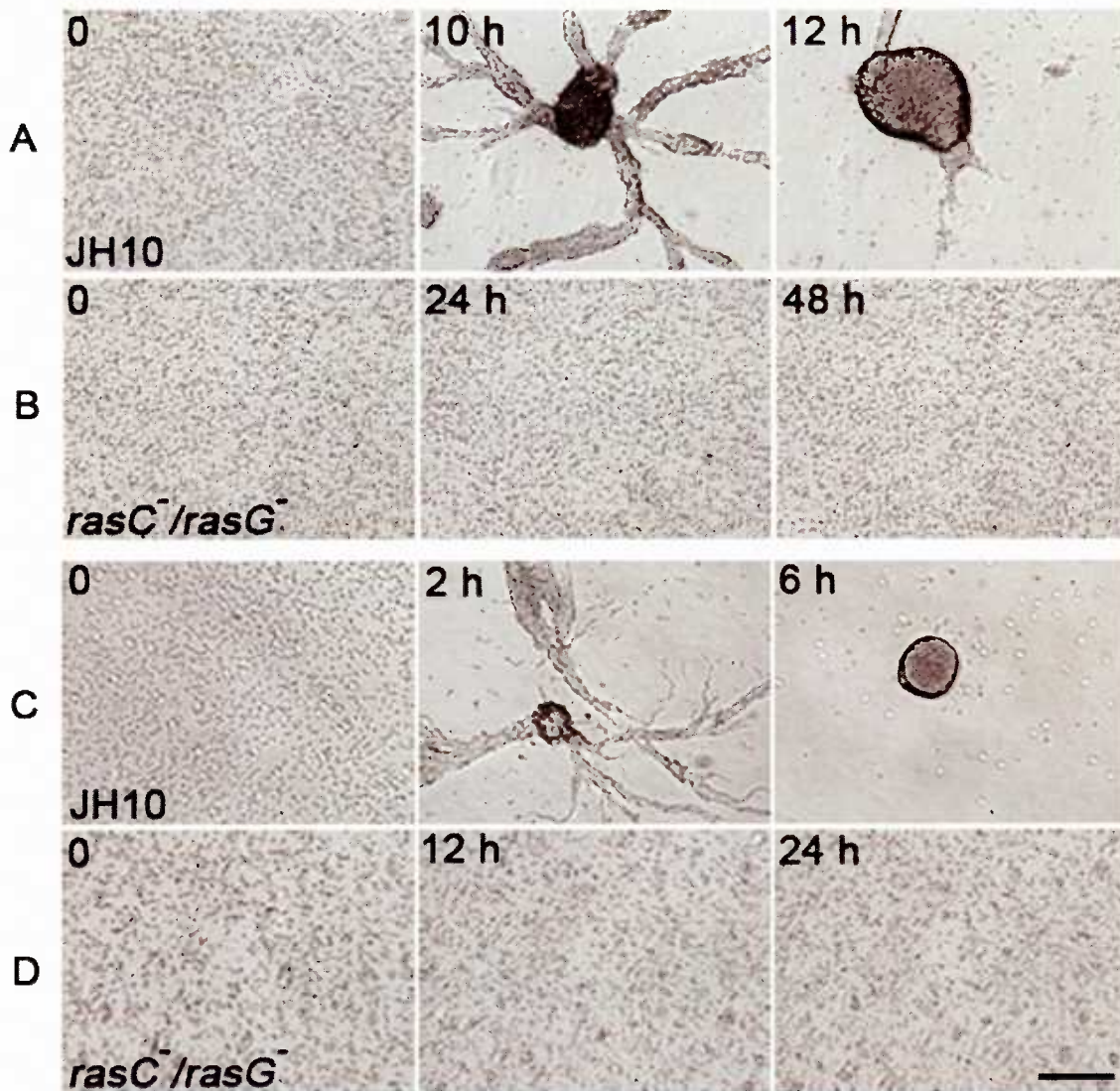


**Figure 20. Aggregation of JH10, and *rasC/rasG* on a plastic surface .** Without (A and B) or with (C and D) 5 h of prior pulsing with cAMP (see Materials and Methods). Strains JH10 (A and C), and *rasC*<sup>-</sup>/*rasG*<sup>-</sup> (B and D) were photographed at the indicated times after plating. Single experiments are shown, but the results for the strains were highly reproducible. Scale bar is 250  $\mu$ m.

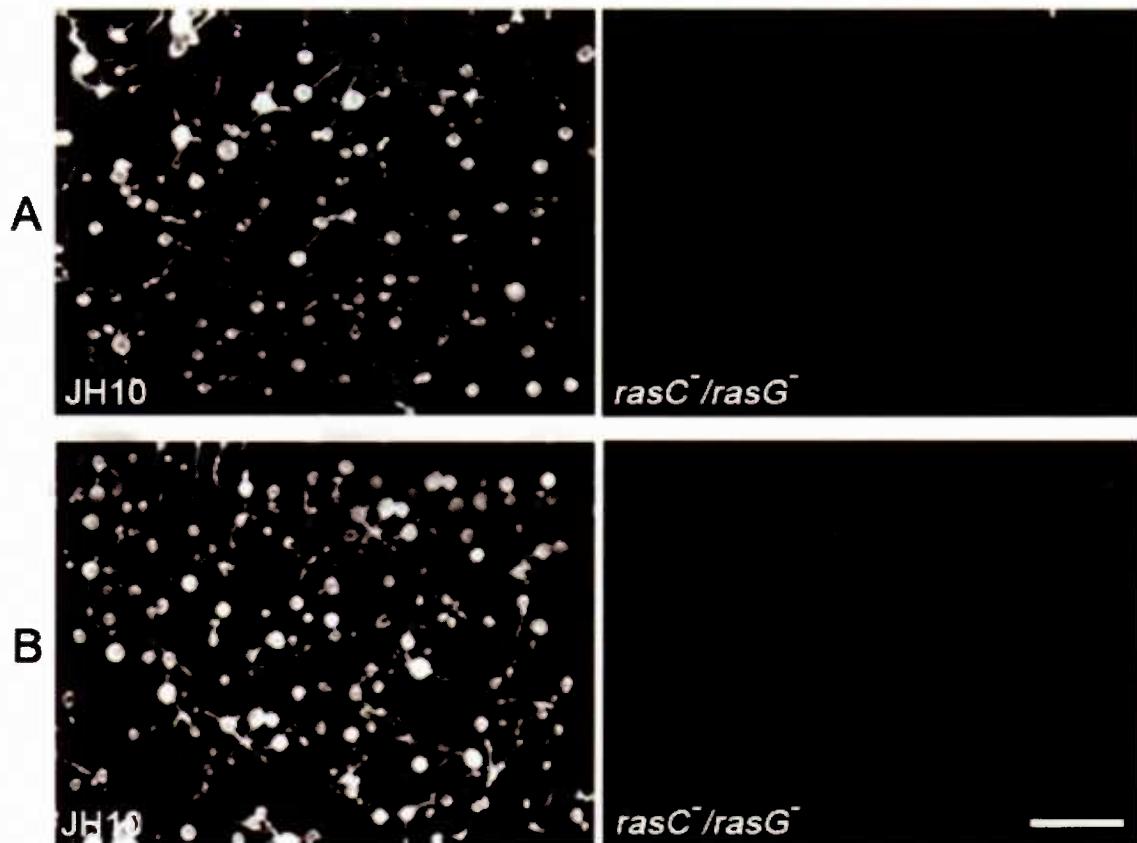


**Figure 21. Development JH10, and *rasC/rasG* on nitrocellulose filters.** (A) Vegetative JH10, and *rasC/rasG* cells or (B) cAMP-pulsed JH10, and *rasC/rasG* cells plated for development on nitrocellulose filters supported by KK2-saturated pads. Images were taken at 22 h after plating using a Wild Leitz dissecting microscope. Scale bar is 150  $\mu\text{m}$ .

### 3.2.3 Early developmental gene expression

Since there was a significant reduction in expression of several early developmental genes in the JH10/*rasG*<sup>-</sup> cells (Figure 9B), the pronounced defect in aggregation of the *rasC*/*rasG*<sup>-</sup> strain might be due to a similar, but more pronounced reduction in gene expression. To test this possibility, cells were pulsed with cAMP in shaken suspension under starvation condition and total RNA was prepared from harvested cells at various time points. The RNA was separated by electrophoresis, and the levels of expression of three representative early developmental genes were then determined by northern blot analysis. In the control JH10 cells, the expression of all three genes increased markedly over the first 8 h, *carA* and *gpaB* normally express at the beginning of aggregation while *csaA* express a little later while cells stick to each other as the result of cell aggregation (Figure 22A). In the *rasC*/*rasG*<sup>-</sup> cells, *carA* expression was negligible and the expression of *gpaB* and *csaA* were markedly reduced (Figure 22B). These decreases were far more pronounced than those observed for the JH10/*rasG*<sup>-</sup> cells (Figure 9B). These data suggest that a significant level of signal transduction through a RasC-dependent pathway contributes to the expression of the early developmental genes in *rasG*<sup>-</sup> cells. The expression of the third gene, *csaA*, was also appreciably lower in the *rasC*/*rasG*<sup>-</sup> cells (Figure 22B) than had been observed for the JH10/*rasG*<sup>-</sup> and JH10/*rasC*<sup>-</sup> cells (Figure 9B and 9C). This low level of early gene expression could explain the total absence of aggregation in the *rasC*/*rasG*<sup>-</sup> strain, since the *rasC*/*rasG*<sup>-</sup> double null strain might have insufficient levels of key essential components of the cAMP signaling pathways.

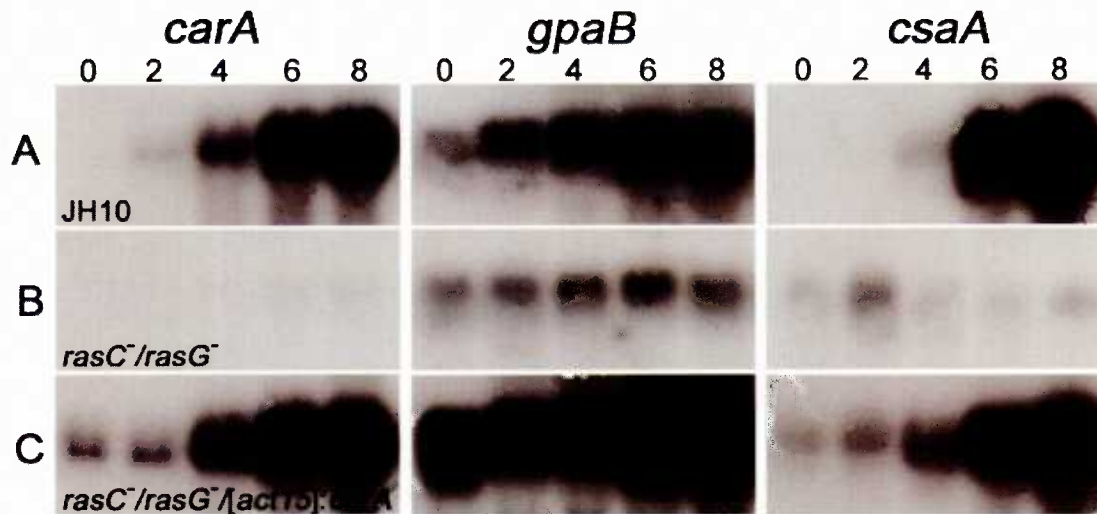


**Figure 22. Northern-blot analysis of early developmental gene expression of JH10, *rasC/rasG*, and *rasC/rasG*/[*act15*]:*carA*.** RNA was isolated from JH10 (A), *rasC*<sup>-</sup>/*rasG*<sup>-</sup> (B), and *rasC*<sup>-</sup>/*rasG*<sup>-</sup>/[*act15*]:*carA* (C) cells, that had been pulsed with cAMP for the indicated times (in hours), and then subjected to electrophoretic fractionation. Blots were hybridized with cDNA probes corresponding to the indicated genes.

### 3.2.4 Restoration of early developmental gene expression in a *rasC/rasG* strain by the ectopic expression of *carA*

Characterization of a *rasC/rasG* double mutant by northern blot analysis had revealed that expression of the early developmentally genes, *carA*, *gpaB* and *csaA* was dramatically reduced, with the effect on *carA* expression being the most pronounced. Since *carA* expression was the most defective, I expressed the gene encoding cAR1 in the *rasC/rasG* strain, in an attempt to provide sufficient cAR1 to allow at least some cAMP signaling. To generate *rasC/rasG*/[*act15*]:*carA* strain, 20 µg of undigested pcAR1-B18 expression vector which contains *carA* cDNA under the control of the constitutively active *actin 15* promoter and a neomycin-resistance cassette (Johnson *et al.*, 1991), was electroporated into *rasC/rasG* cells. Following 10 days of selection, ten G418-resistant clones were selected for further analysis by northern blotting. The northern analysis of one of the clones is shown in Figure 22. *carA* was found to be expressed constitutively in vegetative cells at low level (Figure 22C), and unexpectedly its expression increased dramatically over the course of development. In addition, the expression of the other two early developmental genes was restored (Figure 22C).

To investigate the generality of this phenomenon, the regulatory effect of *carA* on gene expression, the expression of developmentally regulated genes was determined by microarray analysis. Cells were pulsed with cAMP in shaken suspension under starvation condition for 6 h and total RNA was prepared from harvested cells at the indicated time point. The prepared RNAs were subjected to microarray analysis by Dr. Gareth Bloomfield at the 'The Wellcome Trust Sanger Institute'. An expression profile of this analysis, a heatmap, is shown in Figure 23. The heatmap plot shows an overview

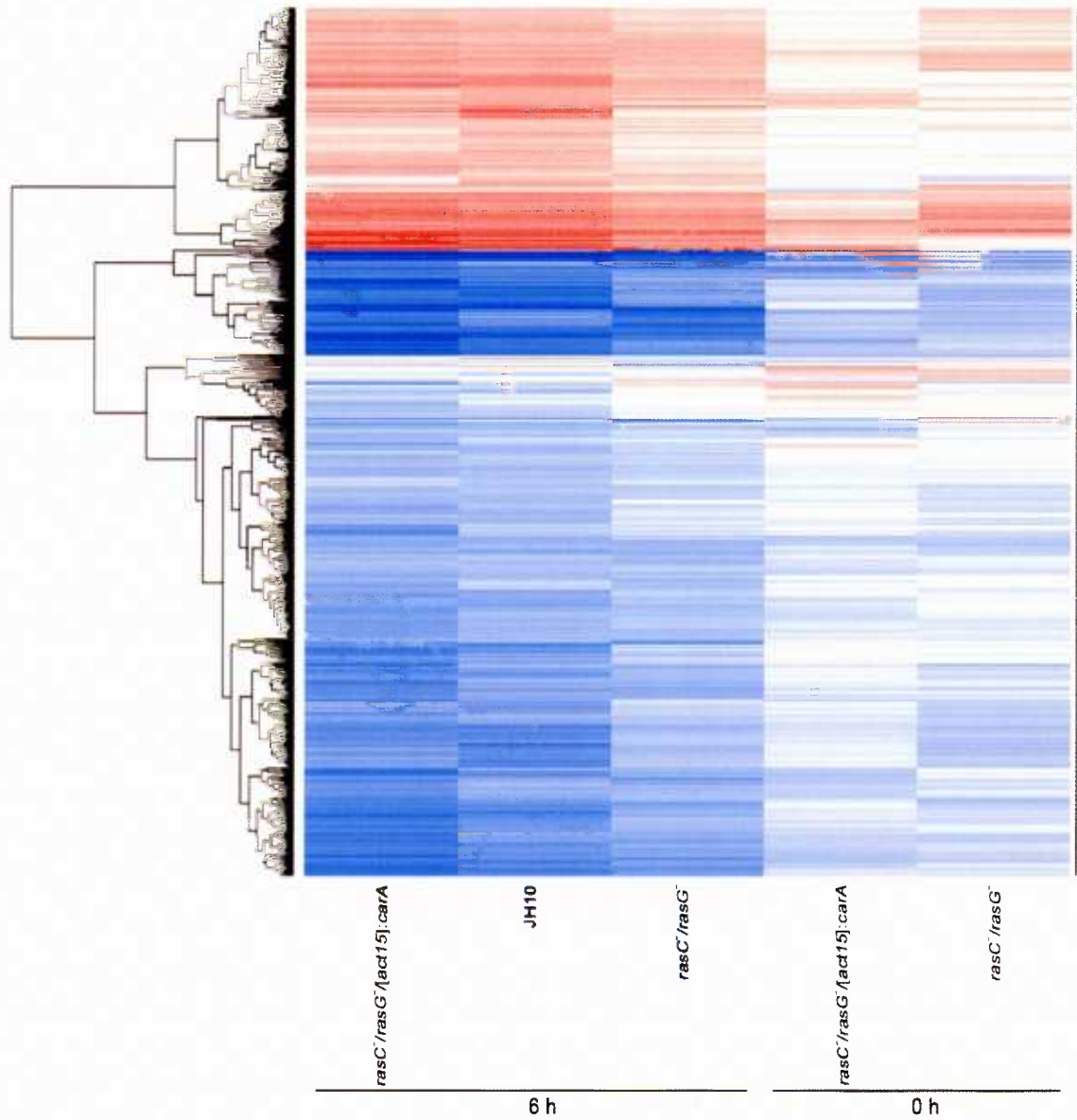
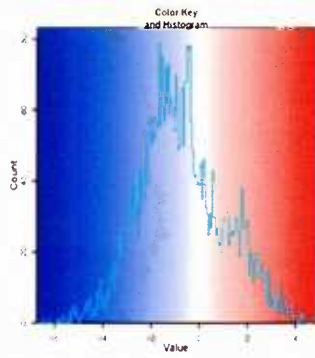


**Figure 23. Expression profiles of early developmental genes.** Heatmap plot displays the gene expression data for the 6 h pulsed *rasC/rasG*/ $\Delta$ *act15*:*carA*, JH10, and *rasC/rasG* and vegetative (0 h) of *rasC/rasG*/ $\Delta$ *act15*:*carA* and *rasC/rasG* relative to wild type cells at 0 h. Each row of the plot represents a gene. The genes with similar expression level relative to wild type cells at 0 h are clustered together and are colored according to the change in expression. Red means the gene has been induced between 0 h and 6 h, blue means it has been repressed. In the top left of the plot there's a scale representing the magnitude of the change, the values are  $\log_2$  ratios.

of the global picture regarding the gene expression. It displays levels of expression of genes differentially regulated in *rasC/rasG*/[*act15*]:*carA*, JH10, and *rasC/rasG* (at 6 h of development) and *rasC/rasG*/[*act15*]:*carA* and *rasC/rasG* (at 0 h of development) relative to wild type cells at 0 h. Each row of the plot represents a gene. The findings indicate that approximately 20% of the estimated 9000 genes were induced in 6 h developed wild type cells. For simplicity, I focused the analysis on the 129 genes that were expressed at least a fivefold-higher after 6 h of development. Of these 129 genes, 68 were not five-fold induced in *rasC/rasG* cells. This overexpression of *carA* in vegetative cells restored the developmentally regulated expression of most of the developmental genes that were suppressed in the *rasC/rasG* strain. A visual inspection of the microarray data (Figure 23) indicated that the expression of a few of the developmentally regulated genes was not apparently rescued. Further analysis of the quantitative data for the most prominent three genes in this category revealed (Dicty ID number: DDB0219883, DDB0217914, DDB0198869) that they were only 2.5 fold developmentally induced. The first two genes are identical and encode a hypothetical 127 KDa protein with uncharacterized function and the third is a putative DEAD/DEAH box helicase. However, other than these three exceptions, ectopic expression of *carA* in the *rasC/rasG* cells provided a strain (*rasC/rasG*/[*act15*]:*carA*) in which the expression of the cAMP signaling components was restored. This strain was then used to investigate the role of RasG and RasC proteins in cAMP induced signal transduction pathway. Overexpression of *carA* in vegetative *rasC/rasG* cells also resulted in a five fold increase in expression of an additional 32 genes. One of these genes, *atr1* (DDB0183856), encodes a phosphatidylinositol 3-kinase-related protein kinase similar to

protein kinase ATR, which belongs to the PIKK family of protein kinases and modulates cell cycle progression and DNA repair and in other organisms (Abraham, 2001). This observation was not pursued further in this thesis, but is certainly worthy of further investigation.

### 3.2.5 cAMP binding assay

In order to demonstrate that the restored *carA* expression in the *rasC/rasG*  $\Delta$ [*act15*]:*carA* strain produced functional cAR1, I determined the binding of cAMP to the cell surface of cAMP pulsed cells. *rasC/rasG*, and *rasC/rasG*  $\Delta$ [*act15*]:*carA* cells were pulsed with cAMP, treated with caffeine, washed and then incubated with <sup>3</sup>H-cAMP. The binding of <sup>3</sup>H-cAMP to the cell surface was measured by the ammonium sulfate stabilization assay as explained in Materials and Methods. The results, shown in Table 7, indicated that cAMP binding was reduced, as expected, in the *rasC/rasG* relative to JH10, but restored to greater than wild type levels in the *rasC/rasG*  $\Delta$ [*act15*]:*carA* cells. This result was consistent with the idea that the overexpression of *carA* indicated in Figure 22 resulted in functional protein being localized on the surface of the *rasC/rasG*  $\Delta$ [*act15*]:*carA* cells.

**Table 7. Cell surface associated-cAMP binding activity.**

<b>Strain</b>	<b>cAMP bound (nmoles /10<sup>7</sup> cells) <sup>a</sup></b>
<b>JH10</b>	<b>4.3 ± 0.4</b>
<b><i>rasC/rasG</i></b>	<b>0.8 ± 0.2</b>
<b><i>rasC/rasG</i> /<i>act15</i>:<i>carA</i></b>	<b>6.6 ± 0.5</b>

<sup>a</sup> The values are the means ± SEM of two independent experiments.

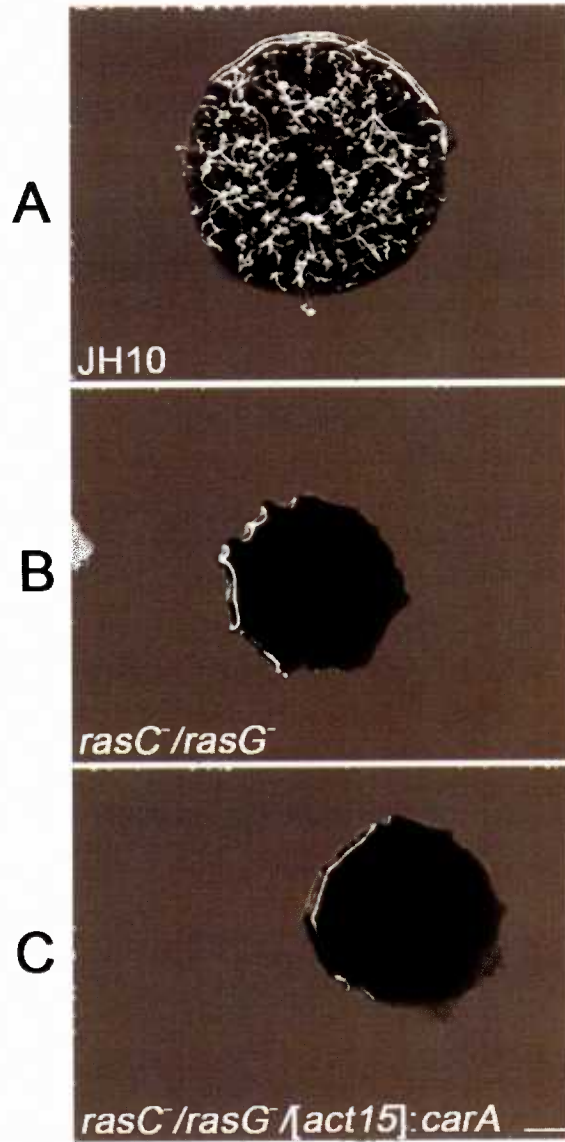


**Figure 24. Multicellular development of JH10, *rasC/rasG*, and *rasC/rasG*  $\Delta$ *act15*:*carA* on bacterial growth plates.** Clonal plaque of parental JH10 and JH10/*rasC*<sup>-</sup>/*rasG*<sup>-</sup> and *rasC*<sup>-</sup>/*rasG*<sup>-</sup>/ $\Delta$ *act15*:*carA* strains after 5 days growth on a bacterial lawn. Images were taken using a Wild Leitz dissecting microscope. Scale bar is 150  $\mu$ m.

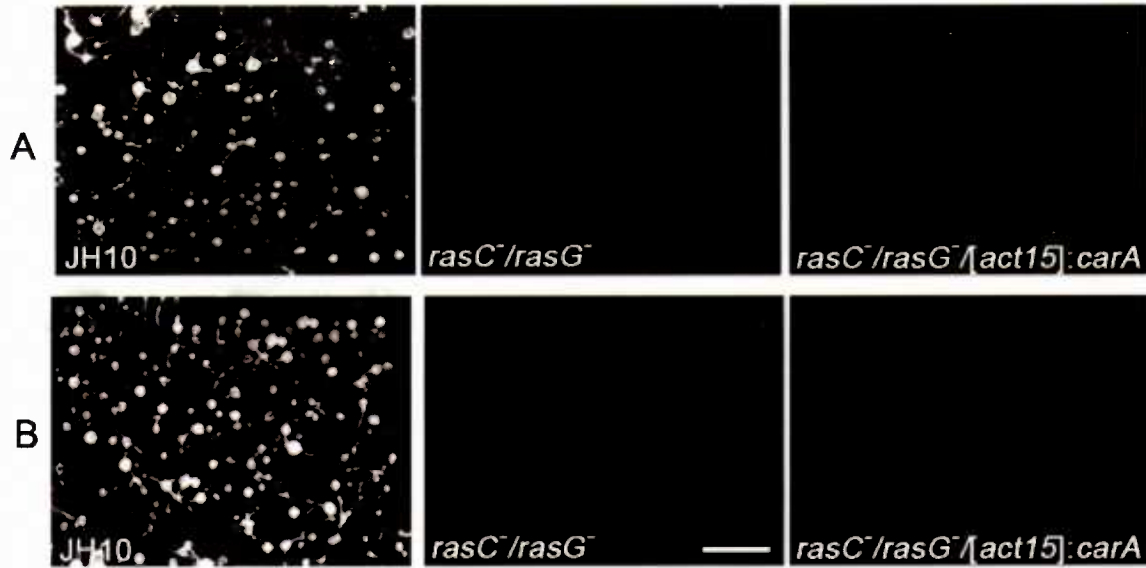


**Figure 25. Development of JH10, *rasC*/*rasG*, and *rasC*/*rasG*[*act15*]:*carA* on nitrocellulose filters.** (A) Vegetative JH10, *rasC*/*rasG*, and *rasC*/*rasG*[*act15*]:*carA* cells or (B) cAMP-pulsed JH10, *rasC*/*rasG*, and *rasC*/*rasG*[*act15*]:*carA* cells plated for development on nitrocellulose filters supported by KK2-saturated pads. Images were taken at 22 h after plating using a Wild Leitz dissecting microscope. Scale bar is 150  $\mu$ m.

### 3.2.6 Developmental phenotype of the *rasC/rasG* $\Delta$ *act15*:*carA* cells

When grown in association with bacteria, the *rasC/rasG*  $\Delta$  *act15*:*carA* cells did not form aggregates on bacterial lawns (Figure 24). In addition, the *rasC/rasG*  $\Delta$  *act15*:*carA* cells did not aggregate or form any developmental structures when cells were plated on nitrocellulose filters under starvation conditions (Figure 25A), the same phenotype observed for the *rasC/rasG* cells. To check whether cAMP pulses allowed a bypass of the aggregation minus phenotype of *rasC/rasG*  $\Delta$  *act15*:*carA* cells, cells in suspension were pulsed for 5 h and then plated on nitrocellulose filters. Under these conditions, the *rasC/rasG*  $\Delta$  *act15*:*carA* cells again failed to form any developmental structures (Figure 25B).

Next, I examined the developmental phenotype of *rasC/rasG*  $\Delta$  *act15*:*carA* cells on plastic dishes. Aggregation streams were not observed when unpulsed *rasC/rasG*  $\Delta$  *act15*:*carA* cells were plated in plastic dishes under non-nutrient buffer, although small clumps of cells were formed after prolonged incubation (Figure 26C), similar to those observed previously for *AX2/rasC* (Lim *et al.*, 2001) and *JH10/rasC* cells (Figure 7C). The *rasC/rasG* cells did not clump under these conditions (Figure 26B). Aggregation streams of the control *JH10* cells were observed 10 h after plating and typical tight aggregates formed by 12 h (Figure 26A). When pulsed with cAMP for 5 h before plating in plastic dishes, *rasC/rasG*  $\Delta$  *act15*:*carA* exhibited the same phenotype as the non pulsed cells (data not shown). This phenotype is quite different from that of the *JH10/rasC* cells that formed large clumps, although without detectable aggregate stream formation, under these conditions (Figure 7F). These results demonstrate clearly that cells containing neither RasG nor RasC are incapable of aggregation under any of the

experimental conditions tested and suggest that the cAMP relay and chemotaxis signals transduced from cAMP are transmitted only by the RasC or RasG pathways.

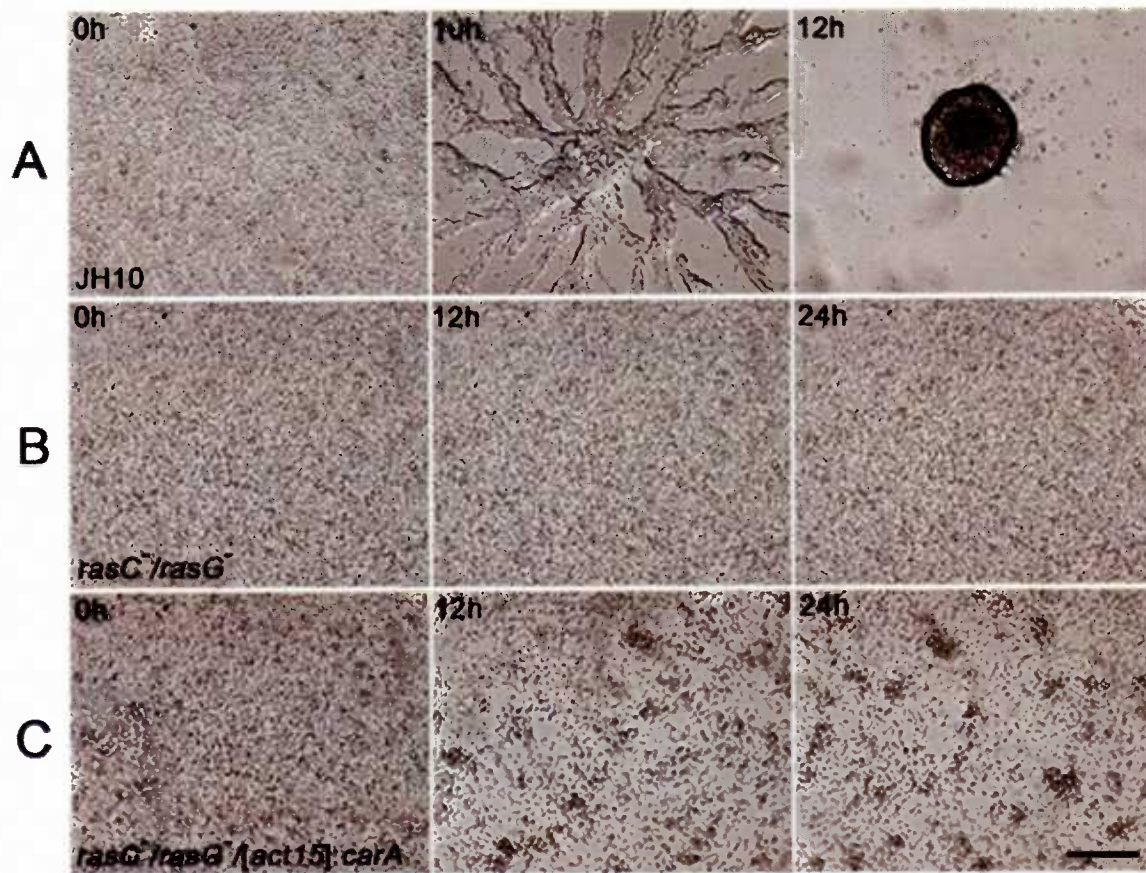


**Figure 26.** Aggregation of JH10, *rasC/rasG*, and *rasC/rasG[act15]:carA* on a plastic surface . Strains JH10 (A), *rasC/rasG* (B), and *rasC/rasG[act15]:carA* (C) were photographed at the indicated times after plating. Single experiments are shown, but the results for the strains were highly reproducible. Scale bar is 250  $\mu$ m.

### 3.2.7 The RasG and RasC pathways are essential for adenylyl cyclase (ACA) activation

As described in section 1, the activation of ACA is essential during aggregation to provide the extracellular cAMP to relay the signal through the population (Parent and Devreotes, 1996). The level of ACA activity can be measured using GTP $\gamma$ S which stimulates ACA activity in cell lysates by efficiently uncoupling the G $\beta\gamma$  subunit from the heterotrimeric G-protein (Theibert and Devreotes, 1986; Parent and Devreotes, 1996). As indicated previously (Figure 15B and 16B), the basal ACA activity was similar for JH10, JH10/*rasG*<sup>-</sup> and JH10/*rasC*<sup>-</sup> cells, indicating that the lower levels of ACA activation in these strains were not due to reduced basal levels of enzyme. However, the ACA activity was reduced in *rasC/rasG*<sup>-</sup> cells (Figure 27), suggesting that these cells expressed less enzyme, a result consistent with the defect in early gene expression (Figure 22). In contrast, cAMP pulsed *rasC/rasG*<sup>-</sup>/*act15*:*carA* cells, had the same basal level of ACA activity as wild type cells. When stimulated with GTP $\gamma$ S, there was no increase in ACA activity in either *rasC/rasG*<sup>-</sup> or in *rasC/rasG*<sup>-</sup>/*act15*:*carA* cells (Figure 27). These results indicate that *rasC/rasG*<sup>-</sup>/*act15*:*carA* cells are incapable of cAMP induced signal relay and are in marked contrast to those obtained for cells with single *ras* gene disruptions (Figure 15B). Thus, signal transduction from the heterotrimeric G protein to ACA must involve either RasC or RasG.

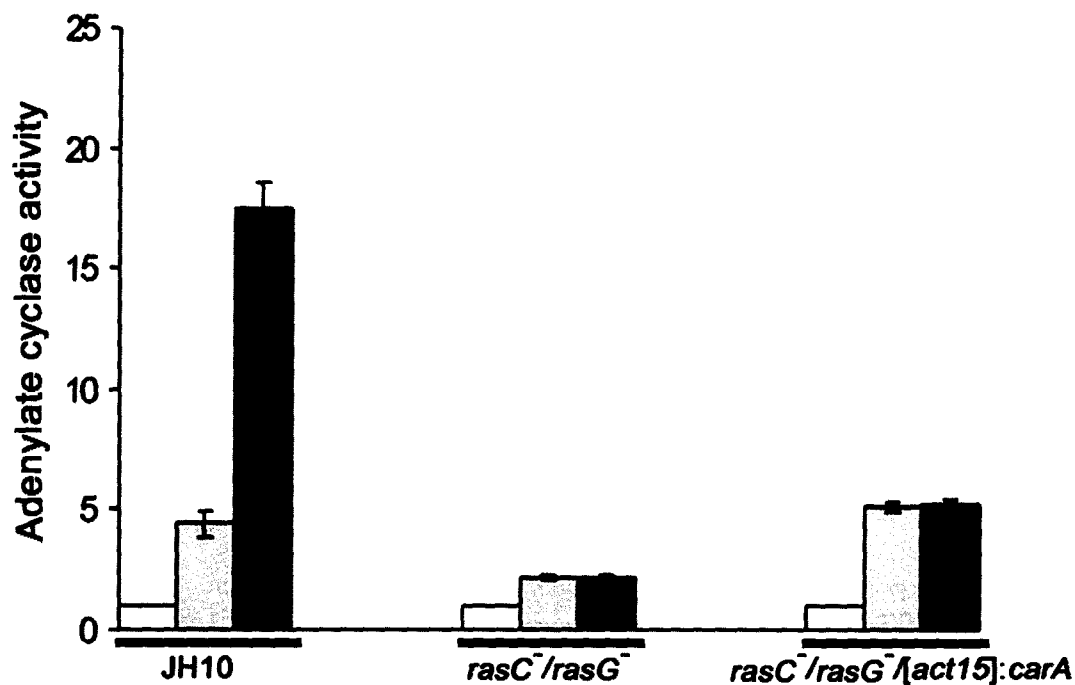


**Figure 27.** *In vitro* GTPγS stimulation of adenylyl cyclase activity of JH10, *rasC*<sup>-</sup>/*rasG*<sup>-</sup>, and *rasC*<sup>-</sup>/*rasG*<sup>-</sup>[*act15*]:*carA*. JH10, *rasC*<sup>-</sup>/*rasG*<sup>-</sup>, and *rasC*<sup>-</sup>/*rasG*<sup>-</sup>[*act15*]:*carA* cells were pulsed with cAMP for 5 h and lysates were assayed for ACA activity in the presence of 5 mM MnSO<sub>4</sub> (gray bar), 40 μM GTPγS (black bar), or no additional component (white bar). Plotted values are normalized relative to the unstimulated activity in the absence of MnSO<sub>4</sub> or GTPγS (white bar). Unstimulated activity defined as 1.0. The means and standard deviations for three independent experiments are shown.

### 3.2.8 The RasG and RasC pathways are essential for chemotaxis, PKB phosphorylation, and guanylyl cyclase activation

To test the cells for their chemotaxis response, *rasC/rasG* cells and *rasC/rasG*  $\Delta$ [*act15*]:*carA* cells were pulsed for 5 hours with cAMP and subjected to a spatial gradient created by diffusion of cAMP from the tip of a micropipet. JH10 cells were highly polarized at the beginning, responded quickly and migrated rapidly toward the cAMP source as in Figure 28A. *rasC/rasG* cells and *rasC/rasG*  $\Delta$ [*act15*]:*carA* cells exhibited no net migration to the pipette tip (Figure 28B and 28C). A few cells did show slight movement toward the tip but then dispersed.

Chemotactic indices were calculated as described for Table 6 and the values confirmed the negligible levels of chemotaxis towards cAMP in the *rasC/rasG* and the *rasC/rasG*  $\Delta$ [*act15*]:*carA* cells (Table 8). The very low levels of chemotaxis in these strains indicate that the vast majority of signaling requires RasG or RasC, but does not preclude the possibility of a very low level of chemotaxis that does not require signaling through either RasC or RasG. The results for the double *ras* gene deletion strains are in contrast to those obtained for the single *ras* gene deletion strains, which both exhibited appreciable chemotaxis (see Table 6). The calculated average instantaneous velocities of the *rasC/rasG* and *rasC/rasG*  $\Delta$ [*act15*]:*carA* cells were lower than those for the wild type, but both strains are clearly still capable of appreciable motility (Table 8). Thus the defect observed in chemotaxis is due to lack of directed motion, not a general loss of motility.

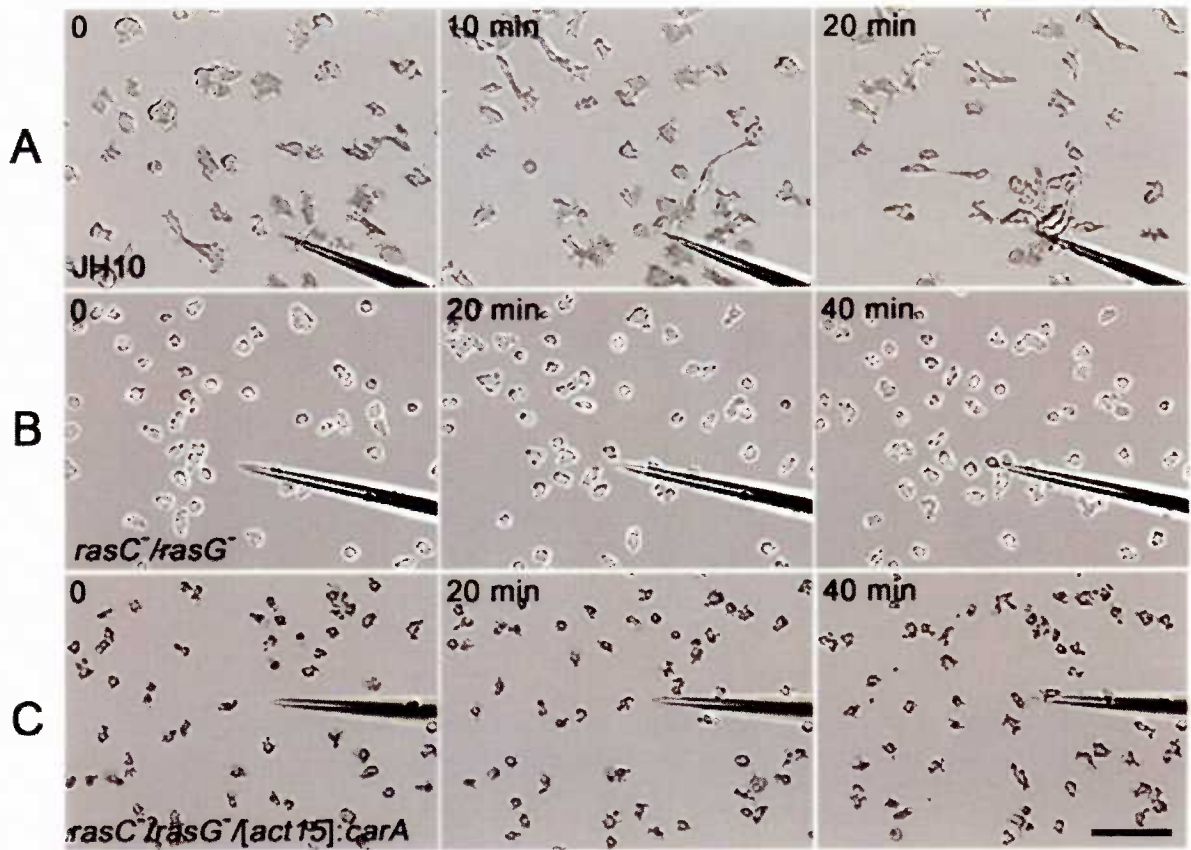


**Figure 28. Chemotaxis of JH10, *rasC/rasG*, and *rasC/rasG*  $\Delta$ [*act15*]:*carA* cells towards a source of cAMP .** Cells of strains JH10 (A), *rasC/rasG* (B), and *rasC/rasG*  $\Delta$ [*act15*]:*carA* (C) had been pulsed with cAMP for 5 h were photographed at the indicated times following the release of cAMP from the micropipette tip. Scale bar is 50  $\mu$ m.

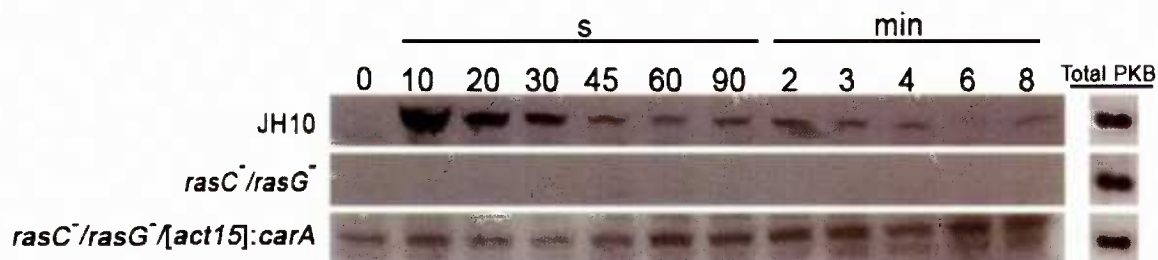
**Table 8. Chemotaxis analysis of *Dictyostelium* cells in a spatial gradient of cAMP.**

Strain	Instantaneous velocity ( $\mu\text{m}/\text{min}$ )	Chemotaxis index <sup>a</sup>
JH10 (n = 20)	11.2 $\pm$ 1.5	0.62 $\pm$ 0.12
<i>rasC/rasG</i> (n = 20)	6.6 $\pm$ 3.3	0.05 $\pm$ 0.02
<i>rasC/rasG</i> $\Delta$ <i>act15</i> ; <i>carA</i> (n = 20)	5.9 $\pm$ 3.4	0.04 $\pm$ 0.01

Values are mean  $\pm$  SD; n = number of cells

<sup>a</sup> Chemotaxis index was calculated as the net distance traveled towards the source of chemoattractant divided by the total distance traveled in that time period.

It has been suggested that PI3K-mediated signaling pathway is important for *Dictyostelium* chemotaxis (Iijima *et al.*, 2002; Manahan *et al.*, 2004; Postma *et al.*, 2004; Loovers *et al.*, 2006; Takeda *et al.*, 2007). To analyze PI3K activation in response to cAMP, the phosphorylation of PKB, a downstream target of PI3K, was monitored by probing the lysates of cAMP-stimulated *rasC/rasG* and *rasC/rasG*  $\Delta$  *act15*; *carA* cells by western blotting using a phosphothreonine-specific antibody that is capable of unambiguously detecting the phosphorylation of PKB (Lim *et al.*, 2001). In JH10 cells, PKB was transiently phosphorylated after 10 s in response to cAMP (Figure 29). In the *rasC/rasG* cells the increase in phosphorylation was totally absent. In *rasC/rasG*  $\Delta$  *act15*; *carA* cells transient activation of PKB was also absent although the basal level of phosphorylated PKB was higher compared to wild type (Figure 29). The elevated basal levels of phosphorylated PKB suggest an upstream kinase that is upregulated (or a

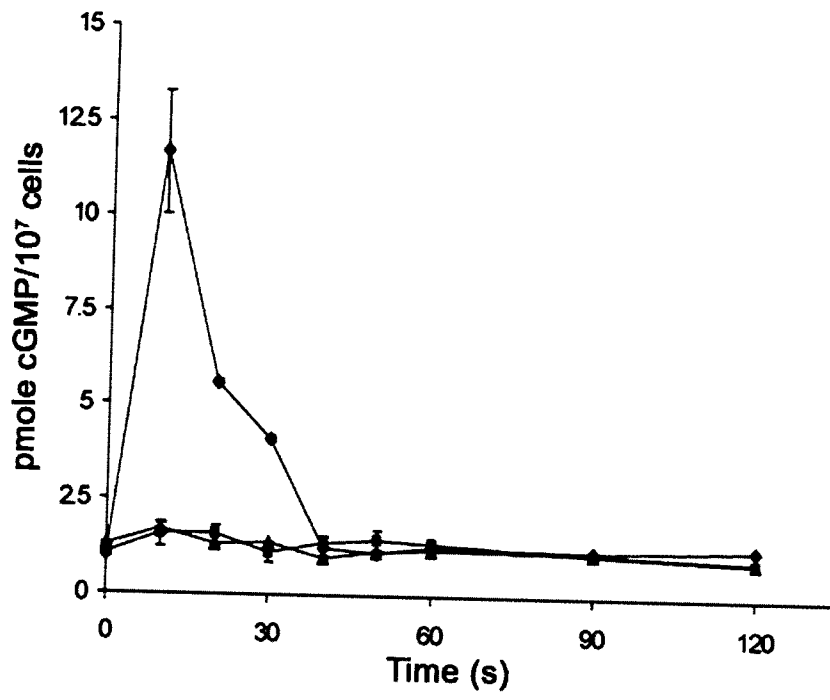
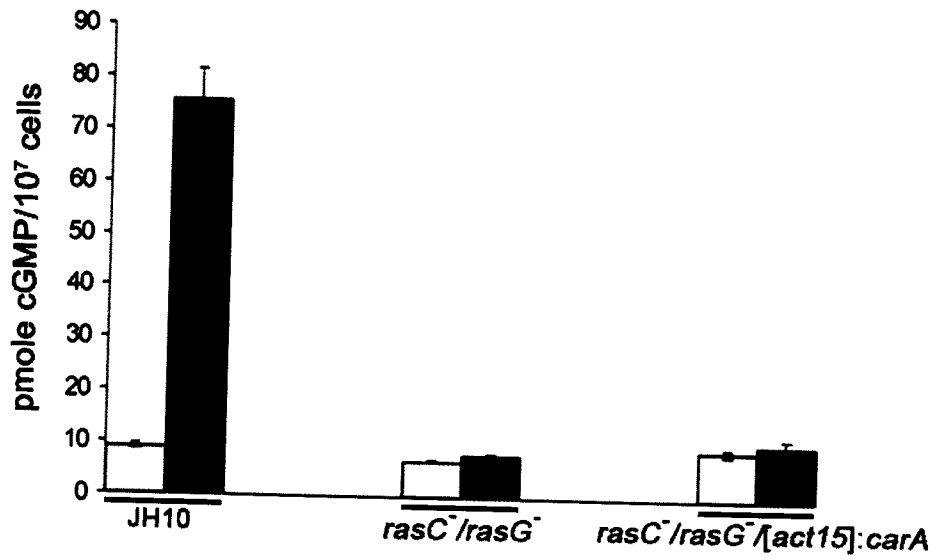


**Figure 29. PKB phosphorylation of JH10, *rasC*/*rasG*, and *rasC*/*rasG* [*act15*]:*carA* cells in response to cAMP.** Extracts from JH10, *rasC*/*rasG*<sup>-</sup>, and *rasC*/*rasG*<sup>-</sup> [*act15*]:*carA* cells that had been pulsed with cAMP for 5 h, were prepared at the indicated times after a single 100 nM cAMP stimulus and subjected to Western-blot analysis using a phosphothreonine-specific antibody.

downstream phosphatase that is downregulated) by the overexpression of *carA*. The microarray data could help to identify potential candidate molecules. The total amounts of PKB protein, as detected using a PKB specific antibody, were identical in all three strains. These results demonstrate that all cAMP-dependant signal transduction leading to PKB phosphorylation occurs through either RasG or RasC.

cGMP production in response to cAMP was also monitored in the *ras* mutant strains. To do these studies, cAMP pulsed cells were washed and treated with caffeine, stimulated with cAMP and the cGMP levels were then measured using a cGMP-[<sup>3</sup>H] assay kit as described in Materials and Methods. In the JH10 parental cell line, there was a burst of cGMP production 10 s after the application of cAMP, which then returned to the basal level after about 30 s. However, this response was not detectable in *rasC/rasG*  $\Delta$ [*act15*]:*carA* cells or *rasC/rasG* cells (Figure 30A), consistent with a requirement of either RasC or RasG for the burst of cGMP after stimulation.

It has been shown previously that GTP $\gamma$ S stimulates guanylyl cyclase activity (van Haastert and Kuwayama, 1997) and the involvement of a monomeric G protein has therefore been proposed (Wu *et al.*, 1995). The availability of the *rasC/rasG*  $\Delta$ [*act15*]:*carA* strain allowed an investigation of the possibility that RasC or RasG are the previously invoked monomeric G proteins required for GTP $\gamma$ S stimulation of guanylyl cyclase activity in cell lysates. GTP $\gamma$ S-stimulated activity of guanylyl cyclase was not detectable in either the *rasC/rasG* or *rasC/rasG*/ $\Delta$ [*act15*]:*carA* cell lysates (Figure 30B). These results are consistent with the conclusion that all cAMP signal transduction responsible for guanylyl cyclase activation is mediated through pathways involving either RasG or RasC.

**A****B**

**Figure 30. cGMP production in response to cAMP and *In vitro* GTP $\gamma$ S stimulation of guanylyl cyclase activity of JH10, *rasC/rasG*, and *rasC/rasG* $\Delta$ *act15*:*carA* cells .** (A) JH10 ( $\blacklozenge$ ), *rasC/rasG* ( $\blacksquare$ ), and *rasC/rasG* $\Delta$ *act15*:*carA* ( $\blacktriangle$ ) cells were pulsed for 5 h with cAMP, washed, and then stimulated with 100 nM cAMP. Samples were taken at the indicated times and assayed for cGMP accumulation (see Material and Methods). The means and standard deviations for three independent experiments are shown. (B) JH10, *rasC/rasG*, and *rasC/rasG* $\Delta$ *act15*:*carA* cells were pulsed with cAMP for 5 h and lysates were then assayed for guanylyl cyclase activity in the absence (gray bar), or the presence of GTP $\gamma$ S (black bar). The means and standard deviations for three independent experiments are shown.

### 3.2.9 Rap activation in *ras*<sup>-</sup> cells

Rap1 in *Dictyostelium discoideum*, has been linked to cytoskeletal regulation, response to osmotic stress, and phagocytosis (Rebstein *et al.*, 1993; Rebstein *et al.*, 1997; Kang *et al.*, 2002). It has been shown that the reduction of Rap1 expression suppresses cGMP production and impairs cell viability, whereas the expression of constitutively active Rap1<sup>G12V</sup> enhances cGMP production (Kang *et al.*, 2002). The recent finding that Rap1 is also activated in response to cAMP (Jeon *et al.*, 2007) suggests that Rap1 might be able to compensate for RasG and RasC in the *rasC*<sup>-</sup>/*rasG*<sup>-</sup>/*act15*:*carA* mutant and this activation might account for the fact that this strain does exhibit very low levels of chemotaxis. Rap1 activation was therefore determined in the various *ras* null strains. For this experiment, cAMP pulsed cells treated with caffeine and then stimulated with cAMP to 15 μM. Aliquots were then taken at the indicated time points, lysed, and the level of activated Rap was measured using the RBD binding assay as described in Materials and Methods. There was a high basal level of activated Rap1 in JH10 cells, and there was an additional activation in response to cAMP that tested over 60 s (Figure 31). The initial, maximum activation was only slightly reduced (if at all) in *rasC*<sup>-</sup> cells compared to JH10 cells, but was not detectable in *rasG*<sup>-</sup>, *rasC*<sup>-</sup>/*rasG*<sup>-</sup> and *rasC*<sup>-</sup>/*rasG*<sup>-</sup>/*act15*:*carA* cells, and the basal level of Rap1 was lower in the in the *rasG*<sup>-</sup>, *rasC*<sup>-</sup>/*rasG*<sup>-</sup> strains (Figure 31). These data indicate that Rap1 activation occurs mainly downstream of RasG and that signaling through RasG is essential for Rap1 activation. Since there may have been slightly lower activation of Rap1 in *rasC*<sup>-</sup> cells, I cannot preclude the possibility that some signaling goes through RasC.

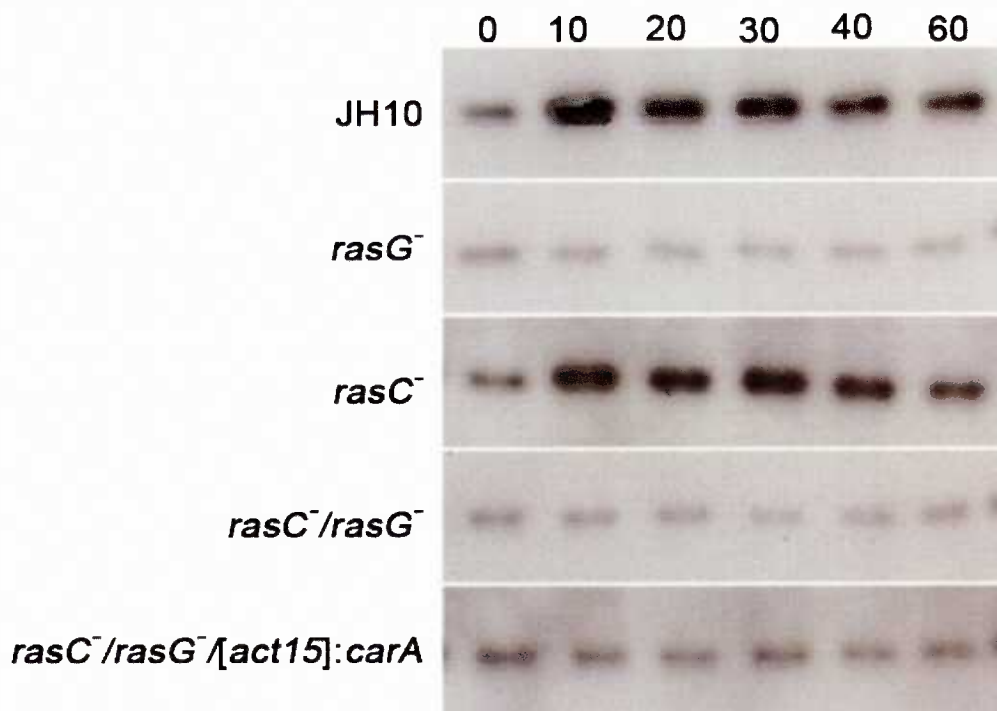


**Figure 31. Rap activation in response to cAMP.** Extracts from JH10, *rasG*<sup>-</sup>, *rasC*<sup>-</sup>, *rasC*<sup>-</sup>/*rasG*<sup>-</sup>, and *rasC*<sup>-</sup>/*rasG*<sup>-</sup>/[*act15*]:*carA* cells, that had been pulsed with cAMP and then subjected to a single cAMP stimulus for the indicated times (in seconds), were bound to GST-Byr2-RBD. The bound material was analyzed by western blots, using an antibody specific for Rap1.

### 3.2.10 Summary

The ectopic expression of *carA* restored early developmental gene expression to the *rasC*/*rasG*<sup>-</sup> strain, rendering it suitable for an analysis of cAMP signal transduction. The results indicated that RasG and RasC are the only two Ras subfamily proteins that directly control cAMP chemotactic and the adenylyl cyclase activation pathways. Rap1 is also activated in response to cAMP and the results suggests that Rap1 activation occurs downstream of the Ras proteins and predominantly, if not exclusively, downstream of RasG (Bolourani *et al.*, 2008).

### **3.3 Identification of the amino acid residues in RasC and RasG required for specificity during aggregation**

#### **3.3.1 RasC and RasG expression from introduced *rasC* and *rasG* transgenes in *rasG*<sup>-</sup> and *rasC*<sup>-</sup> strains**

The results from the analysis of the *rasC*<sup>-</sup>/*rasG*<sup>-</sup>/[*act15*]:*carA* mutant strain indicated that the chemotactic and ACA activation responses to cAMP are mediated through either RasG or RasC. The comparison of cAMP relay and chemotaxis in the single null strains indicated that RasC is predominantly involved in ACA activation and RasG is predominantly involved in chemotaxis. The partial ACA activation and chemotaxis observed in both single null strains could reflect differences in the affinity of the two Ras proteins for common effectors. To test whether RasC could substitute for RasG, the effects of overexpressing RasC in the *rasG*<sup>-</sup> strain was determined. To generate *rasG*<sup>-</sup>/[*rasC*]:*rasC* strain, plasmid pJLW30 containing the complete *rasC* gene including the promoter, and a G418 resistance marker was transformed into *rasG*<sup>-</sup> cells. The resistant colonies were picked and RasC expression levels were determined by western blot analysis using a RasC specific antibody. None of the isolated clones expressed more than a slight increase in RasC compared to the level in the *rasG*<sup>-</sup> cell lines (Figure 32). Thus although *rasG*<sup>-</sup> cells have a higher level of RasC (Figure 4 and 32), expression of RasC transgene did not induce an obvious further increase in RasC protein. Two of the *rasG*<sup>-</sup>/[*rasC*]:*rasC* transformants were selected and their streaming, chemotaxis and ACA activation capabilities were determined. The results obtained were identical to those obtained for the *rasG*<sup>-</sup> strain (data not shown) indicating that the slight increase in RasC protein level had no effect on the phenotypes, a result consistent with

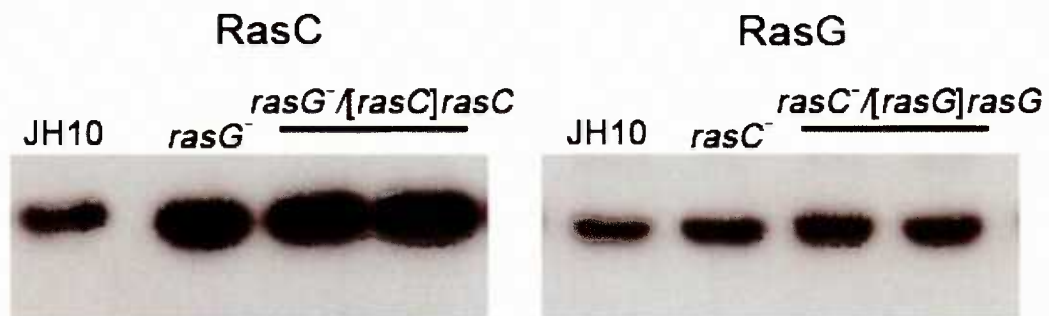


**Figure 32.** Western blot analysis of Ras protein levels of JH10, *rasG*, *rasG*/[*rasC*]:*rasC*, *rasC*, and *rasC*/[*rasG*]:*rasG*. Cell lysates from the JH10, *rasG*<sup>-</sup>, *rasG*<sup>-</sup>/[*rasC*]:*rasC*, *rasC*<sup>-</sup>, and *rasC*<sup>-</sup>/[*rasG*]:*rasG* were probed with RasC and RasG specific antibodies, as indicated.

the idea that the *rasC* promoter is regulated, not only by the level of RasG but also, by the amount of RasC protein in the cell (Figure 32).

To generate a *rasC*/[*rasG*]:*rasG* strain, expressing additional RasG, the pRasG-G418 plasmid containing the complete *rasG* gene including the promoter, and a G418 resistance marker was transformed into *rasC* cells. Resistant colonies were picked and RasG expression levels were determined by western blot analysis using a RasG specific antibody. None of the isolated clones expressed more than a slight increase in RasG compared to the level in the *rasC* cell lines (Figure 32). Two of the *rasC*/[*rasG*]:*rasG* transformants were selected and their streaming, chemotaxis and ACA activation capabilities were determined. Transformants exhibited the same phenotype in all mentioned experiments as *rasC* cells (data not shown) indicating that the slight increase in RasG protein level had no effect on the phenotypes, a result consistent with the idea that the *rasG* promoter is regulated by the amount of RasG protein in the cell (Figure 32).

RasG is expressed maximally during growth and early development, and is subsequently down regulated during aggregation (Khosla 1990, Robbins 1989) whereas RasC expression increases markedly during early development reaching a peak during late aggregation (Lim *et al.*, 2001). To ensure the expression of the transgene, *rasC* in *rasG* cells and *rasG* in *rasC* cells, at the correct time of development, RasC was expressed from the *rasG* promoter in the *rasG* cells and RasG was expressed from the *rasC* promoter in the *rasC* cells by the introduction of the plasmids pBM1 and pBM2, respectively. The resulting G418 resistant colonies, *rasG*/[*rasG*]:*rasC* and *rasC*/[*rasC*]:*rasG* transformants, were picked and subjected to western blotting to determine Ras protein levels. Again levels in excess of a 10-20% increase were not detected

confirming again that the RasC and RasG protein levels in the cell are highly regulated (Figure 33). However, in the experiments, it is not possible to determine how much of the Ras protein was expressed from the transgene promoter and how much was expressed from the endogenous promoter. Two *rasG*<sup>-</sup>/*[rasG]:rasC* and *rasC*<sup>-</sup>/*[rasC]:rasG* transformants, one with the same protein level as the single null and one which exhibited a higher protein level, were subjected to further analysis.

The aggregation of *rasG*<sup>-</sup>/*[rasG]:rasC* cells was observed by plating cells in plastic dishes under non-nutrient buffer. The expression of *rasC* from the *rasG* promoter resulted in cells (*rasG*<sup>-</sup>/*[rasG]:rasC*) that aggregated 2 h earlier than *rasG*<sup>-</sup> cells (data not shown). Next the ability of the cells to synthesize and accumulate cAMP was tested. The *rasG*<sup>-</sup>/*[rasG]:rasC* cells pulsed with cAMP, washed, stimulated with 2'-deoxy-cAMP, and assayed for cAMP accumulation at various times after stimulation. There was a ~20% increase in cAMP production compared to *rasG*<sup>-</sup> cells (Figure 34). Thus surprisingly, the small increase in RasC in the *rasG*<sup>-</sup>/*[rasG]:rasC* cells enhanced the developmental phenotype of the *rasG*<sup>-</sup> cells.

The aggregation of *rasC*<sup>-</sup>/*[rasC]:rasG* cells was observed by plating cells in plastic dishes under non-nutrient buffer. The *rasC*<sup>-</sup>/*[rasC]:rasG* cells did not aggregate when plated on plastic surfaces (data not shown). The *rasC*<sup>-</sup>/*[rasC]:rasG* cells pulsed with cAMP, washed, stimulated with 2'-deoxy-cAMP, and assayed for cAMP accumulation at various times after stimulation. There was negligible increase in cAMP accumulation in response to 2'-deoxy cAMP, results similar to those observed in *rasC*<sup>-</sup> cells (Figure 34), indicating that the small increase in RasG was not able to substitute for RasC.

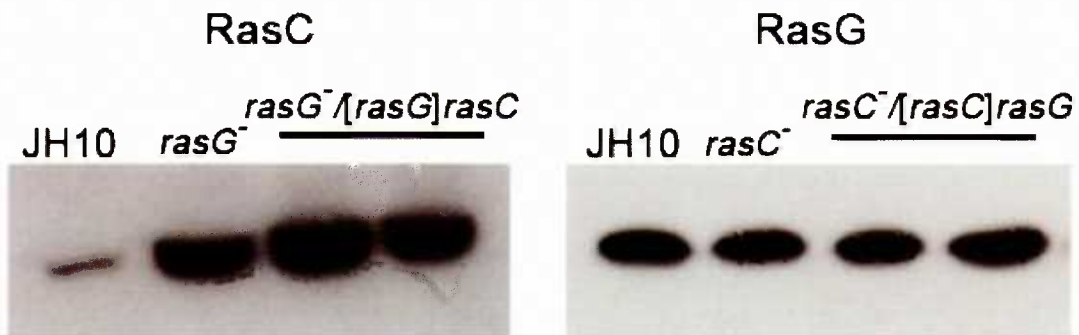


**Figure 33.** Western blot analysis of Ras protein levels of JH10, *rasG*<sup>-</sup>, *rasG*<sup>-</sup>/[*rasG*]:*rasC*, *rasC*<sup>-</sup>, and *rasC*<sup>-</sup>/[*rasC*]:*rasG*. Cell lysates from the JH10, *rasG*<sup>-</sup>, *rasG*<sup>-</sup>/[*rasG*]:*rasC*, *rasC*<sup>-</sup>, and *rasC*<sup>-</sup>/[*rasC*]:*rasG* were probed with RasC and RasG specific antibodies, as indicated.

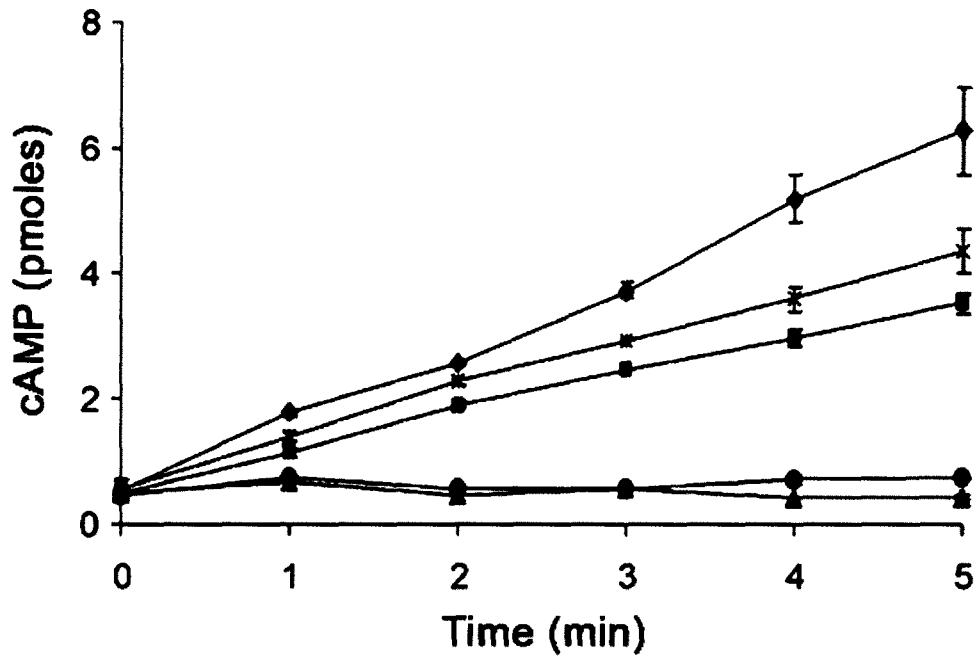


**Figure 34. cAMP accumulation in JH10, *rasG*, *rasC*, *rasC*/[*rasC*]:*rasG*, and *rasG*/[*rasG*]:*rasC* strains .** Cells of strains JH10 (◆), *rasG* (■), *rasC* (▲), *rasC*/[*rasC*]:*rasG* (●), and *rasG*/[*rasG*]:*rasC* (×) were pulsed with cAMP for 5 h, washed, and then stimulated with 2'-deoxy cAMP (see Materials and Methods). Samples taken at the indicated times were assayed for cAMP accumulation. The means and standard deviations for three independent experiments are shown.

### 3.3.2 Determination of the residues important for RasC activity

The finding that the absence of streaming and the reduced levels of cAMP production in the *rasC* cells could not be compensated by the slight over expression of RasG, provided an experimental basis for determining which residues in the key signaling portion of RasC are important for the activity in the cAMP relay. RasC and RasG have a total of nine amino acid differences in the switch I domain and the region flanking the switch II domain (Figure 35), regions that have been implicated in determining effector specificity in mammalian Ras (Herrmann, 2003; Biou and Cherfils, 2004; Mitin *et al.*, 2005). To look for which amino acids are important, RasG was modified by substituting each of the nine non-conserved amino acids, one by one, with the corresponding amino acid from RasC (Figure 35) and the constructs (Table 2) were individually transformed into *rasC* cells. Approximately fifty G418 resistant colonies were picked for each transformation. Five clones for each transformation were analyzed by western blotting with an antibody that was totally specific for the RasG protein. I found that most transformants showed a RasG protein level similar to that found in the *rasC* cells, although a few clones did exhibit a slight increase (10-20%) in RasG protein levels (data not shown). Each of the isolated clones was tested for the ability to stream under non-nutrient buffer. Only one transformant formed aggregates. In this strain aspartic acid 30 was changed to alanine (*rasC*/[*rasC*]:RasG<sup>D30A</sup>). Three clones from each transformation (one with same level and two with the slight increase in RasG protein level) were analyzed for the 2'-deoxy-cAMP-stimulated increase in cAMP. The *rasC*/[*rasC*]:RasG<sup>D30A</sup> transformants was the only one that exhibited an increase in cAMP accumulation (~50% of the wild type)

Protein	Region	amino acid sequence
RasC	Switch I	22 QLT <b>Q</b> N <b>Q</b> FIAEYDPTIEN <b>S</b> Y 40
RasG	Switch I	22 QLI <b>Q</b> N <b>H</b> FID <b>E</b> YDPTIED <b>S</b> Y 40
RasC	Switch II	50 <b>V</b> YMLDI LD <b>T</b> AGQEEYSAMRDQY <b>I</b> R <b>S</b> 74
RasG	Switch II	50 <b>T</b> CLLDI LD <b>T</b> AGQEEYSAMRDQY <b>M</b> R <b>T</b> 74

**Figure 35. Amino acid comparison of switch I and switch II regions of RasC and RasG.** Sequences 22-40 (switch I) and 50-74 (switch II) of RasC and RasG aligned. Amino acid differences are shown in bold.

(Figure 36 and Table 9). These results showed that alanine at position 30 in RasC is important for the activation of ACA.

### 3.3.3 Chimeric constructs

RasG was also modified by two block switches of sequence with RasC. These allowed substitution of all nine non-conserved amino acids in the switch I and II regions (Figure 35). This was accomplished by ligating DNA coding the first 78 amino acids of RasC to DNA encoding amino acids 79-190 of RasG (CSA). In addition a chimeric construct encoding amino acids 1-78 of RasG and 79-190 of RasC was generated (CSB) (Table 2). Both constructs contained the *rasC* promoter. The chimeric constructs were transformed into *rasC* cells and selected resistant isolates analyzed as described above. The *rasC*/[*rasC*]:RasC<sup>1-78</sup>+RasG<sup>79-190</sup> cells (containing the CSA construct) exhibited the same aggregation phenotype to that previously observed for *rasC*/[*rasC*]:RasG<sup>D30A</sup> cells and also accumulated similar levels of cAMP as the *rasC*/[*rasC*]:RasG<sup>D30A</sup> cells (Figure 36 and Table 10). The *rasC*/[*rasC*]:RasG<sup>1-78</sup>+RasC<sup>79-190</sup> cells (containing the CSB construct) accumulated almost 1/5 of the wild type level of cAMP but did not show any sign of aggregate stream formation (Figure 36 and Table 10). Interestingly the replacement of the first 78 amino acids of RasG with the corresponding sequence of RasC did not produce a more pronounced rescue of the *rasC* phenotype than did changing the single position 30 substitution, emphasizing the importance of this position for function. However, the RasG/RasC chimera (CSB) was capable of restoring some adenylate cyclase activity to the *rasC* cells. These results emphasize that the C-terminal portion of the RasC molecule is important for function. This finding is further explored in the discussion.

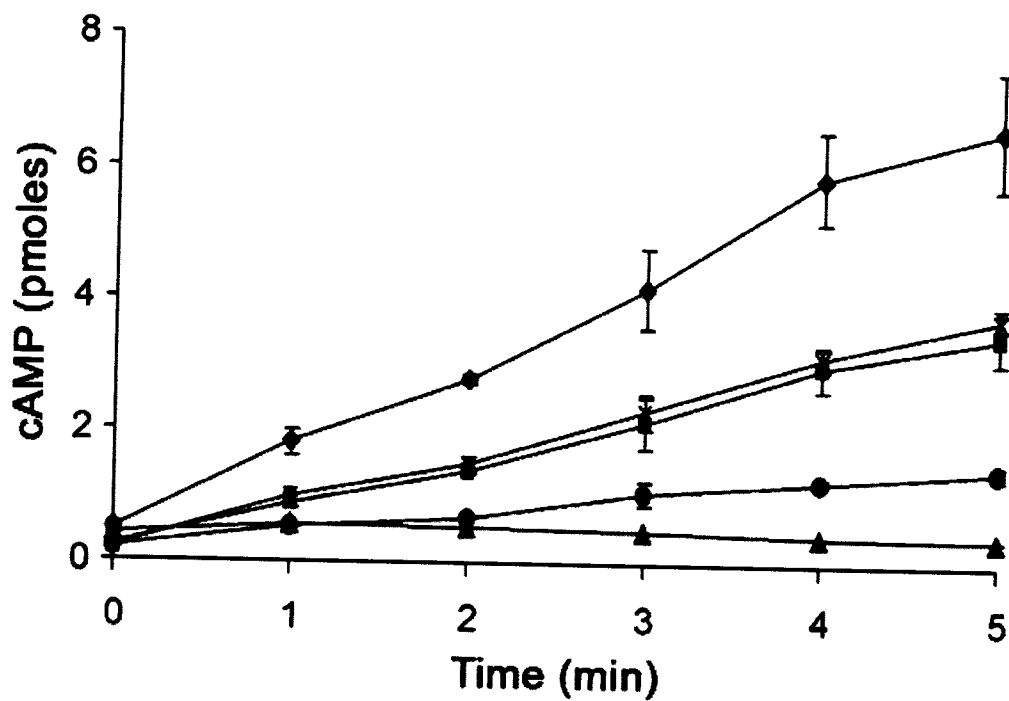


**Figure 36. cAMP accumulation in the various *ras* mutant strains.** Cells of strains JH10 (◆), *rasC*/[*rasC*]:RasG<sup>D30A</sup> (■), *rasC* (▲), *rasC*/[*rasC*]:RasG<sup>1-78</sup>+RasC<sup>79-190</sup> (●), and *rasC*/[*rasC*]:RasC<sup>1-78</sup>+RasG<sup>79-190</sup> (×) were pulsed with cAMP for 5 h, washed, and then stimulated with 2'-deoxy cAMP (see Materials and Methods). Samples taken at the indicated times were assayed for cAMP accumulation. The means and standard deviations for three independent experiments are shown.

**Table 9: Aggregation and cAMP accumulation in cells expressing RasG with a variety of point mutations.**

Strain	Aggregation	cAMP accumulation (pmoles in 5 min)
JH10	Yes	6.62 ± 0.88
<i>rasC</i>	None	0.39 ± 0.01
<i>rasC</i> /[ <i>rasC</i> ]:RasG <sup>I24I</sup>	None	0.43 ± 0.07
<i>rasC</i> /[ <i>rasC</i> ]:RasG <sup>H27Q</sup>	None	0.40 ± 0.05
<i>rasC</i> /[ <i>rasC</i> ]:RasG <sup>D30A</sup>	Cells are polarized, and form clumps	3.56 ± 0.39
<i>rasC</i> /[ <i>rasC</i> ]:RasG <sup>D38N</sup>	None	0.41 ± 0.02
<i>rasC</i> /[ <i>rasC</i> ]:RasG <sup>I50V</sup>	None	0.38 ± 0.03
<i>rasC</i> /[ <i>rasC</i> ]:RasG <sup>C51Y</sup>	None	0.43 ± 0.02
<i>rasC</i> /[ <i>rasC</i> ]:RasG <sup>L52M</sup>	None	0.44 ± 0.06
<i>rasC</i> /[ <i>rasC</i> ]:RasG <sup>M72I</sup>	None	0.39 ± 0.02
<i>rasC</i> /[ <i>rasC</i> ]:RasG <sup>T74S</sup>	None	0.43 ± 0.02

**Table 10: Aggregation and cAMP accumulation in cells expressing chimeric constructs of RasG and RasC.**

<b>Strain</b>	<b>Aggregation</b>	<b>cAMP accumulation (pmoles in 5 min)</b>
JH10	Yes	6.62 ± 0.88
<i>rasC</i>	None	0.39 ± 0.01
<i>rasC</i> /[ <i>rasC</i> ]:RasC <sup>1-78</sup> +RasG <sup>79-190</sup>	Cells are polarized, and form clumps	3.76 ± 0.16
<i>rasC</i> /[ <i>rasC</i> ]:RasG <sup>1-78</sup> +RasC <sup>79-190</sup>	None	1.42 ± 0.09

### 3.4 Role of RasG and RasC proteins in vegetative cells

Previous studies of the *rasG*<sup>-</sup> strains isolated by R. H. Insall (IR15 and IR17) indicated that RasG was important for cell growth (Tuxworth *et al.*, 1997; Khosla *et al.*, 2000). In addition AX2/*rasC*<sup>-</sup> vegetative cells exhibit some abnormal properties (Lim *et al.*, 2005). It was therefore pertinent to compare the vegetative cell phenotypes of the *rasG*<sup>-</sup>, *rasC*<sup>-</sup>, *rasC*<sup>-</sup>/*rasG*<sup>-</sup>, and *rasC*<sup>-</sup>/*rasG*<sup>-</sup>/*act15*:*carA* cells generated here since all of these strains were now derived from a common wild type background and were stable.

#### 3.4.1 RasG is important for cell growth

The JH10/*rasG*<sup>-</sup> and AX2/*rasG*<sup>-</sup> cells grow slightly slower than wild type cells (13.5 h and 13.7 h vs 12.5 h doubling times) on plastic surfaces (data not shown). However in shaken suspension, the *rasG*<sup>-</sup> strains grew considerably slower than wild type cells and ceased growth at much lower cell density (Figure 37). This defect is similar to that found for strains IR15 and IR17 (Tuxworth *et al.*, 1997; Khosla *et al.*, 2000). The growth of JH10/*rasC*<sup>-</sup> was similar to that of JH10 cells and both cultures reached similar final cell densities (Figure 37). *rasC*<sup>-</sup>/*rasG*<sup>-</sup> and *rasC*<sup>-</sup>/*rasG*<sup>-</sup>/*act15*:*carA* cells did not grow at all in shaken suspension (Figure 37). Even after 5 days without growth in suspension, these cells retained full viability as determined by plating cells onto bacterial lawns despite not having increased in cell number. Both the *rasC*<sup>-</sup>/*rasG*<sup>-</sup> and *rasC*<sup>-</sup>/*rasG*<sup>-</sup>/*act15*:*carA* cells grew only slightly slower than the JH10 cells in plastic dishes (data not shown).

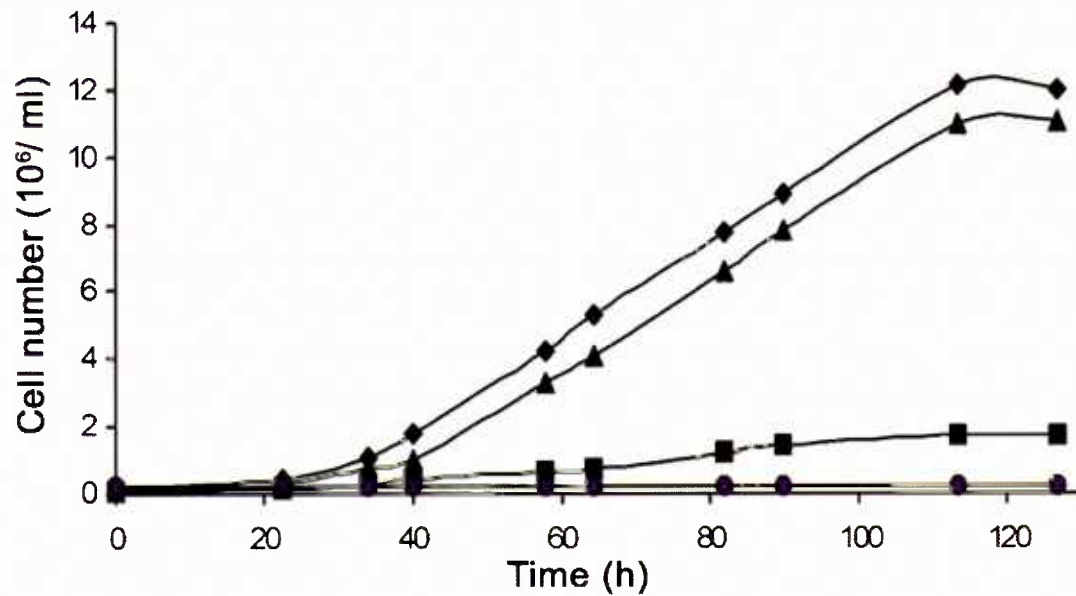


**Figure 37. Cell growth in suspension culture.** Strains JH10 (◆), *rasG*<sup>-</sup> (■), *rasC*<sup>-</sup> (▲), *rasC*<sup>-</sup>/*rasG*<sup>-</sup> (●), and *rasC*<sup>-</sup>/*rasG*<sup>-</sup>/*act15*:*carA* (×) were transferred from Petri plates into axenic medium at time zero and counted at intervals thereafter. The plotted values are the means of duplicate hemocytometer counts. The data plotted are for a single experiment, but similar data were obtained for three independent experiments.

### 3.4.2 RasG is important for cytokinesis

It was shown previously that the poor growth of IR15 and IR17 cells in shaken suspension was accompanied by a defect in cytokinesis, indicated by the fact that cells were multinucleate (Tuxworth *et al.*, 1997; Khosla *et al.*, 2000). The newly isolated JH10/*rasG*<sup>-</sup>, JH10/*rasC*<sup>-</sup> and the *rasC*<sup>-</sup>/*rasG*<sup>-</sup> cells were all grown in shaken suspension for five days and then subjected to nuclear staining.  $3 \times 10^3$  cells/cm<sup>2</sup> were allowed to adhere to glass coverslips for 30 minutes, washed, permeabilised, and stained with DAPI. The majority of the JH10 and JH10/*rasC*<sup>-</sup> cells were binucleate (Figure 38), and the average nuclei number was 1.8 (Table 11). Similar results were obtained previously for AX2/*rasC*<sup>-</sup> and AX2 cells (Lim *et al.*, 2005). In contrast JH10/*rasG*<sup>-</sup>, *rasC*<sup>-</sup>/*rasG*<sup>-</sup>, and *rasC*<sup>-</sup>/*rasG*<sup>-</sup>/*act15*]:*carA* cells were multinucleate with some cells having as many as 16 nuclei (Figure 38) although the average number was close to 4 (Table 11). Multinucleate cells the size of the one shown in Figure 38 are common and considerably larger examples are sometimes observed.

### 3.4.3 Chemotaxis to folate

Bacteria secrete folic acid which chemotactically attracts the vegetative amoebae, resulting in successful predation and feeding (Blusch and Nellen 1994). The chemotaxis to folate was examined by plating vegetative cells in axenic media on plastic dishes to a density of  $\sim 4 \times 10^5$  cells/cm<sup>2</sup>. The media was then replaced with diluted media and the response of JH10, *rasG*<sup>-</sup>, *rasC*<sup>-</sup>, *rasC*<sup>-</sup>/*rasG*<sup>-</sup>, and *rasC*<sup>-</sup>/*rasG*<sup>-</sup>/*act15*]:*carA* cells to a folate filled micropipet was determined. As shown in Figure 39A and 39C, a number of JH10 and JH10/*rasC*<sup>-</sup> cells had moved toward the micropipet after 50 minutes with the cells somewhat slower than the JH10 cells. In contrast, chemotaxis by *rasG*<sup>-</sup> cells was

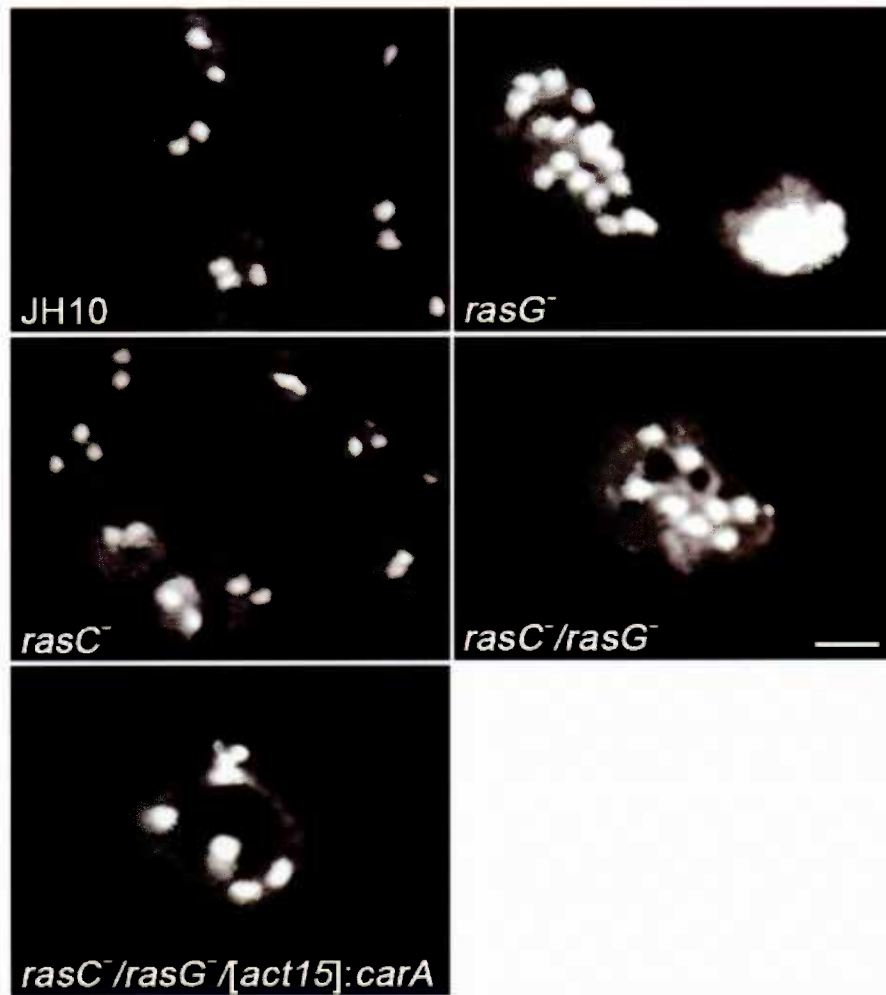


**Figure 38. Nuclear staining.** Cells were grown in shaken suspension for five days, and allowed to adhere to glass coverslips for 30 min, washed and then fixed with formaldehyde. Fixed cells were stained with DAPI as described in Materials and Methods. Epifluorescence images of random fields of view were captured using an Olympus IX-70 inverted microscope. The cells shown are representative of all the cells in the population. Scale bar is 50  $\mu$ m.

**Table 11. Nuclei number of *Dictyostelium* cells grown in suspension.**

<b>Strain</b>	<b>Number of nuclei per cell <sup>a</sup></b>
<b>JH10 (n = 303)</b>	<b>1.82 ± 0.05</b>
<b><i>rasG</i> (n = 315)</b>	<b>4.81 ± 0.55</b>
<b><i>rasC</i> (n = 360)</b>	<b>1.85 ± 0.06</b>
<b><i>rasC/rasG</i> (n = 389)</b>	<b>4.22 ± 0.16</b>
<b><i>rasC/rasG</i> [<i>act15</i>];<i>carA</i> (n = 350)</b>	<b>4.00 ± 0.14</b>

Values are mean ± SD; n = number of cells

<sup>a</sup> An mean value calculated by counting the number of nuclei in 300-390 cells

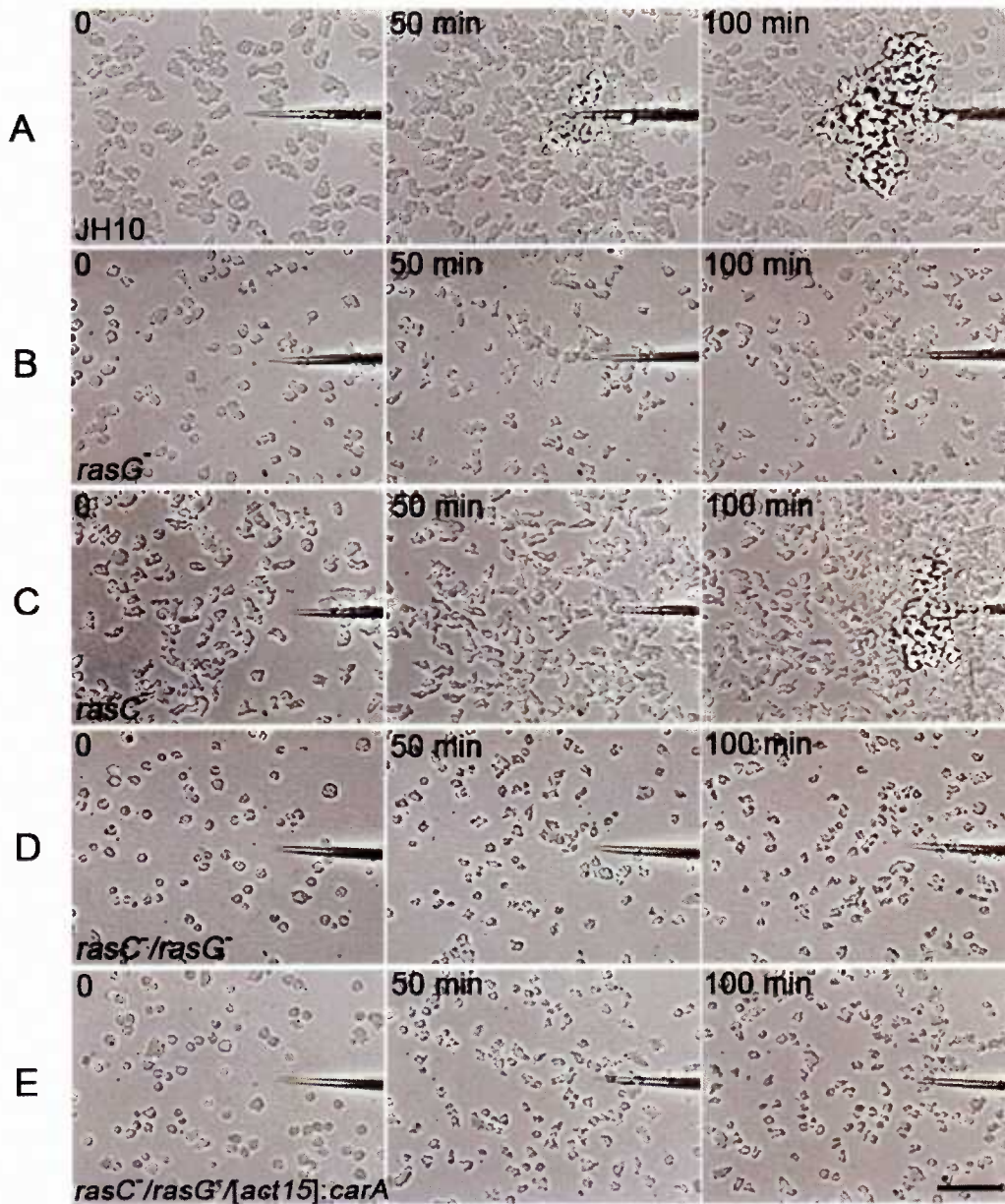


**Figure 39. Chemotaxis in a spatial folate chemoattractant gradient.** JH10 (A), *rasG*<sup>-</sup> (B), *rasC*<sup>-</sup> (C), *rasC/rasG*<sup>-</sup> (D), and *rasC/rasG*<sup>-</sup>/*act15*:*carA* (E) cells were grown to a density of  $\sim 4 \times 10^5$  cells/cm<sup>2</sup> in Nunc dishes. At  $t = 0$ , a micropipette filled with 25 mM folate was positioned in the field of view and cell movements were monitored by time-lapse microscopy. Single experiments are shown, but the results for the strains were highly reproducible. Scale bar is 50  $\mu$ m.

much slower (Figure 39B) and the *rasC/rasG*<sup>-</sup> and *rasC/rasG*<sup>-</sup>/*act15*:*carA* cells exhibited no obvious migration (Figures 39D and 39E). A calculation of chemotactic indices using *Openlab* software revealed a slight reduction in the values for the *rasC*<sup>-</sup> cells relative to JH10 cells, but a considerable reduction in the values for the *rasG*<sup>-</sup> cells and negligible values for the *rasC/rasG*<sup>-</sup> and *rasC/rasG*<sup>-</sup>/*act15*:*carA* cells (Table 12). Calculation of the rates of instantaneous velocity revealed similar values for the JH10 and *rasC*<sup>-</sup> cells, but lower values for the *rasG*<sup>-</sup>, *rasG/rasC*<sup>-</sup> and *rasC/rasG*<sup>-</sup>/*act15*:*carA* strains (Table 12). These results indicate that use of RasG is more significant than the use of RasC for both vegetative cell motility and chemotaxis to folate. However, while motility was not further impaired in the double null strains relative to *rasG*<sup>-</sup> cell; chemotaxis to folate was severely impaired, suggesting a compensation of RasC for RasG for chemotaxis to folate, similar to the situation observed for cAMP chemotaxis.

#### 3.4.4 F-actin distribution

It is clear that F-actin polymerization is required for the complex cell shape changes during cytokinesis and it was shown that actin distribution was altered in the original *rasG*<sup>-</sup> cells (Tuxworth *et al.*, 1997). I decided to reinvestigate this with the mutants generated in JH10 background. To visualize F-actin, vegetative cells were grown in HL5 media in Nunc tissue culture dishes,  $2 \times 10^3$  cells/cm<sup>2</sup> reseeded onto glass coverslips and allowed to adhere for 3 hours. Cells were fixed, permeabilized and stained with FITC-phalloidin (Figure 40). There were obvious differences in actin staining between the null strains and the wild type cells. While in vegetative wild type cells actin was distributed throughout the periphery of the cell, it was distributed in a punctate pattern in vegetative *rasG*<sup>-</sup> cells. Vegetative *rasC*<sup>-</sup> cells exhibit more intense actin staining at the periphery of

the cell than do wild type cells, suggesting that RasC may also play some role in actin distribution. The patches of F-actin in *rasG*<sup>-</sup> cells are indicative of multiple pseudopodia extension and this may explain the lower polarity and abnormal cytokinesis observed in *rasG*<sup>-</sup> cells. This result suggests that RasG plays an important role in F-actin distribution and its ablation could affect the machinery required for normal cell division and cell polarity. The double null cells tended to be more rounded and smaller but with a denser, even actin distribution than the single null cells (Figure 40).

**Table 12. Chemotaxis analysis of *Dictyostelium* cells in a spatial folate chemoattractant gradient.**

<b>Strain</b>	<b>Instantaneous velocity (<math>\mu\text{m}/\text{min}</math>)</b>	<b>Chemotaxis index <sup>a</sup></b>
<b>JH10 (n = 30)</b>	<b>13.70 <math>\pm</math> 0.93</b>	<b>0.90 <math>\pm</math> 0.05</b>
<b><i>rasG</i> (n = 31)</b>	<b>6.85 <math>\pm</math> 0.69</b>	<b>0.31 <math>\pm</math> 0.05</b>
<b><i>rasC</i> (n = 32)</b>	<b>11.78 <math>\pm</math> 0.82</b>	<b>0.70 <math>\pm</math> 0.06</b>
<b><i>rasC/rasG</i> (n = 28)</b>	<b>7.00 <math>\pm</math> 0.75</b>	<b>0.06 <math>\pm</math> 0.02</b>
<b><i>rasC/rasG</i> [<i>act15</i>]:<i>carA</i> (n = 29)</b>	<b>7.32 <math>\pm</math> 0.67</b>	<b>0.06 <math>\pm</math> 0.01</b>

Values are mean  $\pm$  SD; n = number of cells

<sup>a</sup> Chemotaxis index was calculated as the net distance traveled towards the source of chemoattractant divided by the total distance traveled in that time period.

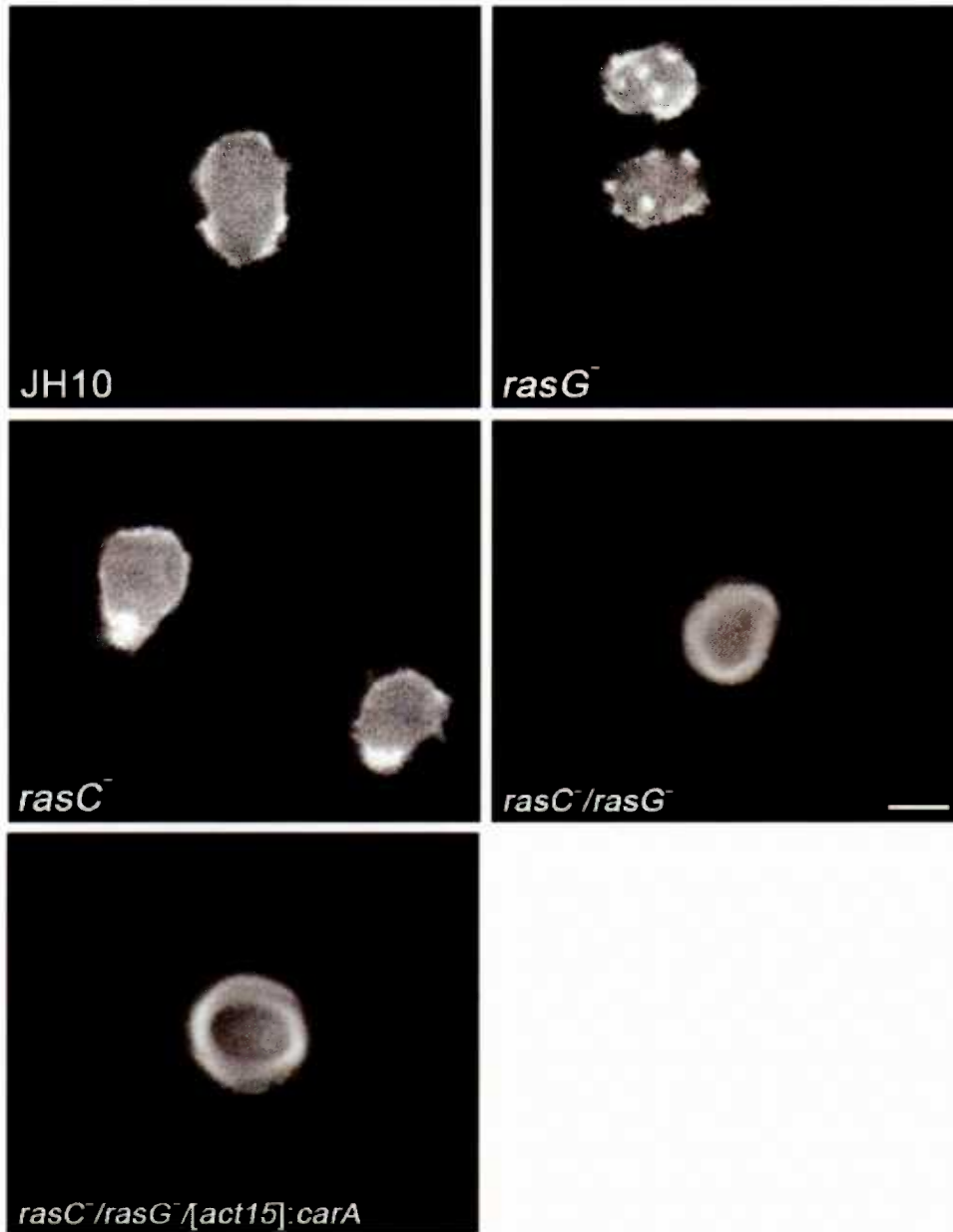


**Figure 40. F-actin distribution.** Cells JH10 , *rasG*<sup>-</sup> , *rasC*<sup>-</sup> , *rasC*<sup>-</sup>/*rasG*<sup>-</sup> , and *rasC*<sup>-</sup>/*rasG*<sup>-</sup>/*act15*:*carA* were seeded onto glass coverslips and allowed to adhere for 3 h. The cells were then fixed with glutaraldehyde, permeabilized with Triton-X100 and stained with FITC-phalloidin conjugate. Epi-fluorescent images were taken on a Zeiss Axiovert microscope (100×). Scale bar is 50 μm.

## 4 DISCUSSION

### 4.1 RasG is involved in *Dictyostelium* aggregation

The initial evidence for a role of Ras signaling pathways in regulating the *Dictyostelium* aggregation process came from the disruption of the RasGEFA gene, which prevented aggregation (Insall *et al.*, 1996). More direct evidence for a role for Ras came with the disruption of the *rasC* gene, which also produced cells that failed to aggregate (Lim *et al.*, 2001). *rasC* null cells exhibited reduced activation of ACA and reduced phosphorylation of PKB in response to cAMP, suggesting a role for RasC in the signal transduction pathways that regulate both the cAMP relay and chemotaxis.

Previous studies with *Dictyostelium rasG* null mutants, IR15 and IR17, had indicated a predominant role for RasG in growth and vegetative-cell functions (Tuxworth *et al.*, 1997; Khosla *et al.*, 2000; Lim *et al.*, 2001). These *rasG* null cells grew very slowly and the only defect observed in development was a slight but inconsistent delay in the onset of aggregation (R. H. Insall, and M. Khosla unpublished observations). However, both IR15 and IR17 were unstable and difficult to work with (Tuxworth *et al.*, 1997; Khosla *et al.*, 2000). Within a relatively short time, the cells regained the ability to grow and differentiate normally, despite the absence of the RasG protein. Because *rasG* cells grow slowly, there is clearly an opportunity for a suppressor strain to take over the population.

Other studies had suggested a possible additional role for RasG in early development. For example, PI3K plays an important role in the chemotactic response to cAMP (Meili *et al.*, 1999; Funamoto *et al.*, 2001; Huang *et al.*, 2003), and because RasG interacts with the Ras binding domains (RBDs) of two of the *Dictyostelium* PI3Ks

(PI3K1 and PI3K2), it had been postulated that RasG is a regulator of PI3K activity and hence of the chemotactic response (Funamoto *et al.*, 2002). In addition, the *Dictyostelium* protein RIP3 was identified by its ability to interact with RasG in yeast two hybrid analyses and cells lacking RIP3 are also defective in aggregation (Lee *et al.*, 1999). Finally, both RasC and RasG are activated in response to cAMP, further indicating a role for RasG in aggregation (Kae *et al.*, 2004). However, definitive proof for a role of RasG was lacking.

In view of the variable defects in development and the relative instability of the previously described *rasG* null strains (Khosla *et al.*, 2000; R. H. Insall and M. Khosla, unpublished observations), new *rasG* null strains were generated in two different backgrounds, AX2 and JH10, in order to study more definitively the possible role of RasG in early development. The new *rasG* strains exhibited all the previously described vegetative cell phenotypes, but both strains were stable and exhibited a consistent delay of about four hours in aggregation. Normal aggregation was restored by the ectopic expression of RasG, verifying that the aggregation defect was a direct result of the lack of the RasG protein. It is not apparent why the new strains are less susceptible than the originals to the presumptive extragenic suppression, but it did not appear to be related to parental background, because mutants generated in both AX2 and AX3 (JH10) backgrounds were stable.

#### **4.2 Chemotaxis and ACA activation during *Dictyostelium* aggregation**

During *Dictyostelium* aggregation, cAMP induces both the activation of ACA, and chemotaxis (Figure 41). Both processes require the cAMP receptor (cAR1) and the associated heterotrimeric G protein ( $G\alpha_2\beta\gamma$ ) (Kimmel and Parent, 2003). Earlier

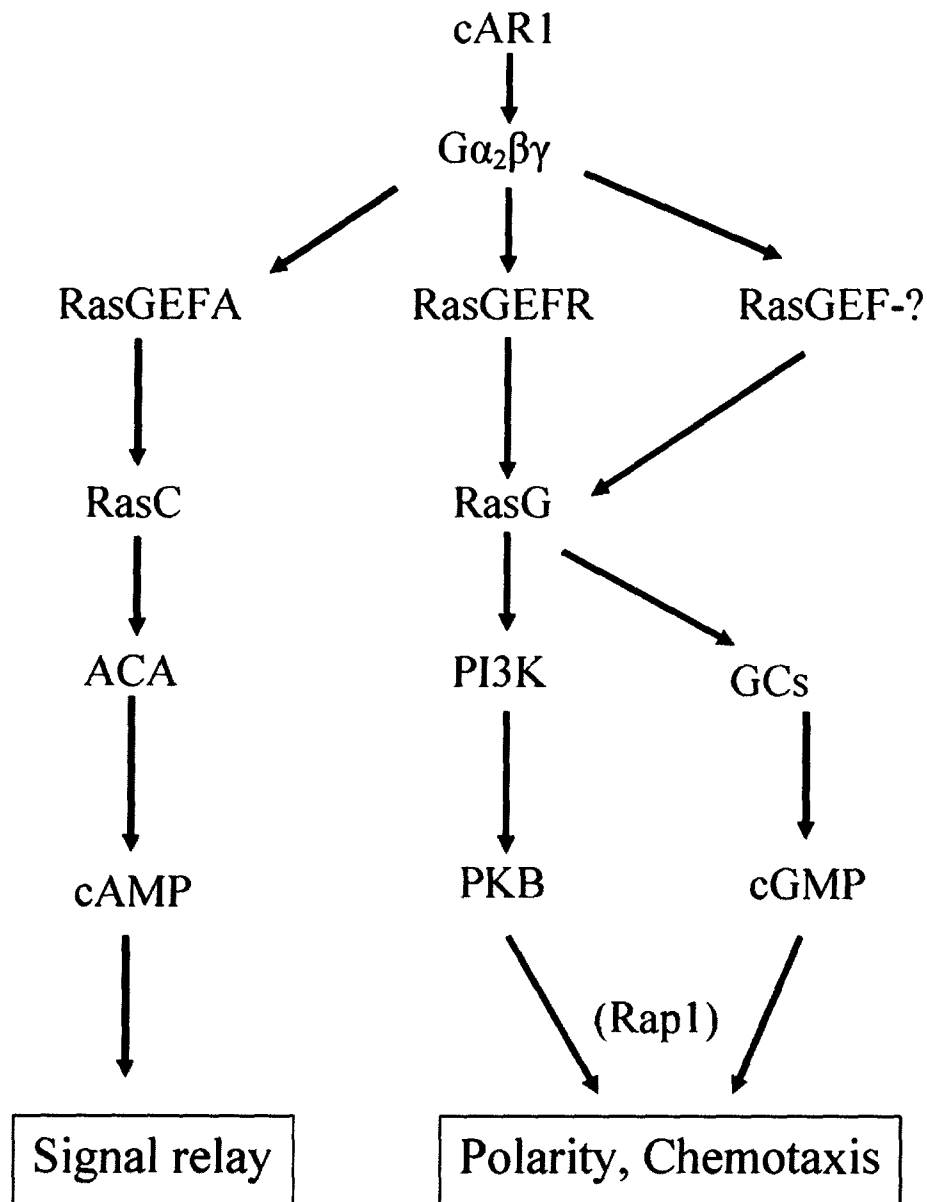


**Figure 41. Model of cAMP signaling via RasC and RasG.** The cAMP signaling pathway branches at the level of RasGEF specificity. Signaling through guanylyl cyclase (GC) and signaling through PI3K appear to constitute parallel pathways during the chemotactic response to cAMP. Rap1 is activated downstream of RasG but its precise site of action is as yet unknown.

experiments showed that there was no increase in the levels of activated RasC and RasG, following the cAMP stimulation, in mutant strains disrupted in the genes encoding the aggregation-stage cAMP receptors (*carA*/*carC*) and components of the  $G\alpha_2\beta\gamma$  complex (*gpaB* and *gpbA*) indicating that RasC and RasG, act downstream of  $G\alpha_2\beta\gamma$  (Kae *et al.*, 2004).

When compared to wild type cells, both JH10/*rasG*<sup>-</sup> and AX2/*rasG*<sup>-</sup> strains after being pulsed with cAMP exhibited reduced polarity and reduced cAMP chemotaxis in a spatial gradient of cAMP. These strains also accumulated less cGMP and lower PKB phosphorylation in response to cAMP than wild type strains. These effects were far more pronounced than those observed for *rasC*<sup>-</sup> mutant cells, suggesting that RasG is more important than RasC for signal transduction leading to chemotaxis. In contrast, the defects in cAMP production and ACA activation were more pronounced in *rasC*<sup>-</sup> cells than in *rasG*<sup>-</sup> cells, suggesting that signaling through RasC was more important for the cAMP relay than signaling through RasG. However, neither ACA activation nor chemotaxis was completely eliminated in either the *rasC*<sup>-</sup> or the *rasG*<sup>-</sup> strains. These results suggested three possibilities: (i) there is some overlap of function of RasC and RasG, (ii) both RasC and RasG are required for optimal chemotaxis and for optimal ACA activation, or (iii) that an additional Ras protein, such as Rap1, that is also activated in response to cAMP (Jeon *et al.*, 2007), plays an important role at this point in the signal transduction pathway. A *rasC*<sup>-</sup>/*rasG*<sup>-</sup> strain in the JH10 background was isolated to directly address these points.

The finding that early gene expression is markedly repressed in the *rasC*<sup>-</sup>/*rasG*<sup>-</sup> strain indicates an important role for RasC and RasG in the response to starvation that

induces early gene expression. Expression of the *carA* gene from the constitutive *actin 15* promoter elevated the level of *carA* expression in vegetative cells. In addition, this vegetative cell expression clearly restored the developmentally regulated expression of *carA* and the expression of other developmental genes known to be involved in cAMP signaling, that were suppressed in the *rasC/rasG*<sup>-</sup> strain. It should be noted that two genes that were suppressed ~2.5 times were not rescued. The mechanism by which early gene expression is repressed in the *rasC/rasG*<sup>-</sup> strain and the mechanism by which such expression is restored in the *rasC/rasG*<sup>-</sup>/*act15*:*carA* strain were not pursued further in this study, which was designed specifically to look at the role of Ras proteins in cAMP induced signal transduction, but these mechanisms are certainly worthy of further investigation. The experiments using the *rasC/rasG*<sup>-</sup>/*act15*:*carA* mutant strain with its restored early developmental gene expression revealed that were negligible levels of cAMP generation and chemotaxis, providing strong evidence that all chemotactic and signal relay responses to cAMP are mediated through either RasG or RasC as shown in Figure 41.

The partial chemotaxis and ACA activation observed in the single *rasG* and *rasC* null mutants could be due to an overlap of RasC and RasG function, since there is close amino acid similarity between the two proteins. Thus, there may be an interaction of the one Ras protein with the effectors of the other, with one Ras protein out-competing the other for its own effectors in the wild type strains. However, in the single null strains, where one protein is missing, the competition would be removed, allowing functional compensation by the interaction of the remaining Ras protein with both sets of effectors. Consistent with this idea of a compensatory mechanism, is the finding that there is an

increase in RasC activation in *rasG* cells (Figure 17A), although there was no reciprocal increase in RasG activation in *rasC* cells (Figure 17B). However its activation was more prolonged which could also indicate a compensatory signaling mechanism. It also remains possible that there is a dual role for RasG and RasC in both ACA activation and in chemotaxis. This idea is attractive, since a requirement for the two Ras proteins for ACA activation could explain the enhancement in the cAMP signal relay as aggregation progresses (Kay, 1979; Chisholm *et al.*, 1984). Thus, RasG might be responsible for initiating the process, but RasC might be important for the amplification of the signal that is needed to entrain the cells into aggregation streams. Similarly, if there is a dual role for RasG and RasC in chemotaxis, RasC might be required early in aggregation for a response to low concentrations of cAMP and RasG required later in aggregation for a response to higher concentrations of cAMP. This interpretation is consistent with the delayed aggregation by the *rasG* cells and the absence of aggregation of the *rasC* cells. However, since there is as yet no experimental support to distinguish these possibilities, they have not been included in the model depicted in Figure 41. The use of GFP-RBD can provide important information about the *in vivo* localization of activated Ras. However, the relative unrestrained of the Ras-RBD interaction makes it difficult to be able to differentiate between the different Ras isoforms. One way is to use isoform specific RBDs. For example, thus far, the RBD of the protein kinase Phg2 has proven to be specific for Rap1 when tested for its ability to bind to five members of the *Dictyostelium* Ras subfamily (Gebbie *et al.*, 2004). Random mutagenizing of RBDs and screening for those that bind to only one Ras protein via a yeast two hybrid assay could be an another method of obtaining isoform specific RBDs. A similar strategy has been

used to generate more efficient fluorescent probes of different colours (Zhang *et al.*, 2002).

### 4.3 Rap1 activation occurs downstream of RasG activation

Rap1 overexpression leads to shape changes and enhanced cell adhesion of vegetative *Dictyostelium* cells (Rebstein *et al.*, 1993; Rebstein, 1996; Rebstein *et al.*, 1997). In addition, the available evidence suggests that Rap1 is essential for vegetative cell viability (Kang *et al.*, 2002). Activated Rap1 is capable of binding to the RBD of Phg2 and it has been suggested that this binding leads to an increase in cell adhesion (Kortholt *et al.*, 2006) and is also important in regulating cell motility (Jeon *et al.*, 2007). It has also been shown that Rap1 is activated by the RasGEF activity of GbpD in vegetative cells (Kortholt *et al.*, 2006). A potential role for Rap1 during aggregation has been recently suggested by the finding that the protein is activated in response to cAMP in aggregation competent cells (Jeon *et al.*, 2007). This activation was found to be absent in *rasC/rasG/[act15]:carA* and *rasG* cells (Figure 31), indicating that it occurs downstream of signaling through RasG. Rap1 activation in response to cAMP was slightly reduced in *rasC* cells and the possibility that some Rap1 activation is mediated through RasC cannot, therefore, be ruled out but this possibility has also not been considered in the final model (Figure 41). The levels of activated Rap1 that were present prior to the cAMP stimulation were also reduced in *rasG* cells but not reduced in *rasC* cells, indicating a role for RasG in regulating basal levels of Rap1 activation. Since GbpD is involved in Rap activation in vegetative cells (Kortholt *et al.*, 2006), it might also be involved in the activation of Rap1 in chemotaxing cells in response to cAMP and it will be interesting to investigate the nature of the possible link between RasG and

GbpD. However, since there is as yet no evidence for the precise role for Rap1 in this signal transduction pathway, it has simply been placed downstream of RasG, and upstream of polarity/chemotaxis (Figure 41).

#### **4.4 The production of cGMP plays a more important role in the chemotactic process than does the production of PIP3**

Since RasG interacts with the RBD of two of the *Dictyostelium* PI3Ks (PI3K1 and PI3K2), it was postulated that RasG is a regulator of PI3K activity (Funamoto *et al.*, 2002). Initially it was suggested that the production of PIP3 by the activity of PI3K plays a pivotal role in the chemotactic response to cAMP (Meili *et al.*, 1999; Funamoto *et al.*, 2001; Huang *et al.*, 2003). However, there have been two reports recently indicating that strains with several deleted *pi3k* genes remain chemotactic, although they have reduced polarity and do move more slowly in response to cAMP (Hoeller and Kay, 2007; Takeda *et al.*, 2007). It would appear that PI3K is not essential for chemotaxis but is, nonetheless, an important determinant for the establishment of polarity, which streamlines the chemotaxis process. In contrast, mutants that have disruptions in the genes encoding the enzymes responsible for cGMP production, *gca* and *sgc*, are only slightly chemotactic to cAMP (Bosgraaf *et al.*, 2002). Taken together, these results indicate that the generation of cGMP plays a more important role in the chemotactic process than the production of PIP3. A comparison of the rates of chemotaxis of the various *ras* null strains relative to levels of PKB phosphorylation (as a measure of PI3K activity) and cGMP production is consistent with this interpretation. Thus, both chemotaxis and cGMP production were only slightly reduced in *rasG*<sup>-</sup> cells, while in contrast, PKB phosphorylation was barely detectable. The *rasG*<sup>-</sup> cells were

predominantly rounded, with no obvious leading edge, even though they performed relatively efficient chemotaxis, consistent with the idea that cGMP pathway is more important for chemotaxis, but that the PI3K pathway is important for establishing polarity. In *rasC* cells, the rate of chemotaxis and the production of cGMP were very similar to those of the parental cell line. However, PKB phosphorylation was markedly reduced in these cells although an appreciable level remained which was presumably sufficient to generate normal polarity in these cells.

#### **4.5 Specificity of Ras protein interactions**

There is strong evidence for specificity among the RasGEFs, that act upstream of the Ras proteins in the cAMP signaling pathway (Kae *et al.*, 2007). RasGEFA is specific for RasC and appears to be the only RasGEF capable of converting RasC to the GTP bound form (Figure 41). RasGEFR is specific for RasG but since RasG is still partially activated in a *gefR*<sup>-</sup> strain, other RasGEFs (whose identifies are currently unknown and, therefore, denoted as RasGEF-? in Figure 41) can also activate RasG. Thus, the input to RasG is more complex than is the input to RasC, which may reflect the fact that RasG has multiple functions in the cell. A key question, still to be examined, is how the activation of the RasGEFs is linked to components of the cAMP receptor/heterotrimeric G protein complex.

Downstream of RasG and RasC there is clearly a bifurcation of the signaling pathways (Figure 41). The differential impact of RasG and RasC on ACA activation versus chemotaxis is almost certainly due to differences in the interaction of the Ras proteins with their downstream effectors. There is already evidence for differential affinity, since the Ras Binding Domains (RBDs) of mammalian Raf1 and RalGDS and

*Dictyostelium* PI3K1 and PI3K2 bind more effectively to RasG than to RasC (Kae *et al.*, 2004). The higher affinity of PI3K1 and PI3K2 for RasG is consistent for the proposed roles for PI3K and RasG in establishing polarity. A yeast two-hybrid analysis has shown that RIP3 also interacts strongly with RasG but does not interact with RasC (Lee *et al.*, 1999). However, the *rip3*<sup>-</sup> strain is defective in aggregation (Lee *et al.*, 1999; Lee *et al.*, 2005), a phenotype that closely resembles that of the *rasC*<sup>-</sup> and *gefA*<sup>-</sup> strains, and very different from the delayed aggregation phenotype of *rasG*<sup>-</sup> cells. This genetic data, therefore, indicates a close connection between RIP3, RasGEFA and RasC and provides no evidence for a connection between RIP3 and RasG. The function of RIP3, therefore, remains an enigma, given the marked discrepancy between the biochemical and genetic data. The failure of RIP3 to bind to RasC in yeast two hybrid assays (Lee *et al.*, 1999) is not simply an artifact, resulting from the failure of RasC to express properly in yeast, since RIP3 binds to RasG but does not bind to RasC in a RBD-RIP3 pull down assay (Kae and Weeks, unpublished observations). A further complication is that RIP3 is a component of the TORC2 complex, which is necessary for optimum ACA activation and optimum chemotaxis (Lee *et al.*, 1999; Lee *et al.*, 2005). Understanding these signaling pathways will require a greater understanding of the role(s) of the TORC2 complex. In addition to these affinity considerations, a spatial separation of RasG and RasC may play an important role in the signal bifurcation, since ACA activation occurs at the trailing end of a migrating cell while PI3K stimulation of PKB occurs at the leading edge. The study of this activation in live cells is currently hampered by the lack of specific reagents that can uniquely identify activated RasC and activated RasG. Creating such specific reagents will be an important step for future understanding.

Studies of the interaction of mammalian Ras proteins with their effector molecules have identified two highly flexible Ras domains, Switch I and Switch II, that dominate these interactions. It has been proposed that the essential residues in these regions have “multispecificities” that are influenced by neighboring amino acids; that is, that identical residues can interact with different effectors in different ways (Herrmann, 2003; Biou and Cherfils, 2004; Mitin *et al.*, 2005). RasC and RasG have identical sequences for the Switch II region, although the residues flanking this sequence differ slightly, providing possible explanations for both specificity and overlap of function. Furthermore, although there is considerable sequence conservation in the Switch I region, there are also some significant differences, again perhaps allowing for both functional specificity and overlap of function. Mutational analyses have suggested that not only RBD but also CRR (cysteine-rich region) of Raf1, the major effector of H-Ras, is critical for Ras-dependent activation of Raf1. Although, the exact mechanism of Raf1 CRR in this activation is not clear, but evidence suggest that C terminal post translational modifications of H-Ras is necessary for this interaction (Hu *et al.*, 1995). The mutational analysis that I performed further defined the key residues that generate functional differences between RasC and RasG. However, lack of full ACA restoration in *rasC*<sup>-</sup>/[*rasC*]:RasG<sup>D30A</sup> and in chimeric *rasC*<sup>-</sup>/[*rasC*]:RasC<sup>1-78</sup>+RasG<sup>79-190</sup> cells indicates that although the amino acid 30 is a key determinant of RasC specificity, the C-terminal portion of the RasC molecule is also important. The unique role for each Ras protein could, therefore, be specified at least partially by the hypervariable region playing an important role in localization and perhaps for downstream interaction.

#### **4.6 The role of RasG and RasC in the regulation of the cytoskeleton during aggregation**

*Dictyostelium* cells like the other motile cells migrate in a complex way that requires coordinated regulation of the cytoskeleton and cell adhesion (Franca-Koh *et al.*, 2006). The basic model involves F-actin polymerization at the cell cortex which generates filaments that produce pseudopods and other membrane extensions for forward drive and myosin II assembles at the rear of the cell that provide cortical tension, resulting in uropod retraction. These responses have been reported to be regulated mainly by PI3K and PLA2, acting in parallel pathways, and by cGMP, respectively (Bosgraaf *et al.*, 2002; Chen *et al.*, 2003; Chen *et al.*, 2007) and I have obtained evidence to suggest that RasG is involved in both responses.

It has been shown that the expression of a mutated PI3K1, that carries a mutation in the RBD, is unable to generate PIP3 when expressed in a *pikA/pikB* double null cell line. Constitutive localization of this mutated PI3K1 via a myristoylation motif to the membrane did not rescue this defect, suggesting that the binding of Ras to PI3K does not act by simply anchoring PI3K to the membrane. Furthermore, activated RasG has been shown to bind to *Dictyostelium* PI3K1 and PI3K2 in a yeast two hybrid assay (Funamoto *et al.*, 2002). In addition, I have shown that activation of PKB, a downstream effector of PI3K, was barely detectable in *rasG* cells. All these data suggest that RasG is required for PI3K activation of PIP3 formation and, consequently, for actin polymerization.

It has been suggested that members of the Rho family of small G proteins play a role in regulation of cell polarity, cytoskeletal organization and directional sensing in neutrophils (Drechsel *et al.*, 1997). In these cells, active RhoA accumulates in the rear of

migrating cells, which directs the uropod retraction by regulating the myosin II assembly and its interaction with actin at the cell cortex (Xu *et al.*, 2003). This process is regulated through a cascade involving ROCK (Rho kinase) and MLCK (myosin light-chain kinase). However, myosin filament formation appears to be regulated by a different pathway in *Dictyostelium*, since the *Dictyostelium* genome does not possess Rho homologs. Instead, the *Dictyostelium* p21-activated kinase (PAK) localizes to the back of the chemotaxing cell and is required for the assembly of myosin II filaments, a function that is dependent on cGMP signaling (Chung and Firtel, 1999). Chemotaxing cells rapidly polymerize myosin II to the cortex at the rear and sides of the cell, and this response is defective in a *sgcA*<sup>-</sup>/*gca*<sup>-</sup> double knockout strain that is unable to synthesize cGMP, and also in cells lacking cGMP-binding proteins (Bosgraaf *et al.*, 2002). These mutants are motile, but they exhibit a loss in polarity during chemotaxis, and are severely defective in chemotaxis. *rasG*<sup>-</sup> cells are also unable to properly polarize during chemotaxis, yet still retain the ability to move. In addition, *rasG*<sup>-</sup> cells also display reduced chemotaxis efficiency and, although this defect is not as severe as that for the *sgcA*<sup>-</sup>/*gca*<sup>-</sup> strain, the difference can be explained by the fact that cGMP production is totally abolished in *sgcA*<sup>-</sup>/*gca*<sup>-</sup> cells but only partially reduced in *rasG*<sup>-</sup> cells. However, cGMP synthesis is completely abolished in *rasC*/*rasG*<sup>-</sup> double null cells; and these cells exhibit negligible chemotaxis, a phenotype similar to that of the *sgcA*<sup>-</sup>/*gca*<sup>-</sup> cells. It has also been suggested that PKB activation is important for the assembly of myosin at the rear of the cells (Chung and Firtel, 1999) and that the binding of myosin heavy-chain kinase to filamentous actin at the front of the cell prevents myosin assembly, thus restricting myosin activity to the sides and rear of the cell (Rubin and Ravid, 2002). However, since

*rasG*<sup>-</sup> cells have negligible activation of PKB, but are still capable of chemotaxis, clearly PKB is not essential for motility.

Although the predominant role for RasC is believed to be in the regulation of ACA, the protein also appears to play a role in the pathways leading to actin and myosin II polymerization and this role is different from that of RasG. In *rasC*<sup>-</sup> cells the polymerization of both actin and myosin, in response to cAMP, is similar to that observed in the wild type cells but the subsequent depolymerization of both actin and myosin is different (Wessels *et al.*, 2004). In wild type cells, actin and myosin II depolymerize and move away from the cell cortex to the cytosol, but both remain in the cortex of *rasC*<sup>-</sup> cells, leading to a hyper-polarized cell morphology (Wessels *et al.*, 2004). This suggests that RasC might play a role in the depolymerization of both actin and myosin II filaments during chemotaxis, but clearly this has no effect on cell motility.

#### **4.7 Proposed model of Ras signaling during aggregation**

The work in this thesis demonstrated that all cAMP induced signals transduced through heterotrimeric G proteins and leading to signal relay, polarity and chemotaxis in *Dictyostelium* depend upon RasC and RasG (Figure 41). It appears that all cAMP mediated RasC activation is mediated by RasGEFA, while RasG activation is mediated by RasGEFR and an as yet unidentified additional RasGEF since RasG is still partially activated in a *gefR*<sup>-</sup> strain (Kae *et al.*, 2007). Thus, the signaling pathway leading to RasG activation seems more complex than the one to RasC. Examining other *rasGEF* null strains for RasG activation in addition to measuring *in vitro* nucleotide release activity of the corresponding RasGEF protein should lead to the elucidation of the other GEFs required for RasG activation. Another important question that remains to be

answered is how the specific activation of the RasGEFs is linked to components of the cAMP receptor complex.

The available evidence suggests that RasG regulates at least three signaling pathways: 1) the activation of guanylyl cyclase (Figure 41), 2) the activation of PI3K (Figure 41), and 3) the regulation of the TORC2 complex via an interaction with RIP3 (Lee *et al.*, 2005). Taken together, these observations indicate that the predominant role for RasG is in regulating polarity and chemotaxis. It has been shown that RasG is activated at the leading edge of chemotaxing cells (Sasaki *et al.*, 2004) and that GC, PI3K, and RIP3 all translocate to the leading edge upon cAMP stimulation (Lee *et al.*, 1999; Funamoto *et al.*, 2002; Sasaki *et al.*, 2004; Lee *et al.*, 2005; Veltman *et al.*, 2005).

In contrast, the prominent role for RasC during aggregation is in the activation of ACA. However the precise role that RasC plays in ACA activation is not clear at this point. *In vivo* localization studies indicate that ACA activation occurs at the rear of the cell (Kriebel *et al.*, 2003), suggesting that signals received at the front of the cell must be relayed to the rear for the activation of ACA. The mutational analysis presented in this thesis suggests that the C terminal region of RasC is an important determinant for full ACA activation, and since the C terminal region of Ras proteins is known to be important for localization, this raises the interesting possibility that RasC is activated at the rear of the cell, placing it in proximity to ACA. However, *Dictyostelium* ACA does not have a RBD, so there must be some adaptor protein that mediates the passage of the signal from activated RasC to ACA. We have used a yeast two hybrid screen to search for such an adaptor protein, but this search proved to be unsuccessful, although binding proteins for RasG and Rap1 were detected in analogous screens.

#### 4.8 The role of RasG and RasC in vegetative cells

One of the most dramatic phenotypic defects of vegetative *rasG*<sup>-</sup> cells is the abnormal cytokinesis that occurs when these cells are grown in shaken suspension, although there are several other cytoskeleton related defects, including changes in cell polarity, motility, folate chemotaxis, and the distribution of F-actin (Tuxworth *et al.*, 1997; Khosla *et al.*, 2000). There is also a reduced growth rate in the *rasG*<sup>-</sup> cells which is probably, at least in part, due to the defects in cytokinesis, although additional requirements of RasG for optimum growth can not be precluded. RasG is clearly not essential for growth, and the loss of RasG may be partially compensated by the presence of other Ras proteins, such as RasD, which is identical in the effector and effector-proximal domains and exhibits 82% identity over the entire length of the protein (Daniel, 1995). In this regard it is perhaps significant that growing *rasG*<sup>-</sup> cells show a marked increase in the level of RasD, which is barely detectable in the wild type cells (data not shown). Attempts have been made to generate a *rasG/rasD* strain but failure to obtain such a mutant (D. Secko unpublished observation) is consistent with the idea that RasD is capable of substituting for RasG and that RasG/RasD carry out an essential function.

Cytokinesis is an important part of the cell cycle that divides one cell to two daughter cells. During cytokinesis, the cells undergo a series of stereotypical shape changes. The cells first round up, then elongate and finally constrict at the center. The microtubule network and its associated proteins coordinate the mitotic segregation of chromosomes and distribution of organelles and serve as key regulators of actin cytoskeleton in controlling the cell shape changes that lead to cell separation. It has been shown that proteins such as myosin II, and Rho GTPases associate with the furrow, while

others such as RacE, coronin, and Scar localize to the poles and this distribution is important for normal cytokinesis (De Lozanne and Spudich, 1987; Chen *et al.*, 1994; Drechsel *et al.*, 1997; Kitayama *et al.*, 1997; Bi *et al.*, 1998; Weber *et al.*, 1999). Actin filaments play important roles at both the poles and furrow of the dividing cells. Polymerized actin and actin binding proteins accumulate at the pole, while actin and myosin filaments accumulate in the furrow at the contractile ring (Gerisch *et al.*, 1999; Fukui, 2000; O'Connell *et al.*, 2001). The absence or mislocalization of these cytoskeletal proteins, due to mutation, causes severe defects in cytokinesis. For example, a deletion of myosin II prevents *Dictyostelium* cytokinesis when cells are grown in shaken suspension, although these cells are capable of cell division on a surface by undergoing “traction-mediated cytofission” (De Lozanne and Spudich, 1987). Even multinucleated cells fragment and move apart when plated on a cell surface.

It is clear that *Dictyostelium* cells must establish and maintain cortical asymmetries for many cellular functions, such as chemotaxis and cytokinesis. While *Dictyostelium* cells establish polarity during chemotaxis as a response to an external chemoattractant, polarity during cytokinesis is dependent on internal components. As discussed previously, it has been suggested that the accumulation of actin in front and myosin in the rear of the cells, in response to an internal gradient of PIP3, results in migration. Similar events could occur during cytokinesis. It has been reported that the movement of PTEN to the membrane results in uniform reduction of PIP3 levels leading to the loss of actin polymerization (Iijima and Devreotes, 2002), which allows the cells to abolish the polarity that is established during migration. It has been speculated that for cytokinesis to occur, the poles of the cells become the active site for the formation of

PIP3 and the generation of actin filled projections during cell elongation, whereas the furrow zone which is devoid of PIP3, allows acto-myosin based contractions to occur (Janetopoulos *et al.*, 2005).

Since RasG interacts with the RBD of two of the *Dictyostelium* PI3Ks (PI3K1 and PI3K2) (Funamoto *et al.*, 2002) and given the fact that our data indicates that RasG is required for cell polarity during the chemotactic response, it is likely that RasG is also required for the signaling pathway that regulates polarity during cytokinesis and its absence leads to failure in cytokinesis, resulting in large, multinucleated cells; JH10/*rasG*<sup>-</sup>, *rasC*/*rasG*<sup>-</sup>, and *rasC*/*rasG*<sup>-</sup>/*act15*]:*carA* cells are mostly multinucleate. The various *ras* null and wild type cells also have different patterns of actin staining. While vegetative wild type cells exhibit an even pattern of actin distribution, actin is distributed in a punctate pattern throughout the cell surface in vegetative *rasG*<sup>-</sup> cells. Vegetative *rasC* cells also exhibit more intense actin staining throughout the periphery of the cell than do wild type cells. In *rasC*/*rasG*<sup>-</sup>, and *rasC*/*rasG*<sup>-</sup>/*act15*]:*carA* cells actin is also distributed densely but evenly around the cell periphery. These results suggest a role for both proteins, RasC and RasG, in the establishment of internal cues for the signaling pathways leading to polarity.

The fact that there is a defect in folate chemotaxis in vegetative *rasG* null strains is consistent with the important role that RasG plays in the mobilization of both the actin and myosin cytoskeletons during the establishment of cell polarity for chemotaxis. When grown in shaken suspension *rasG*<sup>-</sup> cells divide slowly and cease division at a lower density than wild type cells. In contrast *rasC*/*rasG*<sup>-</sup>, and *rasC*/*rasG*<sup>-</sup>/*act15*]:*carA* cells become multinucleate and do not divide at all in suspension. The total absence of folate

chemotaxis and the total absence of cell division in suspensions in *rasC*<sup>-</sup>/*rasG*<sup>-</sup>, and *rasC*<sup>-</sup>/*rasG*<sup>-</sup>/*act15*]:*carA* cells suggests a compensatory role of RasC for RasG during both processes, a similar phenomenon to that observed for aggregating cells during cAMP chemotaxis.

#### **4.9 Concluding remarks**

*Dictyostelium* has a relatively large number of Ras subfamily proteins, and its potential for high throughput genetic analysis makes the organism ideal for the study of Ras signaling networks. Results obtained in this study should therefore be relevant to other organisms, such as humans, that also encode numerous Ras subfamily proteins but which require more complex signaling networks. I have clearly shown that RasG and RasC are essential for the cAMP signaling during *Dictyostelium* aggregation, with RasG more important for chemotaxis and RasC more important for signal relay. In addition, the two proteins are essential for vegetative cell growth in suspension and for chemotaxis to folate in vegetative cells. Ideas for further study have been incorporated at the appropriate places in the foregoing discussion.

## REFERENCES

- Abraham, R.T. (2001). Cell cycle checkpoint signaling through the ATM and ATR kinases. *Genes Dev* 15, 2177-2196.
- Adari, H., Lowy, D.R., Willumsen, B.M., Der, C.J., and McCormick, F. (1988). Guanosine triphosphatase activating protein (GAP) interacts with the p21ras effector binding domain. *Science* 240, 518-521.
- Affolter, M., and Weijer, C.J. (2005). Signaling to cytoskeletal dynamics during chemotaxis. *Dev Cell* 9, 19-34.
- Ahmadian, M.R., Stege, P., Scheffzek, K., and Wittinghofer, A. (1997). Confirmation of the arginine-finger hypothesis for the GAP-stimulated GTP-hydrolysis reaction of Ras. *Nat Struct Biol* 4, 686-689.
- Alibaud, L., Cosson, P., and Benghezal, M. (2003). *Dictyostelium discoideum* transformation by oscillating electric field electroporation. *Biotechniques* 35, 78-83.
- Andrew, N., and Insall, R.H. (2007). Chemotaxis in shallow gradients is mediated independently of PtdIns 3-kinase by biased choices between random protrusions. *Nat Cell Biol* 9, 193-200.
- Arbabi, S., and Maier, R.V. (2002). Mitogen-activated protein kinases. *Crit Care Med* 30, S74-79.
- Aubry, L., and Firtel, R. (1999). Integration of signaling networks that regulate *Dictyostelium* differentiation. *Annu Rev Cell Dev Biol* 15, 469-517.
- Barbacid, M. (1987). *ras* genes. *Annu Rev Biochem* 56, 779-827.
- Bellacosa, A., Chan, T.O., Ahmed, N.N., Datta, K., Malstrom, S., Stokoe, D., McCormick, F., Feng, J., and Tsichlis, P. (1998). Akt activation by growth factors is a multiple-step process: the role of the PH domain. *Oncogene* 17, 313-325.
- Bi, E., Maddox, P., Lew, D.J., Salmon, E.D., McMillan, J.N., Yeh, E., and Pringle, J.R. (1998). Involvement of an actomyosin contractile ring in *Saccharomyces cerevisiae* cytokinesis. *J Cell Biol* 142, 1301-1312.
- Biggs, W.H., 3rd, Meisenhelder, J., Hunter, T., Cavenee, W.K., and Arden, K.C. (1999). Protein kinase B/Akt-mediated phosphorylation promotes nuclear exclusion of the winged helix transcription factor FKHR1. *Proc Natl Acad Sci U S A* 96, 7421-7426.

Biou, V., and Cherfils, J. (2004). Structural principles for the multispecificity of small GTP-binding proteins. *Biochemistry* 43, 6833-6840.

Boeckeler, K., Adley, K., Xu, X., Jenkins, A., Jin, T., and Williams, R.S. (2006). The neuroprotective agent, valproic acid, regulates the mitogen-activated protein kinase pathway through modulation of protein kinase A signalling in *Dictyostelium discoideum*. *Eur J Cell Biol* 85, 1047-1057.

Boettner, B., Govek, E.E., Cross, J., and Van Aelst, L. (2000). The junctional multidomain protein AF-6 is a binding partner of the Rap1A GTPase and associates with the actin cytoskeletal regulator profilin. *Proc Natl Acad Sci U S A* 97, 9064-9069.

Boguski, M.S., and McCormick, F. (1993). Proteins regulating Ras and its relatives. *Nature* 366, 643-654.

Bolourani, P., Spiegelman, G.B., and Weeks, G. (2006). Delineation of the roles played by RasG and RasC in cAMP-dependent signal transduction during the early development of *Dictyostelium discoideum*. *Mol Biol Cell* 17, 4543-4550.

Bolourani, P., Spiegelman, G.B., and Weeks, G. (2008). Rap1 Activation in Response to cAMP Occurs Downstream of Ras Activation during Dictyostelium Aggregation. *J Biol Chem* 283, 10232-10240.

Bonfini, L., Karlovich, C.A., Dasgupta, C., and Banerjee, U. (1992). The Son of sevenless gene product: a putative activator of Ras. *Science* 255, 603-606.

Bos, J.L. (1989). *ras* oncogenes in human cancer: a review. *Cancer Res* 49, 4682-4689.

Bos, J.L., Rehmann, H., and Wittinghofer, A. (2007). GEFs and GAPs: critical elements in the control of small G proteins. *Cell* 129, 865-877.

Bosgraaf, L., Russcher, H., Smith, J.L., Wessels, D., Soll, D.R., and Van Haastert, P.J. (2002). A novel cGMP signalling pathway mediating myosin phosphorylation and chemotaxis in Dictyostelium. *Embo J* 21, 4560-4570.

Bosgraaf, L., and van Haastert, P.J. (2006). The regulation of myosin II in Dictyostelium. *Eur J Cell Biol* 85, 969-979.

Bosgraaf, L., Waijer, A., Engel, R., Visser, A.J., Wessels, D., Soll, D., and van Haastert, P.J. (2005). RasGEF-containing proteins GbpC and GbpD have differential effects on cell polarity and chemotaxis in Dictyostelium. *J Cell Sci* 118, 1899-1910.

Bourne, H.R., Sanders, D.A., and McCormick, F. (1991). The GTPase superfamily: conserved structure and molecular mechanism. *Nature* 349, 117-127.

Brenner, M. (1978). Cyclic AMP levels and turnover during development of the cellular slime mold *Dictyostelium discoideum*. *Dev Biol* 64, 210-223.

Broek, D., Toda, T., Michaeli, T., Levin, L., Birchmeier, C., Zoller, M., Powers, S., and Wigler, M. (1987). The *S. cerevisiae* CDC25 gene product regulates the RAS/adenylate cyclase pathway. *Cell* 48, 789-799.

Cabrera-Vera, T.M., Vanhauwe, J., Thomas, T.O., Medkova, M., Preininger, A., Mazzone, M.R., and Hamm, H.E. (2003). Insights into G protein structure, function, and regulation. *Endocr Rev* 24, 765-781.

Campbell, S.L., Khosravi-Far, R., Rossman, K.L., Clark, G.J., and Der, C.J. (1998). Increasing complexity of Ras signaling. *Oncogene* 17, 1395-1413.

Chen, L., Iijima, M., Tang, M., Landree, M.A., Huang, Y.E., Xiong, Y., Iglesias, P.A., and Devreotes, P.N. (2007). PLA2 and PI3K/PTEN pathways act in parallel to mediate chemotaxis. *Dev Cell* 12, 603-614.

Chen, L., Janetopoulos, C., Huang, Y.E., Iijima, M., Borleis, J., and Devreotes, P.N. (2003). Two phases of actin polymerization display different dependencies on PI(3,4,5)P3 accumulation and have unique roles during chemotaxis. *Mol Biol Cell* 14, 5028-5037.

Chen, M.Y., Long, Y., and Devreotes, P.N. (1997). A novel cytosolic regulator, Pianissimo, is required for chemoattractant receptor and G protein-mediated activation of the 12 transmembrane domain adenylyl cyclase in *Dictyostelium*. *Genes Dev* 11, 3218-3231.

Chen, P., Ostrow, B.D., Tafuri, S.R., and Chisholm, R.L. (1994). Targeted disruption of the *Dictyostelium* RMLC gene produces cells defective in cytokinesis and development. *J Cell Biol* 127, 1933-1944.

Chen, X., and Resh, M.D. (2001). Activation of mitogen-activated protein kinase by membrane-targeted Raf chimeras is independent of raft localization. *J Biol Chem* 276, 34617-34623.

Chisholm, R.L., Barklis, E., and Lodish, H.F. (1984). Mechanism of sequential induction of cell-type specific mRNAs in *Dictyostelium* differentiation. *Nature* 310, 67-69.

Chomczynski, p., and Sacchi, N. (1987). Single step method of RNA isolation by guanidinium thiocyanate-phenol-chloroform extraction. *Anal Biochem* 162, 156-159.

Choy, E., Chiu, V.K., Silletti, J., Feoktistov, M., Morimoto, T., Michaelson, D., Ivanov, I.E., and Philips, M.R. (1999). Endomembrane trafficking of ras: the CAAX motif targets proteins to the ER and Golgi. *Cell* 98, 69-80.

Chubb, J.R., Wilkins, A., Thomas, G.M., and Insall, R.H. (2000). The Dictyostelium RasS protein is required for macropinocytosis, phagocytosis and the control of cell movement. *J Cell Sci* 113, 709-719.

Chung, C.Y., and Firtel, R.A. (1999). PAKa, a putative PAK family member, is required for cytokinesis and the regulation of the cytoskeleton in *Dictyostelium discoideum* cells during chemotaxis. *J Cell Biol* 147, 559-576.

Clarke, S. (1992). Protein isoprenylation and methylation at carboxyl-terminal cysteine residues. *Annu Rev Biochem* 61, 355-386.

Colicelli, J. (2004). Human RAS superfamily proteins and related GTPases. *Sci STKE* 2004, RE13.

Corbett, K.D., and Alber, T. (2001). The many faces of Ras: recognition of small GTP-binding proteins. *Trends Biochem Sci* 26, 710-716.

Cullen, P.J. (2001). Ras effectors: buying shares in Ras plc. *Curr Biol* 11, R342-344.

Daniel, J., Bush, J., Cardelli, J., Spiegelman, G.B., and Weeks, G. (1994). Isolation of two novel *ras* genes in *Dictyostelium discoideum*; evidence for a complex, developmentally regulated *ras* gene subfamily. *Oncogene* 9, 501-508.

Daniel, J., Spiegelman, G. and Weeks, D.G. (1995). Dictyostelium *ras* genes. In *Guidebook to the Small GTPases*. Zerial, M. and Huber, L.A. (eds.). NY, Oxford University Press, pp. 100-104.

Datta, S.R., Dudek, H., Tao, X., Masters, S., Fu, H., Gotoh, Y., and Greenberg, M.E. (1997). Akt phosphorylation of BAD couples survival signals to the cell-intrinsic death machinery. *Cell* 91, 231-241.

De Lozanne, A., and Spudich, J.A. (1987). Disruption of the Dictyostelium myosin heavy chain gene by homologous recombination. *Science* 236, 1086-1091.

Dijkers, P.F., Birkenkamp, K.U., Lam, E.W., Thomas, N.S., Lammers, J.W., Koenderman, L., and Coffey, P.J. (2002). FKHR-L1 can act as a critical effector of cell

death induced by cytokine withdrawal: protein kinase B-enhanced cell survival through maintenance of mitochondrial integrity. *J Cell Biol* 156, 531-542.

Drechsel, D.N., Hyman, A.A., Hall, A., and Glotzer, M. (1997). A requirement for Rho and Cdc42 during cytokinesis in *Xenopus* embryos. *Curr Biol* 7, 12-23.

Eichinger, L., Pachebat, J.A., Glockner, G., Rajandream, M.A., Sugang, R., Berriman, M., Song, J., Olsen, R., Szafranski, K., Xu, Q., Tunggal, B., Kummerfeld, S., Madera, M., Konfortov, B.A., Rivero, F., Bankier, A.T., Lehmann, R., Hamlin, N., Davies, R., Gaudet, P., Fey, P., Pilcher, K., Chen, G., Saunders, D., Sodergren, E., Davis, P., Kerhornou, A., Nie, X., Hall, N., Anjard, C., Hemphill, L., Bason, N., Farbrother, P., Desany, B., Just, E., Morio, T., Rost, R., Churcher, C., Cooper, J., Haydock, S., van Driessche, N., Cronin, A., Goodhead, I., Muzny, D., Mourier, T., Pain, A., Lu, M., Harper, D., Lindsay, R., Hauser, H., James, K., Quiles, M., Madan Babu, M., Saito, T., Buchrieser, C., Wardroper, A., Felder, M., Thangavelu, M., Johnson, D., Knights, A., Loulseged, H., Mungall, K., Oliver, K., Price, C., Quail, M.A., Urushihara, H., Hernandez, J., Rabbinowitsch, E., Steffen, D., Sanders, M., Ma, J., Kohara, Y., Sharp, S., Simmonds, M., Spiegler, S., Tivey, A., Sugano, S., White, B., Walker, D., Woodward, J., Winckler, T., Tanaka, Y., Shaulsky, G., Schleicher, M., Weinstock, G., Rosenthal, A., Cox, E.C., Chisholm, R.L., Gibbs, R., Loomis, W.F., Platzer, M., Kay, R.R., Williams, J., Dear, P.H., Noegel, A.A., Barrell, B., and Kuspa, A. (2005). The genome of the social amoeba *Dictyostelium discoideum*. *Nature* 435, 43-57.

Eickholt, B.J., Towers, G.J., Ryves, W.J., Eikel, D., Adley, K., Ylinen, L.M., Chadborn, N.H., Harwood, A.J., Nau, H., and Williams, R.S. (2005). Effects of valproic acid derivatives on inositol trisphosphate depletion, teratogenicity, glycogen synthase kinase-3beta inhibition, and viral replication: a screening approach for new bipolar disorder drugs derived from the valproic acid core structure. *Mol Pharmacol* 67, 1426-1433.

Fath, I., Apiou, F., Schweighoffer, F., Chevallier-Multon, M.C., Ciora, T., Dutrillaux, B., and Tocque, B. (1993). Identification of two human homologues to *Drosophila* SOS (son of sevenless) localized on two different chromosomes. *Nucleic Acids Res* 21, 4398.

Feig, L.A. (2003). Ral-GTPases: approaching their 15 minutes of fame. *Trends Cell Biol* 13, 419-425.

Firtel, R.A., and Chung, C.Y. (2000). The molecular genetics of chemotaxis: sensing and responding to chemoattractant gradients. *Bioessays* 22, 603-615.

Franca-Koh, J., and Devreotes, P.N. (2004). Moving forward: mechanisms of chemoattractant gradient sensing. *Physiology (Bethesda)* 19, 300-308.

Franca-Koh, J., Kamimura, Y., and Devreotes, P. (2006). Navigating signaling networks: chemotaxis in *Dictyostelium discoideum*. *Curr Opin Genet Dev* 16, 333-338.

Fresno Vara, J.A., Casado, E., de Castro, J., Cejas, P., Belda-Iniesta, C., and Gonzalez-Baron, M. (2004). PI3K/Akt signalling pathway and cancer. *Cancer Treat Rev* 30, 193-204.

Fukui, Y. (2000). Real-time high-resolution optical sectioning suggests biphasic cytokinetic mechanism in *Dictyostelium discoideum*. *Microsc Res Tech* 49, 183-189.

Funamoto, S., Meili, R., Lee, S., Parry, L., and Firtel, R.A. (2002). Spatial and temporal regulation of 3-phosphoinositides by PI3-kinase and PTEN mediates chemotaxis. *Cell* 109, 611-623.

Funamoto, S., Milan, K., Meili, R., and Firtel, R.A. (2001). Role of phosphatidylinositol 3' kinase and a downstream pleckstrin homology domain-containing protein in controlling chemotaxis in *Dictyostelium*. *J Cell Biol* 153, 795-810.

Gebbie, L., Benghezal, M., Cornillon, S., Froquet, R., Cherix, N., Malbouyres, M., Lefkir, Y., Grangeasse, C., Fache, S., Dalous, J., Bruckert, F., Letourneur, F., and Cosson, P. (2004). Phg2, a kinase involved in adhesion and focal site modeling in *Dictyostelium*. *Mol Biol Cell* 15, 3915-3925.

Genot, E., and Cantrell, D.A. (2000). Ras regulation and function in lymphocytes. *Curr Opin Immunol* 12, 289-294.

Gerisch, G., Maniak, M., and Neujahr, R. (1999). Patterns of cellular activities based on protein sorting in cell motility, endocytosis and cytokinesis. *Biochem Soc Symp* 65, 1-14.

Gibbs, J.B., Schaber, M.D., Allard, W.J., Sigal, I.S., and Scolnick, E.M. (1988). Purification of ras GTPase activating protein from bovine brain. *Proc Natl Acad Sci U S A* 85, 5026-5030.

Goldfinger, L.E., Ptak, C., Jeffery, E.D., Shabanowitz, J., Han, J., Haling, J.R., Sherman, N.E., Fox, J.W., Hunt, D.F., and Ginsberg, M.H. (2007). An experimentally derived database of candidate Ras-interacting proteins. *J Proteome Res* 6, 1806-1811.

Hadwiger, J.A., and Firtel, R.A. (1992). Analysis of G alpha 4, a G-protein subunit required for multicellular development in Dictyostelium. *Genes Dev* 6, 38-49.

Harwood, A.J., Hopper, N.A., Simon, M.N., Driscoll, D.M., Veron, M., and Williams, J.G. (1992). Culmination in Dictyostelium is regulated by the cAMP-dependent protein kinase. *Cell* 69, 615-624.

Heid, P.J., Geiger, J., Wessels, D., Voss, E., and Soll, D.R. (2005). Computer-assisted analysis of filopod formation and the role of myosin II heavy chain phosphorylation in Dictyostelium. *J Cell Sci* 118, 2225-2237.

Herrmann, C. (2003). Ras-effector interactions: after one decade. *Curr Opin Struct Biol* 13, 122-129.

Hoeller, O., and Kay, R.R. (2007). Chemotaxis in the absence of PIP3 gradients. *Curr Biol* 17, 813-817.

Hu, C.D., Kariya, K., Tamada, M., Akasaka, K., Shirouzu, M., Yokoyama, S., and Kataoka, T. (1995). Cysteine-rich region of Raf-1 interacts with activator domain of post-translationally modified Ha-Ras. *J Biol Chem* 270, 30274-30277.

Huang, Y.E., Iijima, M., Parent, C.A., Funamoto, S., Firtel, R.A., and Devreotes, P. (2003). Receptor-mediated regulation of PI3Ks confines PI(3,4,5)P3 to the leading edge of chemotaxing cells. *Mol Biol Cell* 14, 1913-1922.

Iijima, M., and Devreotes, P. (2002). Tumor suppressor PTEN mediates sensing of chemoattractant gradients. *Cell* 109, 599-610.

Iijima, M., Huang, Y.E., and Devreotes, P. (2002). Temporal and spatial regulation of chemotaxis. *Dev Cell* 3, 469-478.

Insall, R., Kuspa, A., Lilly, P.J., Shaulsky, G., Levin, L.R., Loomis, W.F., and Devreotes, P. (1994). CRAC, a cytosolic protein containing a pleckstrin homology domain, is required for receptor and G protein-mediated activation of adenylyl cyclase in Dictyostelium. *J Cell Biol* 126, 1537-1545.

Insall, R.H., Borleis, J., and Devreotes, P.N. (1996). The *aimless* RasGEF is required for processing of chemotactic signals through G-protein-coupled receptors in Dictyostelium. *Curr Biol* 6, 719-729.

Janetopoulos, C., Borleis, J., Vazquez, F., Iijima, M., and Devreotes, P. (2005). Temporal and spatial regulation of phosphoinositide signaling mediates cytokinesis. *Dev Cell* 8, 467-477.

Jeon, T.J., Lee, D.J., Merlot, S., Weeks, G., and Firtel, R.A. (2007). Rap1 controls cell adhesion and cell motility through the regulation of myosin II. *J Cell Biol* 176, 1021-1033.

Johnson, R.L., Vaughan, R.A., Caterina, M.J., Van Haastert, P.J., and Devreotes, P.N. (1991). Overexpression of the cAMP receptor 1 in growing *Dictyostelium* cells. *Biochemistry* 30, 6982-6986.

Jones, S., Vignais, M.L., and Broach, J.R. (1991). The CDC25 protein of *Saccharomyces cerevisiae* promotes exchange of guanine nucleotides bound to *ras*. *Mol Cell Biol* 11, 2641-2646.

Kae, H., Kortholt, A., Rehmann, H., Insall, R.H., Van Haastert, P.J., Spiegelman, G.B., and Weeks, G. (2007). Cyclic AMP signalling in *Dictyostelium*: G-proteins activate separate Ras pathways using specific RasGEFs. *EMBO Rep* 8, 477-482.

Kae, H., Lim, C.J., Spiegelman, G.B., and Weeks, G. (2004). Chemoattractant-induced Ras activation during *Dictyostelium* aggregation. *EMBO Rep* 5, 602-606.

Kang, R., Kae, H., Ip, H., Spiegelman, G.B., and Weeks, G. (2002). Evidence for a role for the *Dictyostelium* Rap1 in cell viability and the response to osmotic stress. *J Cell Sci* 115, 3675-3682.

Katso, R., Okkenhaug, K., Ahmadi, K., White, S., Timms, J., and Waterfield, M.D. (2001). Cellular function of phosphoinositide 3-kinases: implications for development, homeostasis, and cancer. *Annu Rev Cell Dev Biol* 17, 615-675.

Kay, R.R. (1979). Gene expression in *Dictyostelium discoideum*: mutually antagonistic roles of cyclic-AMP and ammonia. *J Embryol Exp Morphol* 52, 171-182.

Kelley, G.G., Reks, S.E., Ondrako, J.M., and Smrcka, A.V. (2001). Phospholipase C(epsilon): a novel Ras effector. *Embo J* 20, 743-754.

Kessin, R.H. (2001). *Dictyostelium*- Evolution, cell biology, and the development of multicellularity. Cambridge University Press: Cambridge, UK.

Khosla, M., Robbins, S.M., Spiegelman, G.B., and Weeks, G. (1990). Regulation of *DdrasG* gene expression during *Dictyostelium* development. *Mol Cell Biol* 10, 918-922.

Khosla, M., Spiegelman, G.B., Insall, R., and Weeks, G. (2000). Functional overlap of the Dictyostelium RasG, RasD and RasB proteins. *J Cell Sci* 113 ( Pt 8), 1427-1434.

Khosla, M., Spiegelman, G.B., and Weeks, G. (2005). The effect of the disruption of a gene encoding a PI4 kinase on the developmental defect exhibited by Dictyostelium *rasC* cells. *Dev Biol* 284, 412-420.

Khosla, M., Spiegelman, G.B., Weeks, G., Sands, T.W., Viridy, K.J., and Cotter, D.A. (1994). RasG protein accumulation occurs just prior to amoebae emergence during spore germination in *Dictyostelium discoideum*. *FEMS Microbiol Lett* 117, 293-298.

Kimmel, A.R., and Parent, C.A. (2003). The signal to move: *D. discoideum* go orienteering. *Science* 300, 1525-1527.

Kitayama, C., Sugimoto, A., and Yamamoto, M. (1997). Type II myosin heavy chain encoded by the *myo2* gene composes the contractile ring during cytokinesis in *Schizosaccharomyces pombe*. *J Cell Biol* 137, 1309-1319.

Kortholt, A., Rehmann, H., Kae, H., Bosgraaf, L., Keizer-Gunnink, I., Weeks, G., Wittinghofer, A., and Van Haastert, P.J. (2006). Characterization of the GbpD-activated Rap1 pathway regulating adhesion and cell polarity in *Dictyostelium discoideum*. *J Biol Chem* 281, 23367-23376.

Kriebel, P.W., Barr, V.A., and Parent, C.A. (2003). Adenylyl cyclase localization regulates streaming during chemotaxis. *Cell* 112, 549-560.

Lee, S., Comer, F.I., Sasaki, A., McLeod, I.X., Duong, Y., Okumura, K., Yates Iii, J.R., Parent, C.A., and Firtel, R.A. (2005). TOR Complex 2 Integrates Cell Movement during Chemotaxis and Signal Relay in Dictyostelium. *Mol Biol Cell* 16, 4572-4583.

Lee, S., Parent, C.A., Insall, R., and Firtel, R.A. (1999). A novel Ras-interacting protein required for chemotaxis and cyclic adenosine monophosphate signal relay in Dictyostelium. *Mol Biol Cell* 10, 2829-2845.

Li, G., Alexander, H., Schneider, N., and Alexander, S. (2000). Molecular basis for resistance to the anticancer drug cisplatin in Dictyostelium. *Microbiology* 146 ( Pt 9), 2219-2227.

Liang, W., Licate, L., Warrick, H., Spudich, J., and Egelhoff, T. (2002). Differential localization in cells of myosin II heavy chain kinases during cytokinesis and polarized migration. *BMC Cell Biol* 3, 19.

Lim, C.J., Spiegelman, G.B., and Weeks, G. (2001). RasC is required for optimal activation of adenylyl cyclase and Akt/PKB during aggregation. *EMBO J* 20, 4490-4499.

Lim, C.J., Zawadzki, K.A., Khosla, M., Secko, D.M., Spiegelman, G.B., and Weeks, G. (2005). Loss of the Dictyostelium RasC protein alters vegetative cell size, motility and endocytosis. *Exp Cell Res* 306, 47-55.

Liu, G., and Newell, P.C. (1994). Regulation of myosin regulatory light chain phosphorylation via cyclic GMP during chemotaxis of Dictyostelium. *J Cell Sci* 107 ( Pt 7), 1737-1743.

Loomis, W.F. (1996). Genetic networks that regulate development in Dictyostelium cells. *Microbiol Rev* 60, 135-150.

Loomis, W.F., and Smith, D.W. (1990). Molecular phylogeny of *Dictyostelium discoideum* by protein sequence comparison. *Proc Natl Acad Sci U S A* 87, 9093-9097.

Loovers, H.M., Postma, M., Keizer-Gunnink, I., Huang, Y.E., Devreotes, P.N., and van Haastert, P.J. (2006). Distinct roles of PI(3,4,5)P3 during chemoattractant signaling in Dictyostelium: a quantitative in vivo analysis by inhibition of PI3-kinase. *Mol Biol Cell* 17, 1503-1513.

Louis, S.A., Spiegelman, G.B., and Weeks, G. (1997a). Expression of an activated rasD gene changes cell fate decisions during Dictyostelium development. *Mol Biol Cell* 8, 303-312.

Louis, S.A., Weeks, G., and Spiegelman, G.B. (1997b). Rap1 overexpression reveals that activated RasD induces separable defects during Dictyostelium development. *Dev Biol* 190, 273-283.

Lowy, D.R., and Willumsen, B.M. (1993). Function and regulation of *ras*. *Annu Rev Biochem* 62, 851-891.

Manahan, C.L., Iglesias, P.A., Long, Y., and Devreotes, P.N. (2004). Chemoattractant signaling in *Dictyostelium discoideum*. *Annu Rev Cell Dev Biol* 20, 223-253.

Marinissen, M.J., and Gutkind, J.S. (2001). G-protein-coupled receptors and signaling networks: emerging paradigms. *Trends Pharmacol Sci* 22, 368-376.

Marshall, C.J. (1996). Ras effectors. *Curr Opin Cell Biol* 8, 197-204.

- Meili, R., Ellsworth, C., Lee, S., Reddy, T.B., Ma, H., and Firtel, R.A. (1999). Chemoattractant-mediated transient activation and membrane localization of Akt/PKB is required for efficient chemotaxis to cAMP in *Dictyostelium*. *EMBO J* 18, 2092-2105.
- Melien, O. (2007). Heterotrimeric G proteins and disease. *Methods Mol Biol* 361, 119-144.
- Mitin, N., Rossman, K.L., and Der, C.J. (2005). Signaling interplay in Ras superfamily function. *Curr Biol* 15, R563-574.
- Morrison, D.K., and Cutler, R.E. (1997). The complexity of Raf-1 regulation. *Curr Opin Cell Biol* 9, 174-179.
- Nimnual, A.S., Yatsula, B.A., and Bar-Sagi, D. (1998). Coupling of Ras and Rac guanosine triphosphatases through the Ras exchanger Sos. *Science* 279, 560-563.
- O'Connell, C.B., Warner, A.K., and Wang, Y. (2001). Distinct roles of the equatorial and polar cortices in the cleavage of adherent cells. *Curr Biol* 11, 702-707.
- Olsen, G.J., McCarroll, R., and Sogin, M.L. (1983). Secondary structure of the *Dictyostelium discoideum* small subunit ribosomal RNA. *Nucleic Acids Res* 11, 8037-8049.
- Olson, M.F., and Marais, R. (2000). Ras protein signalling. *Semin Immunol* 12, 63-73.
- Palmieri, S.J., Nebl, T., Pope, R.K., Seastone, D.J., Lee, E., Hinchcliffe, E.H., Sluder, G., Knecht, D., Cardelli, J., and Luna, E.J. (2000). Mutant Rac1B expression in *Dictyostelium*: effects on morphology, growth, endocytosis, development, and the actin cytoskeleton. *Cell Motil Cytoskeleton* 46, 285-304.
- Parent, C.A. (2004). Making all the right moves: chemotaxis in neutrophils and *Dictyostelium*. *Curr Opin Cell Biol* 16, 4-13.
- Parent, C.A., and Devreotes, P.N. (1996). Molecular genetics of signal transduction in *Dictyostelium*. *Annu Rev Biochem* 65, 411-440.
- Pawson, T., and Schlessingert, J. (1993). SH2 and SH3 domains. *Curr Biol* 3, 434-442.
- Pechlivanis, M., and Kuhlmann, J. (2006). Hydrophobic modifications of Ras proteins by isoprenoid groups and fatty acids-More than just membrane anchoring. *Biochim Biophys Acta* 1764, 1914-1931.
- Postma, M., Bosgraaf, L., Looovers, H.M., and Van Haastert, P.J. (2004). Chemotaxis: signalling modules join hands at front and tail. *EMBO Rep* 5, 35-40.

Prinster, S.C., Hague, C., and Hall, R.A. (2005). Heterodimerization of G protein-coupled receptors: specificity and functional significance. *Pharmacol Rev* 57, 289-298.

Prior, I.A., Harding, A., Yan, J., Sluimer, J., Parton, R.G., and Hancock, J.F. (2001). GTP-dependent segregation of H-ras from lipid rafts is required for biological activity. *Nat Cell Biol* 3, 368-375.

Pupillo, M., Insall, R., Pitt, G.S., and Devreotes, P.N. (1992). Multiple cyclic AMP receptors are linked to adenylyl cyclase in *Dictyostelium*. *Mol Biol Cell* 3, 1229-1234.

Quilliam, L.A., Rebhun, J.F., and Castro, A.F. (2002). A growing family of guanine nucleotide exchange factors is responsible for activation of Ras-family GTPases. *Prog Nucleic Acid Res Mol Biol* 71, 391-444.

Radziwill, G., Erdmann, R.A., Margelisch, U., and Moelling, K. (2003). The Bcr kinase downregulates Ras signaling by phosphorylating AF-6 and binding to its PDZ domain. *Mol Cell Biol* 23, 4663-4672.

Rebstein, P.J. (1996). Analysis of the effects of the *rap1* and *rasG* genes on *Dictyostelium discoideum* cell morphology, Ph.D. Thesis. University of British Columbia, Vancouver, BC.

Rebstein, P.J., Cardelli, J., Weeks, G., and Spiegelman, G.B. (1997). Mutational analysis of the role of Rap1 in regulating cytoskeletal function in *Dictyostelium*. *Exp Cell Res* 231, 276-283.

Rebstein, P.J., Weeks, G., and Spiegelman, G.B. (1993). Altered morphology of vegetative amoebae induced by increased expression of the *Dictyostelium discoideum* *ras*-related gene *rap1*. *Dev Genet* 14, 347-355.

Reymond, C.D., Gomer, R.H., Mehdy, M.C., and Firtel, R.A. (1984). Developmental regulation of a *Dictyostelium* gene encoding a protein homologous to mammalian ras protein. *Cell* 39, 141-148.

Reymond, C.D., Gomer, R.H., Nellen, W., Theibert, A., Devreotes, P., and Firtel, R.A. (1986). Phenotypic changes induced by a mutated *ras* gene during the development of *Dictyostelium* transformants. *Nature* 323, 340-343.

Robbins, S.M., Suttorp, V.V., Weeks, G., and Spiegelman, G.B. (1990). A *ras*-related gene from the lower eukaryote *Dictyostelium* that is highly conserved relative to the human *rap* genes. *Nucleic Acids Res* 18, 5265-5269.

- Robbins, S.M., Williams, J.G., Jermyn, K.A., Spiegelman, G.B., and Weeks, G. (1989). Growing and developing Dictyostelium cells express different *ras* genes. *Proc Natl Acad Sci U S A* 86, 938-942.
- Rodriguez-Viciano, P., Warne, P.H., Khwaja, A., Marte, B.M., Pappin, D., Das, P., Waterfield, M.D., Ridley, A., and Downward, J. (1997). Role of phosphoinositide 3-OH kinase in cell transformation and control of the actin cytoskeleton by Ras. *Cell* 89, 457-467.
- Roelofs, J., Snippe, H., Kleineidam, R.G., and Van Haastert, P.J. (2001). Guanylate cyclase in *Dictyostelium discoideum* with the topology of mammalian adenylyl cyclase. *Biochem J* 354, 697-706.
- Roelofs, J., and Van Haastert, P.J. (2002). Characterization of two unusual guanylyl cyclases from Dictyostelium. *J Biol Chem* 277, 9167-9174.
- Rubin, H., and Ravid, S. (2002). Polarization of myosin II heavy chain-protein kinase C in chemotaxing Dictyostelium cells. *J Biol Chem* 277, 36005-36008.
- Rupper, A., and Cardelli, J. (2001). Regulation of phagocytosis and endo-phagosomal trafficking pathways in *Dictyostelium discoideum*. *Biochim Biophys Acta* 1525, 205-216.
- Salomon, Y. (1979). Adenylyl cyclase assay. *Adv Cyclic Nucleotide Res* 10, 35-55.
- Sambrook, J., Fritsch, E. F. and Maniatis, T. (1989). *Molecular Cloning. A Laboratory Manual.*, 2 edn. Cold Spring Harbor, Cold Spring Harbor Laboratory Press.
- Saran, S., Meima, M.E., Alvarez-Curto, E., Weening, K.E., Rozen, D.E., and Schaap, P. (2002). cAMP signaling in Dictyostelium. Complexity of cAMP synthesis, degradation and detection. *J Muscle Res Cell Motil* 23, 793-802.
- Sarbassov, D.D., Guertin, D.A., Ali, S.M., and Sabatini, D.M. (2005). Phosphorylation and regulation of Akt/PKB by the rictor-mTOR complex. *Science* 307, 1098-1101.
- Sasaki, A.T., Chun, C., Takeda, K., and Firtel, R.A. (2004). Localized Ras signaling at the leading edge regulates PI3K, cell polarity, and directional cell movement. *J Cell Biol* 167, 505-518.
- Sasaki, A.T., and Firtel, R.A. (2006). Regulation of chemotaxis by the orchestrated activation of Ras, PI3K, and TOR. *Eur J Cell Biol* 85, 873-895.

Schenk, P.W., Epskamp, S.J., Knetsch, M.L., Harten, V., Lagendijk, E.L., van Duijn, B., and Snaar-Jagalska, B.E. (2001). Lysophosphatidic acid- and Gbeta-dependent activation of Dictyostelium MAP kinase ERK2. *Biochem Biophys Res Commun* 282, 765-772.

Schlessinger, J. (2000). Cell signaling by receptor tyrosine kinases. *Cell* 103, 211-225.

Schulkes, C., and Schaap, P. (1995). cAMP-dependent protein kinase activity is essential for preaggregative gene expression in Dictyostelium. *FEBS Lett* 368, 381-384.

Seastone, D.J., Zhang, L., Buczynski, G., Rebstein, P., Weeks, G., Spiegelman, G., and Cardelli, J. (1999). The small Mr Ras-like GTPase Rap1 and the phospholipase C pathway act to regulate phagocytosis in *Dictyostelium discoideum*. *Mol Biol Cell* 10, 393-406.

Segall, J.E., Kuspa, A., Shaulsky, G., Ecke, M., Maeda, M., Gaskins, C., Firtel, R.A., and Loomis, W.F. (1995). A MAP kinase necessary for receptor-mediated activation of adenylyl cyclase in Dictyostelium. *J Cell Biol* 128, 405-413.

Shaulsky, G., and Loomis, W.F. (1993). Cell type regulation in response to expression of ricin A in Dictyostelium. *Dev Biol* 160, 85-98.

Shields, J.M., Pruitt, K., McFall, A., Shaub, A., and Der, C.J. (2000). Understanding Ras: 'it ain't over 'til it's over'. *Trends Cell Biol* 10, 147-154.

Snaar-Jagalska, B.E., and Van Haastert, P.J. (1994). G-protein assays in Dictyostelium. *Methods Enzymol* 237, 387-408.

Souza, G.M., Lu, S., and Kuspa, A. (1998). YakA, a protein kinase required for the transition from growth to development in Dictyostelium. *Development* 125, 2291-2302.

Steimle, P.A., Licate, L., Cote, G.P., and Egelhoff, T.T. (2002). Lamellipodial localization of Dictyostelium myosin heavy chain kinase A is mediated via F-actin binding by the coiled-coil domain. *FEBS Lett* 516, 58-62.

Sternberg, P.W., and Han, M. (1998). Genetics of RAS signaling in *C. elegans*. *Trends Genet* 14, 466-472.

Stokoe, D., Macdonald, S.G., Cadwallader, K., Symons, M., and Hancock, J.F. (1994). Activation of Raf as a result of recruitment to the plasma membrane. *Science* 264, 1463-1467.

Sussman, M. (1987). Cultivation and synchronous morphogenesis of Dictyostelium under controlled experimental conditions. *Methods Cell Biol* 28, 9-29.

- Sutherland, B.W. (2001). Investigation of the function of the *Dictyostelium discoideum* RasB protein., Ph.D. Thesis. University of British Columbia, Vancouver, BC.
- Sutherland, B.W., Spiegelman, G.B., and Weeks, G. (2001). A Ras subfamily GTPase shows cell cycle-dependent nuclear localization. *EMBO Rep* 2, 1024-1028.
- Takai, Y., Sasaki, T., and Matozaki, T. (2001). Small GTP-binding proteins. *Physiol Rev* 81, 153-208.
- Takeda, K., Sasaki, A.T., Ha, H., Seung, H.A., and Firtel, R.A. (2007). Role of phosphatidylinositol 3-kinases in chemotaxis in *Dictyostelium*. *J Biol Chem* 282, 11874-11884.
- Tall, G.G., Barbieri, M.A., Stahl, P.D., and Horazdovsky, B.F. (2001). Ras-activated endocytosis is mediated by the Rab5 guanine nucleotide exchange activity of RIN1. *Dev Cell* 1, 73-82.
- Theibert, A., and Devreotes, P.N. (1986). Surface receptor-mediated activation of adenylate cyclase in *Dictyostelium*. Regulation by guanine nucleotides in wild-type cells and aggregation deficient mutants. *J Biol Chem* 261, 15121-15125.
- Tuxworth, R.I., Cheetham, J.L., Machesky, L.M., Spiegelmann, G.B., Weeks, G., and Insall, R.H. (1997). *Dictyostelium* RasG is required for normal motility and cytokinesis, but not growth. *J Cell Biol* 138, 605-614.
- Van Haastert, P.J., and Devreotes, P.N. (2004). Chemotaxis: signalling the way forward. *Nat Rev Mol Cell Biol* 5, 626-634.
- van Haastert, P.J., Keizer-Gunnink, I., and Kortholt, A. (2007). Essential role of PI3-kinase and phospholipase A2 in *Dictyostelium discoideum* chemotaxis. *J Cell Biol* 177, 809-816.
- Van Haastert, P.J., and Kien, E. (1983). Binding of cAMP derivatives to *Dictyostelium discoideum* cells. Activation mechanism of the cell surface cAMP receptor. *J Biol Chem* 258, 9636-9642.
- van Haastert, P.J.M. (1984). A method for studying cAMP-relay in *Dictyostelium discoideum*: the effect of temperature on cAMP-relay. *J Gen Microbiol* 130, 2559-2564.
- van Haastert, P.J.M., and Kuwayama, H. (1997). cGMP as second messenger during *Dictyostelium* chemotaxis. *FEBS Lett* 410, 25-28.

- Vanhaesebroeck, B., and Waterfield, M.D. (1999). Signaling by distinct classes of phosphoinositide 3-kinases. *Exp Cell Res* 253, 239-254.
- Veltman, D.M., Roelofs, J., Engel, R., Visser, A.J., and Van Haastert, P.J. (2005). Activation of soluble guanylyl cyclase at the leading edge during *Dictyostelium* chemotaxis. *Mol Biol Cell* 16, 976-983.
- Veltman, D.M., and Van Haastert, P.J. (2006). Guanylyl cyclase protein and cGMP product independently control front and back of chemotaxing *Dictyostelium* cells. *Mol Biol Cell* 17, 3921-3929.
- Vetter, I.R., and Wittinghofer, A. (2001). The guanine nucleotide-binding switch in three dimensions. *Science* 294, 1299-1304.
- Villalonga, P., Lopez-Alcala, C., Bosch, M., Chiloeches, A., Rocamora, N., Gil, J., Marais, R., Marshall, C.J., Bachs, O., and Agell, N. (2001). Calmodulin binds to K-Ras, but not to H- or N-Ras, and modulates its downstream signaling. *Mol Cell Biol* 21, 7345-7354.
- Vojtek, A.B., Hollenberg, S.M., and Cooper, J.A. (1993). Mammalian Ras interacts directly with the serine/threonine kinase Raf. *Cell* 74, 205-214.
- Vos, M.D., Martinez, A., Ellis, C.A., Vallecorsa, T., and Clark, G.J. (2003). The pro-apoptotic Ras effector Nore1 may serve as a Ras-regulated tumor suppressor in the lung. *J Biol Chem* 278, 21938-21943.
- Wassarman, D.A., Therrien, M., and Rubin, G.M. (1995). The Ras signaling pathway in *Drosophila*. *Curr Opin Genet Dev* 5, 44-50.
- Watts, D.J., and Ashworth, J.M. (1970). Growth of myxameobae of the cellular slime mould *Dictyostelium discoideum* in axenic culture. *Biochem J* 119, 171-174.
- Weber, I., Niewohner, J., and Faix, J. (1999). Cytoskeletal protein mutations and cell motility in *Dictyostelium*. *Biochem Soc Symp* 65, 245-265.
- Weeks, G., Gaudet, P., and Insall, R.H. (2005). The Small GTPase Superfamily. In: *Dictyostelium* genomics, eds. W.F. Loomis and A. Kuspa: Horizon Bioscience, Norfolk, U.K., 211-234.
- Weeks, G., and Spiegelman, G.B. (2003). Roles played by Ras subfamily proteins in the cell and developmental biology of microorganisms. *Cell Signal* 15, 901-909.

- Weiner, O.D. (2002). Regulation of cell polarity during eukaryotic chemotaxis: the chemotactic compass. *Curr Opin Cell Biol* 14, 196-202.
- Wessels, D., Brincks, R., Kuhl, S., Stepanovic, V., Daniels, K.J., Weeks, G., Lim, C.J., Spiegelman, G., Fuller, D., Iranfar, N., Loomis, W.F., and Soll, D.R. (2004). RasC plays a role in transduction of temporal gradient information in the cyclic-AMP wave of *Dictyostelium discoideum*. *Eukaryot Cell* 3, 646-662.
- Wilkins, A., and Insall, R.H. (2001). Small GTPases in *Dictyostelium*: lessons from a social amoeba. *Trends Genet* 17, 41-48.
- Wilkins, A., Khosla, M., Fraser, D.J., Spiegelman, G.B., Fisher, P.R., Weeks, G., and Insall, R.H. (2000). *Dictyostelium* RasD is required for normal phototaxis, but not differentiation. *Genes Dev* 14, 1407-1413.
- Wittinghofer, F. (1998). Ras signalling. Caught in the act of the switch-on. *Nature* 394, 317, 319-320.
- Wolthuis, R.M., and Bos, J.L. (1999). Ras caught in another affair: the exchange factors for Ral. *Curr Opin Genet Dev* 9, 112-117.
- Wu, L., Valkema, R., Van Haastert, P.J., and Devreotes, P.N. (1995). The G protein beta subunit is essential for multiple responses to chemoattractants in *Dictyostelium*. *J Cell Biol* 129, 1667-1675.
- Xu, J., Wang, F., Van Keymeulen, A., Herzmark, P., Straight, A., Kelly, K., Takuwa, Y., Sugimoto, N., Mitchison, T., and Bourne, H.R. (2003). Divergent signals and cytoskeletal assemblies regulate self-organizing polarity in neutrophils. *Cell* 114, 201-214.
- Zhang, H., Heid, P.J., Wessels, D., Daniels, K.J., Pham, T., Loomis, W.F., and Soll, D.R. (2003a). Constitutively active protein kinase A disrupts motility and chemotaxis in *Dictyostelium discoideum*. *Eukaryot Cell* 2, 62-75.
- Zhang, J., Campbell, R.E., Ting, A.Y., and Tsien, R.Y. (2002). Creating new fluorescent probes for cell biology. *Nat Rev Mol Cell Biol* 3, 906-918.
- Zhang, Y., Luo, Y., Zhai, Q., Ma, L., and Dorf, M.E. (2003b). Negative role of cAMP-dependent protein kinase A in RANTES-mediated transcription of proinflammatory mediators through Raf. *Faseb J* 17, 734-736.